Michael Giebler, BSc

Supercritical fluid impregnation of polycarbonate with copper nanoparticles in carbon dioxide

MASTERARBEIT

zur Erlangung des akademischen Grades
Master of Science

Masterstudium Chemie

eingereicht an der

Technischen Universität Graz

Betreuer

Ao.Univ.Prof. Dipl.-Ing. Dr.techn. Thomas Gamse
Dipl.-Ing. Dániel Varga

Institut für Chemische Verfahrenstechnik und Umwelttechnik

Graz, August 2016

EIDESSTATTLICHE ERKLÄRUNG

Ich erkläre an Eides statt, dass ich die vorliegende Arbeit selbstständig verfasst, andere als die angegebenen Quellen/Hilfsmittel nicht benutzt, und die den benutzten Quellen wörtlich und inhaltlich entnommenen Stellen als solche kenntlich gemacht habe. Das in TUGRAZonline hochgeladene Textdokument ist mit der vorliegenden Masterarbeit identisch.

Datum

Unterschrift

Acknowledgements

An dieser Stelle möchte ich all jenen danken, die mich während der Erstellung dieser Masterarbeit und im Laufe meines Studiums unterstützt haben.

Zuallererst gebührt mein Dank Ao.Univ.Prof. Dipl.-Ing. Dr.techn. Thomas Gamse und Dipl.-Ing. Dániel Varga.

Dank ihrer Expertise, Geduld und Ratschläge war diese Arbeit möglich. Ich möchte mich herzlich bei beiden für diese tolle Möglichkeit bedanken!

Dipl.-Ing. Dr.techn. Helmar Wiltsche und dem Team des FELMI - ZFE Graz danke ich für die zahlreichen Analysen.

Darüber hinaus möchte ich mich bei all den Kollegen, Freunden und Weggefährten bedanken, die mich in den letzten Jahren begleitet und motiviert haben.

Ein besonderer Dank gilt meiner Familie, die mir vieles ermöglicht und mich in meinen Entscheidungen immer unterstützt hat.

Und ich möchte mich bei meiner Freundin für die Unterstützung der letzten Jahre bedanken.

Abstract

Impregnation of polymers in supercritical fluids offers intermediate steps towards energy-efficient and low-cost processes. Deposition of nano- scaled particles within the polymer matrix induces new properties and has a great potential for the development of new materials. For the copper impregnation, experiments were performed in a high- pressure vessel in the range of 100 – 200 bar, 40 – 50°C and with an impregnation time of 1 – 24 h. For this work, polycarbonate was used as polymer matrix and supercritical CO_2 served as solvent. To increase the efficiency of the impregnation, dithizone was used as carrier. and its properties (e.g. solubility and bonding capacity) were investigated. Dithizone forms complexes with a variety of metals and has a good solubility in supercritical CO_2. The copper concentration was determined with ICP-OES and ICP-MS. Moreover, SEM coupled with EDX served as indicator for an impregnation deep inside the polymer matrix. Four different process approaches were introduced and compared with each other. In three of those four test series successful impregnation of the polycarbonate was achieved. The copper concentration was between 4 and 380 mg/kg polymer. Whereas, the best results were obtained by a 2- step impregnation. This process includes a preliminary dithizone impregnation and a final impregnation with copper(II) nitrate. SEM/ EDX measurements proved the existence of nano- sized copper aggregates (5 –100 nm) within the matrix.

Zusammenfassung

Neue Anforderungen an Industrieprozesse hinsichtlich wirtschaftlicher und ökologischer Faktoren machen die Entwicklung kosten- und energieeffizienter Prozesse notwendig. Die Imprägnierung von Polymeren in überkritischen Fluiden könnte einen Beitrag zu dieser Entwicklung leisten. Zusätzlich ermöglicht das Anlagern von Nanostrukturen innerhalb der Polymermatrix die Schaffung neuer Materialeigenschaften. Ziel dieser Arbeit war die Imprägnierung von Polykarbonat mit Kupfer- Nanopartikel. Hierzu wurden Versuche in einem Druckbereich von 100 – 200 bar, einem Temperaturbereich von 40 – 50°C und einer Imprägnierungszeit von 1 – 24 h durchgeführt. Überkritisches CO_2 wurde als Lösungsmittel verwendet. Um die aufgenommene Kupfermenge zu erhöhen, wurde Dithizon als zusätzliches Trägermaterial verwendet. Dithizon bildet mit einer großen Anzahl an Metallen, Komplexe und zeigt zusätzlich eine gute Löslichkeit in überkritischem CO_2. Um die resultierende Kupferkonzentration zu bestimmen, wurden ICP- OES und ICP- MS zur Analyse genutzt. Darüber hinaus, diente SEM gekoppelt mit EDX als Erfolgskriterium hinsichtlich möglicher Kupferaggregate.

Vier verschiedene Prozessansätze wurden entwickelt und verglichen. Dabei ergaben drei der vier Prozesse eine erfolgreiche Imprägnierung. Eine zweistufige Imprägnierung ergab hierbei die höchsten Konzentrationen von 4 – 380 mg/kg Polymer. Der zweistufige Prozess beinhaltet eine Imprägnierung des Polykarbonates mit Dithizon und eine anschließende Imprägnierung mit Kupfer(II)- nitrat. Die Auswertung der SEM Bilder und die Kopplung mit der EDX Technik zeigte Nanopartikel von der Größe 5 - 100 nm tief innerhalb der Polymermarix.

Table of content

1 Introduction

Constantly growing energy consumption and scarcity of resources, force the industry to develop more efficient and less energy consuming processes.

Based on these environmental concerns and proceeded development of energy efficient processes, supercritical fluids (SCF) offer a good possibility to satisfy these new demands. Unique properties of SCF allow the replacement of organic solvents, and enhanced process operations. One major feature of SCF, is not having a phase boundary between the gas and liquid phases. Therefore, SCF are characterized as hybrids, having properties of gases and of liquids. Examples for their usage are: (a) alternative solvents for classical separation processes such as extraction, fractionation, adsorption, chromatography, and crystallization, (b) as reaction media for polymerization or depolymerisation, or (c) simply as reprocessing fluid like production of particles, fibres or foams [1].

Besides classical applications with supercritical fluids, the preparation of nano- sized particles in supercritical fluids has a great potential for industrial processes.

Combining supercritical fluid methods for the preparation of nanoparticles with polymer processing, is one of the newest topics in this growing field of interest. Properties related to nanoscale composite material are the specific particle morphology, metal dispersion, concentration and electronic properties of the metal within its host environment [2].

SCF have been used to deposit thin metal films onto a wide range of surfaces and incorporate metallic particles for a wide variety of inorganic and organic substrates for microelectronic, optical and catalytic applications [2]. Moreover, covered with nanoparticles, polymers gain antibacterial and antifungal properties.

One potential way to synthesize such metal- containing- polymers is the impregnation with supercritical fluids.

Supercritical fluid impregnation is an environmentally friendly, energy efficient and convenient method for the impregnation of matrices like polymers, textiles, fibres, aerogels and wood.

1.1 Aim and research objective

The aim of this work was the impregnation of polycarbonate with copper nanoparticles deep inside the polymer matrix. To reach a successful impregnation the properties of supercritical CO_2, dithizone and polycarbonate were combined. In this work, four different approaches were used, compared and later studied with regard to their mechanisms. To find ideal process conditions, parameters like temperature, pressure, the amount of additives, co-solvents and different experimental settings were changed and collated.

In order to determine the efficiency of the impregnation, techniques like ICP-OES, ICP-MS, UV-VIS spectroscopy and SEM/EDX were used.

2 Theoretical background

2.1 Basic physical properties of supercritical fluids

Before moving on to the actual topic of this thesis, it is essential to define what a supercritical fluid is.

IUPAC defines this "fluid" as a state of a compound, mixture or element above its critical pressure (p_C) and critical temperature (T_C). Whereas the critical temperature is the maximum temperature, at which a gas can be converted into a liquid by an increase in pressure. The critical pressure is the minimum pressure, which would suffice to liquefy a substance at its critical temperature. Above the critical pressure, an increase in temperature will not cause a fluid to vaporise to give a two- phase system [3].

Technically speaking, a supercritical fluid is not a gas but a vapour [4]. Its properties appear to be a mixture between a gas and a liquid, therefore, at the supercritical point both phases are indistinguishable. However, in comparison to the gaseous and liquid state, compressibility and heat capacity are higher near the critical point [5]. Consequently, by changing their pressure or temperature, the properties of SCF can be tuned from liquid-like to gas-like without crossing a phase boundary [6]. Therefore, it is not possible to liquefy a supercritical fluid under any pressure as long as it is heated above its critical temperature and no phase separation occurs for any substance at pressures or temperatures above its critical values [7].

As mentioned before, the SCF used for all these experiments was supercritical CO_2 ($scCO_2$), which is used as a processing solvent for different polymer applications like polymer modification, formation of polymer composites, polymer blending, microcellular foaming, particle production and polymerization [8].

CO_2 has brilliant dissolving properties regarding hydrophilic substances under liquid and supercritical conditions. One further reason for its frequent use is that CO_2 has a relatively low critical point at a pressure of 73.959 ± 0,005 bar (7.40 MPa) and a temperature of 31.05 ± 0.05 °C (304.5 K) [9].

Figure 2-1 represents a schematic phase diagram for pure CO_2. This diagram shows the state of matter, whereas temperature is in dependence from pressure. To give a short explanation how to read this diagram, the starting point is at 74 bar and -80°C. At this condition CO_2 is solid. Following an isobaric heating, the system crosses the melting curve. After this point CO_2 is liquid (e.g. 74 bar and -20°C). With further heating, the state of CO_2 changes again, from liquid to supercritical. Generally speaking, the critical point can be observed at the critical

temperature (T_C) and the critical pressure (p_C) and marks the end of the vapour-liquid equilibrium line (boiling line), which separates the vapour and liquid regions.

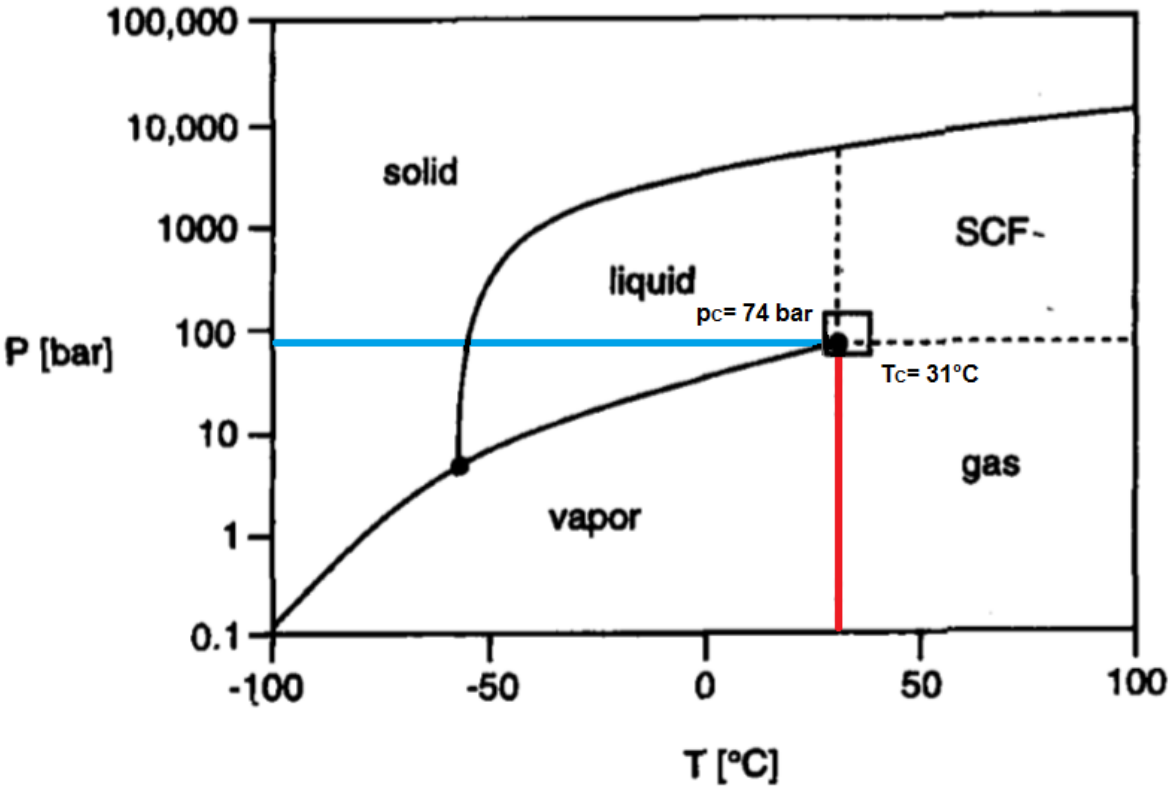

Figure 2-1 Schematic phase diagram for a pure CO_2 [5]

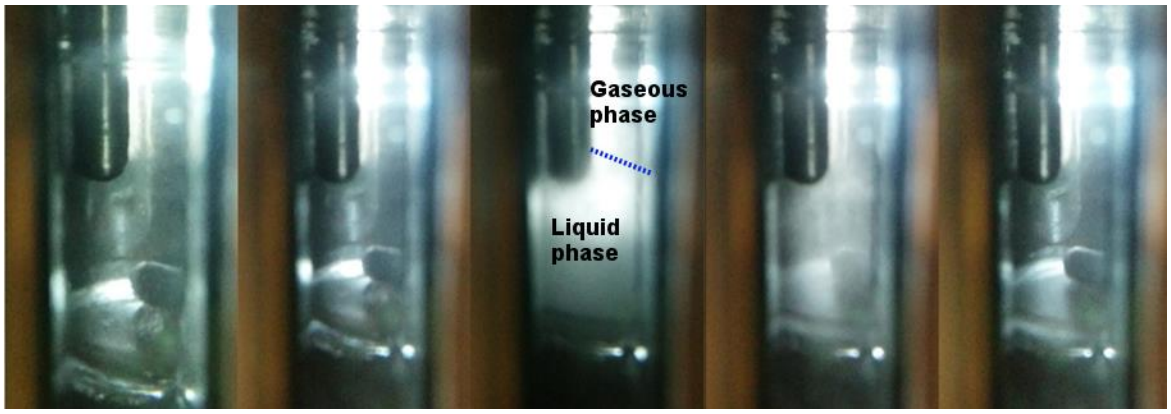

Figure 2-2 Supercritical CO_2 formation in a high- pressure view cell

Figure 2-2 illustrates the formation of $scCO_2$ beginning with gaseous CO_2 (first picture left). By increasing pressure and temperature and getting closer to the supercritical point, a second phase (liquid) appears (picture in the middle). The liquid level increases and the two phases mix. At the supercritical point of CO_2 (73.959 ± 0,005 bar and 31.05 ± 0.05°C) the two phases merge and the phase boundary disappears. Only one-phase exists (picture on the right) and the supercritical state of CO_2 is reached.

2.2 PVT properties of gases

Knowing the density of a gas in its supercritical state is essential for processes like impregnation and extraction. One possible approach to calculate a density of a gas in its ideal state is the ideal gas law (Equation 1). However, this equation cannot be applied to SCF, since their behaviour and properties differ too much from the ideal behaviour

$$p \cdot V = n \cdot R \cdot T \quad \text{(Equation 1)}$$

p…pressure [Pa]

V…volume [m^3]

n… amount of substance of the gas [mol]

R…gas constant 8.3145[$J \cdot K^{-1} \cdot mol^{-1}$]

T…temperature [K]

Adjusting of Equation 1 and multiplication with the molecular weight gives:

$$\rho_{Gas} = \frac{n \cdot M_{Gas}}{V} = M_{Gas} \cdot \frac{p}{R \cdot T} \quad \text{(Equation 2)}$$

and

$$\rho_{Gas} = \frac{M_{Gas}}{V} \quad \text{(Equation 3)}$$

As illustrated in the previous equations, the density of a gas increases with increasing pressure and decreases with decreasing temperature. Furthermore, extensive parameter V gives the specific property volume per mol, which is also connected to the density.

As the title of the ideal gas law suggests, only ideal systems count for this method. Generally, a gas behaves like an ideal gas at higher temperature and lower pressure. Potential energy becomes less significant compared to the particles kinetic energy and the size of the molecules gets less important compared to the empty space between them.

At normal conditions, most real gases behave like an ideal gas, including hydrogen, nitrogen, oxygen and carbon dioxide. Since standard temperature and pressure are not suitable for industrial processes, it is important to use more precise calculation methods. For the sake of completeness, cubic equations of state, non-cubic equations of state, virial equations of state or multiparameter equations of state are more accurate equations [10] [11].

2.3 Selection of suitable supercritical fluids

Since, polycarbonate and the utilized chemicals are limited to certain temperature and pressure ranges, it was essential for the experiments to use a gas, which has beneficial operating conditions to reach the supercritical state. One of the advantages using a supercritical gas as solvent is that no further removal of the solvent is necessary. Simply depressurization removes the gas.

In addition to that, economically speaking, if an extreme high pressure is necessary to reach the supercritical state, this would be very expensive and hence disadvantageous.

Table 2-1 Possible supercritical gases [12]

Gas	Formula	T_c [°C]	p_c [bar]	Lower and upper explosion limit [vol%]
1-Buten	CH_2=CH-CH-CH_3	146.44	40.20	1.6 -10
Chlorodifluoromethane	$CHClF_3$	96,15	96,15	-
Chloromethane	CH_3Cl	143.10	66.79	7.1 - 18.5
Chlorotrifluoromethane	$CClF_3$	28.81	39.46	-
Dichlorodifluoromethane	CCl_2F_2	111.80	41.25	-
Dinitrogen monoxide	N_2O	36.42	72.45	-
Ethane	CH_3- CH_3	32.27	48.80	3 - 12.5
Ethene	CH_2=CH_2	9.21	50.32	2.7 - 34
Carbon dioxide	O=C=O	31.04	73.81	-
n-Butane	CH_3-CH_2-CH_2-CH_3	152.03	37.97	1.5 - 8.5
Propane	CH_3-CH_2-CH_3	96.67	42.49	2.1 - 9.5
Propene	CH_2=CH-CH_3	92.42	46.65	2 - 11.7
Trifluoromethane	CHF_3	25.74	48.36	-
Xenon	Xe	16.59	58.40	-

By comparing the listed gases and having industrial processes in mind, most of the gases can be eliminated due to their high- flammability or high critical temperatures. Halogenated solvents (e.g. Trifluoromethane or Chlorodifluoromethane) are toxic and environmentally hazardous. Regarding health, safety, security and environment, gases like Ethane, Ethene and Propane tend to be explosive at a certain vol%. Furthermore, only a few of the gases are economically justified. The only gas, which meets all these requirements is CO_2. Besides its environmental benefits, CO_2 also provides further advantages like a relatively inertness, a readily accessible critical point, excellent wetting characteristics, low viscosity and highly tuneable behaviour, facilitating easy separation [6].

Furthermore, supercritical CO_2 represents a non-toxic and non-flammable solvent with a low viscosity, high diffusion rate and low surface tension. Since CO_2 is a gas under ambient conditions, its easy removal from the polymeric matrix is another advantage for the use of supercritical carbon dioxide ($scCO_2$) as a solvent.

One major disadvantage of $scCO_2$ is its polarity. Since it has a non- polar character only non-polar compounds are soluble. This property is important for further considerations regarding the complexes and will be discussed in chapter 2.8.4. Nevertheless, CO_2 is a good solvent for most small molecules, either polar or nonpolar.

It may be possible to dissolve a polar solute in $scCO_2$ by applying higher pressure on the system if there is a possibility to make special interactions with the applied solute. For instance, specific interactions such as complex formation and hydrogen bonding can increase the solvent strength of the SCF [13].

By adding polar co-solvents, such as methanol or ethanol, the solubility of polar compounds in $scCO_2$ can be enhanced. Varying the amount of such co-solvent allows for fine-tuning the dissolving capacity of such (e.g. $scCO_2$-ethanol) mixtures.

2.4 Commercial procedures for sc. impregnation with nanostructures and dyeing of polymers

Since nanometer - sized materials offer new properties of industrial interest, the development of techniques for the impregnation of polymers with nanostructure has undertaken a tremendous step forward in the last decade. There are various methods and approaches to produce metal-containing polymers or to create thin films on polymers. To obtain metal-polymer nanocomposites two techniques are used; *in situ* and *ex situ* methods.

For the *in situ* method metal particles are generated inside the polymer matrix by decomposition (e.g. thermolysis, photolysis, radiolysis) or chemical reduction of a metallic precursor reduced within the matrix upon impregnation [14].
In the *ex situ* method, nanoparticles are first produced by soft- chemistry routes and then dispersed into polymeric matrices e.g. via mixing [14].

Examples are reactions of metal salts in polymer solutions, the treatment of polymers with metal vapours, or the polymerization of various metal-monomer systems. Depending on the metal nature and the polymer structure, these processes lead to organometallic units incorporated into polymer chains, metal–polymer complexes, or metal clusters and nanoparticles physically connected with polymer matrix [14].

In this section, the three main methods are discussed:

2.4.1 Solvent cast technology

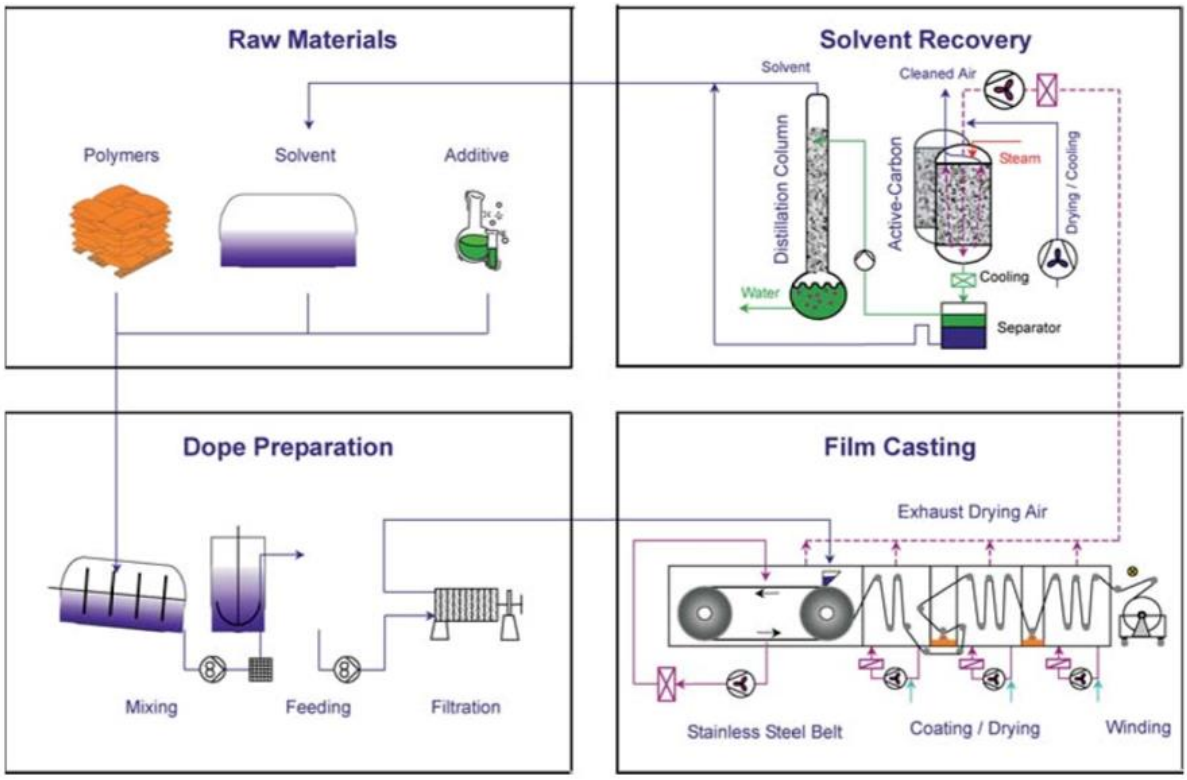

Figure 2-3 Production of solvent cast films [15]

In Figure 2-3 the basic steps for solvent cast technology are presented. This method represents a simple technique for the preparation of µm sized films and flexible plastic components containing additives.

For this technique an inner diameter mould, which is immersed in a tank of polymer solution is used. Using a combination of thermal and frictional properties, the polymer solution forms a thin film around the mould [15].

For that, the mould is extracted from the tank in a controlled manner, followed by a curing or drying process. Once the first polymer layer is solidified, further features can be added e.g. additives. Several casting steps are then used to encapsulate the additives within the polymer. After final solidification, the polymer is removed from the mould.

2.4.2 Melt mixing technology

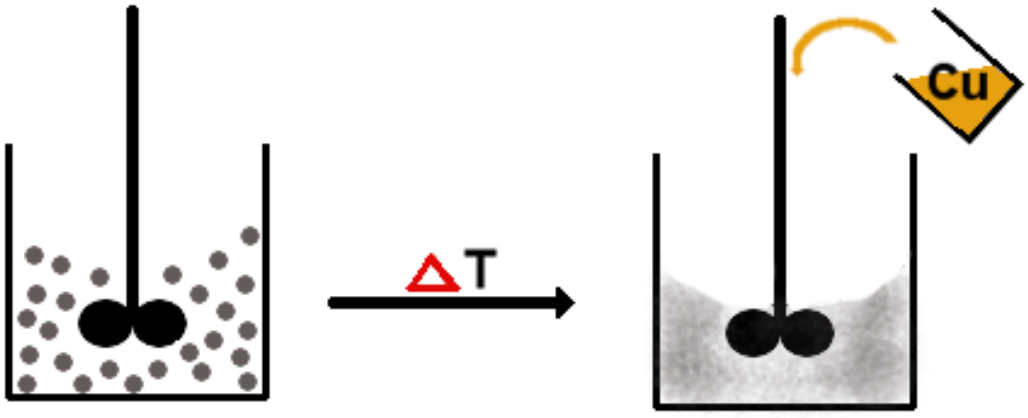

Figure 2-4 Simplified scheme of the melt mixing method

During the melt mixing process blends of polymers are prepared in a melt, which is carried out in rollers, extruders or kneading machines.

The rate - determining step for the intermixing is the diffusion or mobility of the macromolecules inside the highly viscous melt, whereas the morphological architecture of a polymer blend prepared by melt mixing is furthermore dependent on the mixing temperature, the shear gradient, the mixing time, and the rheological properties of the single components [16].

2.4.3 Extrusion technology

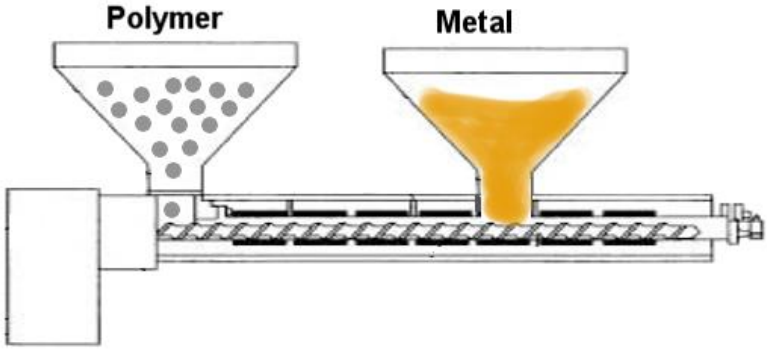

Figure 2-5 Simplified scheme of the extruder technology

Extrusion technology enables the preparation of products or semi-finished items by forcing polymer melts trough a shape-forming orifice (extruder), while this is effected by using mainly single-screw or twin - screw extruders [17].

2.5 Impregnation process

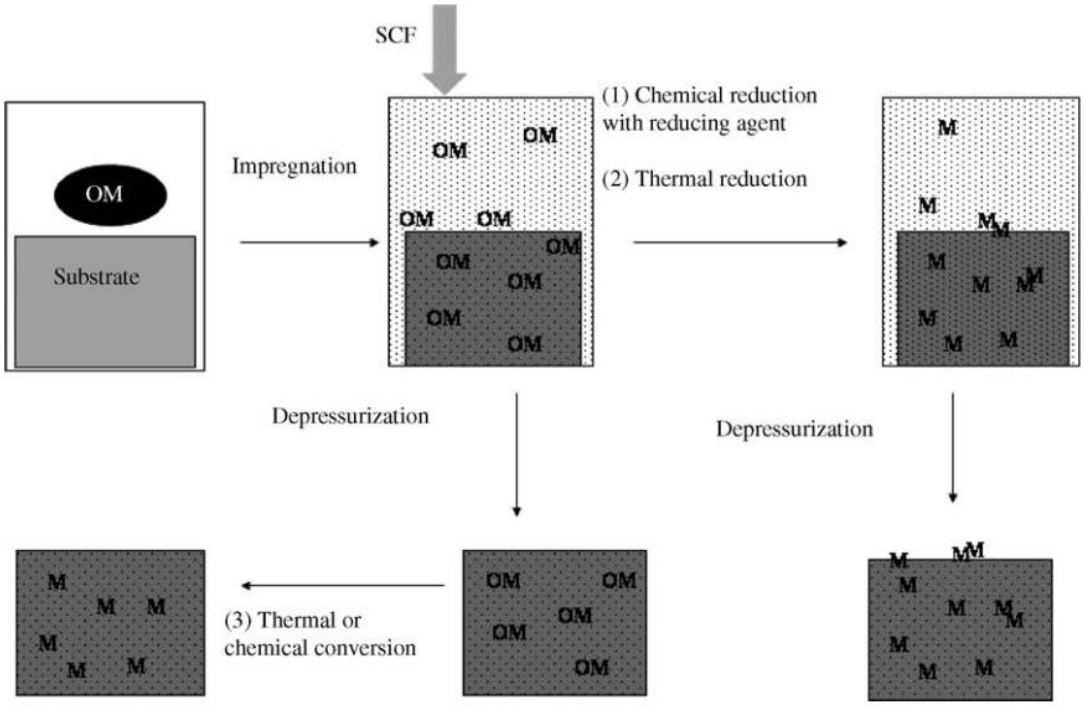

Figure 2-6 Scheme of the impregnation process using sc. fluids as processing solvent [18]

Figure 2-6 illustrates possible processing methods to synthesize supported nanoparticles via deposition or impregnation. OM represents an organometallic compound inside the polymer matrix and M the metal, which is present inside the polymer after the process. In contrast to the processes in Figure 2-6, no additional reduction was performed for this work.

According to Kikic *et.al.* (2003) two properties are essential for the impregnation process [19].

1. the solubility of the solute in the supercritical fluid, which includes two different mechanisms:
   a. deposition of a substance soluble in a supercritical fluid into the polymer matrix upon depressurisation
   b. high affinity of the solute for the polymer matrices
2. the solute modification inside the polymer matrix, while it is possible to distinguish between:
   a. solutes which are not modified in the polymer matrix
   b. solutes which undergo a modification during the impregnation process

Further on, Kikic *et. al.* define (2003), five advantages of this impregnation technique [19].

1. The matrix tends to prevent an agglomeration of metal particles
2. Supercritical CO_2 shows high penetrability into polymers
3. It is possible to control the solvent power and the impregnation rate and therefore, to control the composition and morphology of the obtained composite.
4. The final product does not require special drying
5. Low surface tension allows impregnation even of barrier polymers like Teflon or obtaining of a continuous metal layer on their surface.

To increase binding of the metal, an additive was used for the experiments. Dithizone, a chelate ligand is widely used for analytical applications and forms stable complexes with a variety of transition metals. Additionally, the very good solubility of this compound in supercritical CO_2 will be shown in this work.

2.6 Behaviour of polymers in supercritical fluids like $scCO_2$

Depending on the applied polymer matrix, high pressure during the impregnation process causes different effects. One major effect of high pressure CO_2 is sorption of the CO_2 into the polymer.
It is characterised by increased segmental and chain mobility as well as an increase in interchain distance. This results from polymer-solvent interactions and solvent size [13]. The effect appears in the glass transition temperature (T_G) and melting/crystallization temperature of polymers. Therefore, sorption of CO_2 changes the mechanical and physical properties of the polymer [20]. This phenomenon is called sorption induced glass transition (SIGT), upon which T_g of a given polymer apparently decreases. Moreover, lower polymer viscosity by up to an order of magnitude appears.
It has been proved that CO_2 remarkably accelerates the sorption of many low molecular weight additives into a number of glassy polymers [21].
Berens *et. al*. (1992) states, that two possible interpretations for the mechanism by which CO_2 promotes the impregnation of polymers with additives are possible [21]:

1. The additive is dissolved in the CO_2 and the polymer is then swollen by the CO_2 solution of the additive.
2. CO_2 - assisted impregnation process involves the approach towards an equilibrium distribution of three components (polymer, additive and CO_2) among the phase present.

2.6.1 Swelling

Supercritical CO_2 is able to reversibly swell glass and rubbery polymers and reduce the viscosity of polymer melts [19]. Furthermore, swelling induces a decrease of viscosity, which results from a growing interchain distance, moreover CO_2 acts as a lubricant for polymer chains.

By changing the temperature and the pressure and thereby controlling the density of the solvent, the degree of polymer swelling and the diffusion rate of the substrate can be modified. One way for measuring the swelling of the polymer is to measure the change in one or more dimensions of a polymer sample, whereas one way to calculate the swelling is presented in Equation 4:

$$\frac{\Delta V}{V_0} = \left(\frac{L}{L_0}\right)^3 - 1 \quad \text{(Equation 4)}$$

where ΔV is the volume change while swelling, L and L_0 are the measured lengths of the swollen and unswollen polymer film and V_0 is the volume of the unswollen polymer. The equation is valid for isotropic swelling [22]

The equation is presented only for completeness and will not be used for any calculations in the following work.

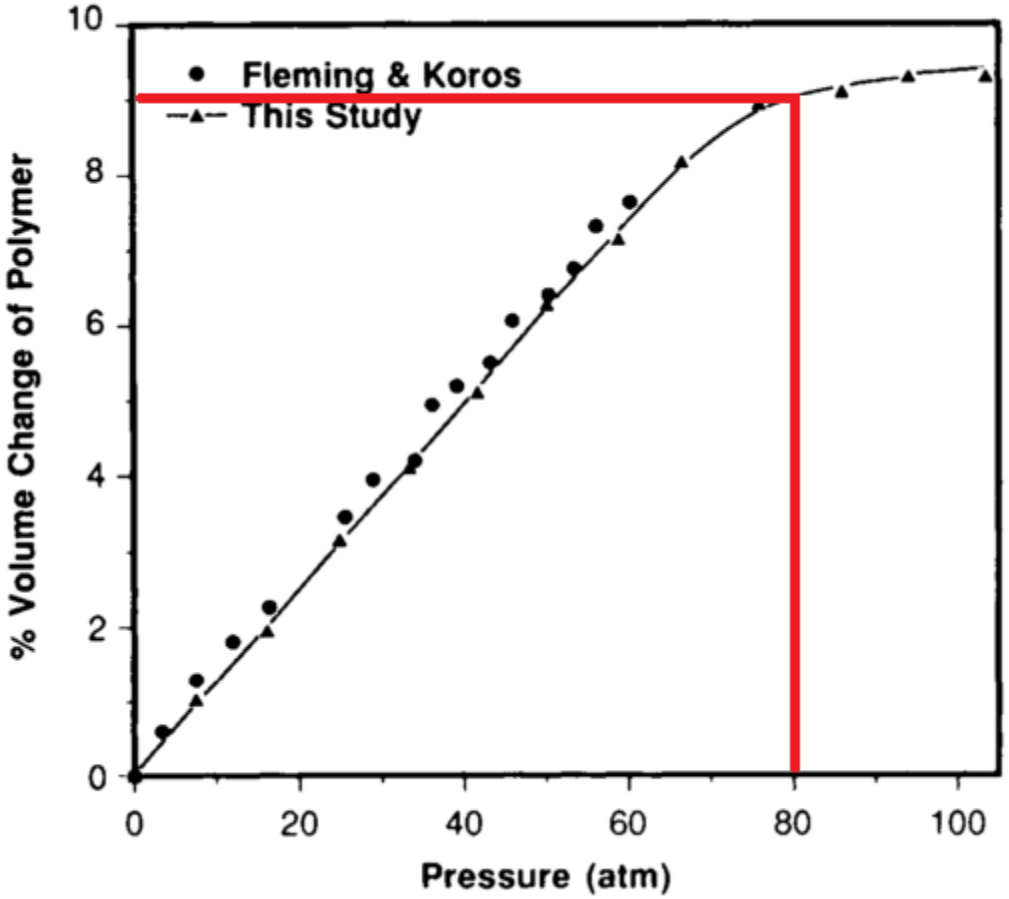

Figure 2-7 Swelling of PC in the presence of CO_2 at 35°C and elevated pressure [22]

Figure 2-7 illustrates the percent change in the volume of the polymer sample versus pressure for two different experiments [22]. The swelling isotherm is essentially linear with pressure up to approximately 80 atm (≈81.06 bar) [22].
The red line shows the point where the supercritical phase of the CO_2 begins. The measured volume change of polycarbonate is constant at around 9% from 80 to 100 atm.

For certain applications, swelling of polymers provides some advantages. There are many examples available in the literature, where the change of polymers' properties caused upon swelling was beneficial. Main examples are producing polymer foams by the use of $scCO_2$, modification through impregnation with dyes or drugs, in-situ polymerization and blending, and viscosity reduction which facilitates the processing of polymer melts [23].

2.6.2 Mass transfer, diffusion and solubility

The mass transfer of large molecules into a polymer matrix involves the coordinated motions of the impregnation material and segmental motions of the polymer chains [24].

Generally speaking, by increasing the temperature and pressure, the diffusion of the $scCO_2$ within polymer matrices can be enhanced.

Regarding solubility and diffusion coefficients of high- pressure CO_2 in polymers, Sun *et. al.* (2014) determined, that in polycarbonate the saturated solubility of $scCO_2$ increased with increasing temperature [20]. Furthermore, under some conditions the solubility decreased with time after showing maximum solubility at a constant sorption temperature and pressure, whereas this resulted from crystallization of the PC [20]. This crystallization occurs due to the plastification effect of dissolved CO_2. Moreover, when the polycarbonate sample was not yet crystallized, the diffusion coefficient increased with an increase in the sorption pressure of carbon dioxide at each temperature [20]. This observation is illustrated in Figure 2-9. The sorption isotherm in Figure 2-8 shows a qualitatively similar dependence on pressure, but is slightly concave downward at low pressure [22].

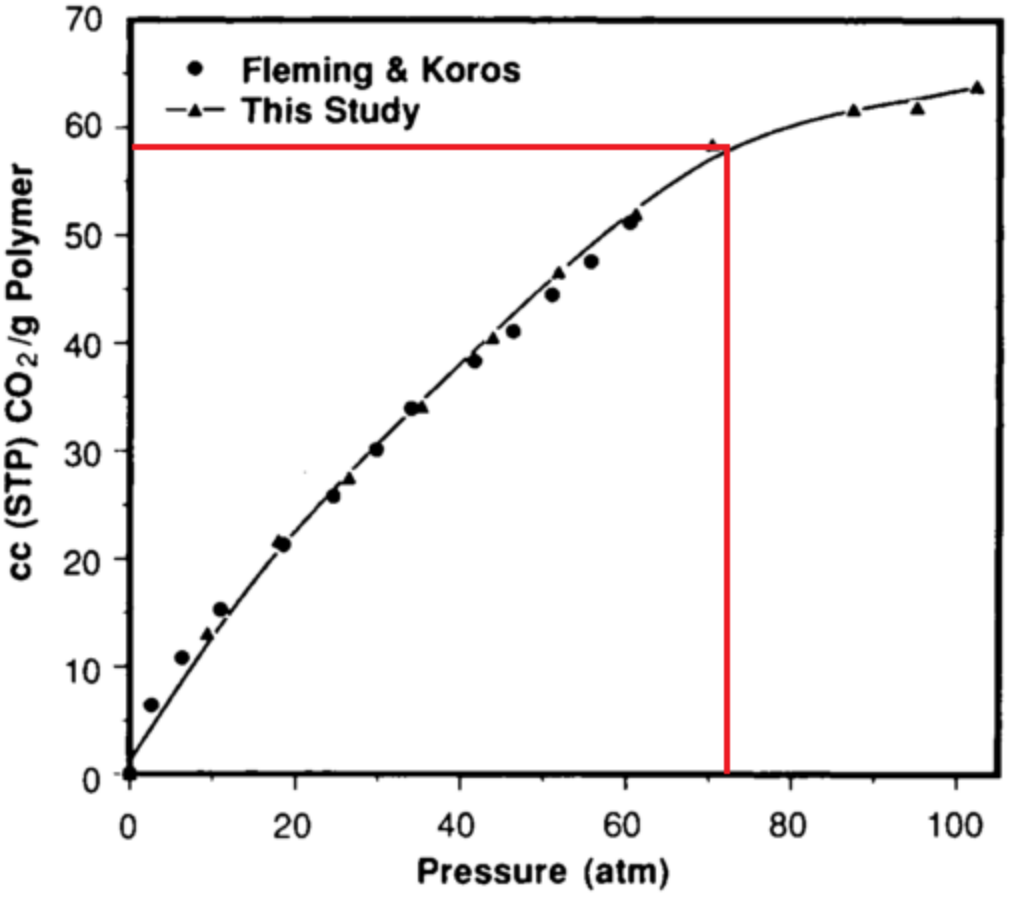

Figure 2-8 Sorption of CO_2 in PC at 35°C and elevated pressure [22]

Regarding the solubility of CO_2 in polymers, Berens and Huvard (1989) stated that near-critical CO_2 behaves like a polar, highly volatile organic solvent when interacting with polymers [25] [26]. Whereas Shieh and Lin (2002) pointed out that the sorption process at or below P_c was mainly driven by the carbonyl groups (in ethylene-vinyl acetate). Above P_c it depends on the degree of crystallinity. The higher the degree of crystallinity, the lower the normalized CO_2 sorption concentration (cm^3 STP CO_2/mol of VA) in the polymer [27].

According to Kazarian *et. al.* (1996), the carbonyl - group of several polymer – systems acts as electron donor and exhibits specific interactions of CO_2 as electron acceptor rather than electron donor [28].

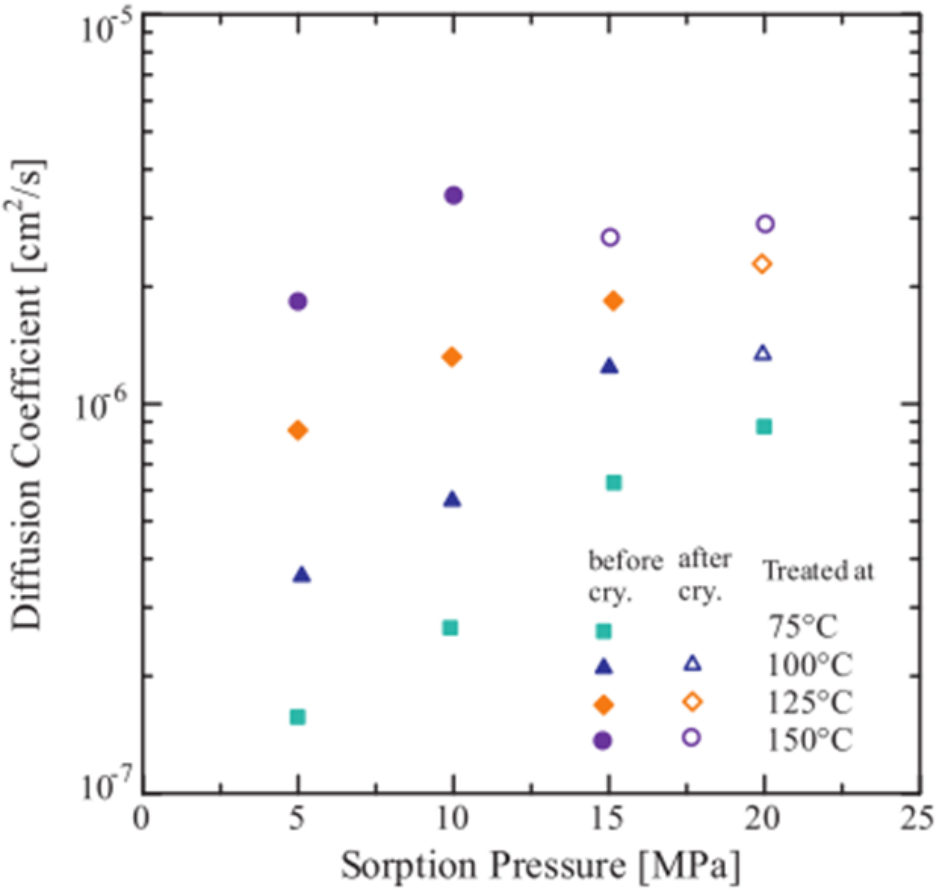

Figure 2-9 Diffusion coefficient of CO_2 in PC [20]

2.6.3 Phase equilibrium between CO_2 and polymer

The interaction between CO_2 and a polymer is rather complex and could not yet be described with an accurate mathematical model. This is not surprising, as equilibrium behaviour differs from one polymer to another. The current state of understanding this equilibrium is, that chain flexibility aids dissolution and e.g. carbonyl groups accessible in the backbone or on side chains can specifically interact with CO_2 [26].

2.7 Nanoclusters:

Nanoclusters have a size of 1 - 50 nm in diameter (or at least one dimension) and contain a vast number of atoms. The electronic, magnetic, and optical properties of nanoclusters (nanocrystals) are size-dependent. In small nanocrystals, the electronic energy levels are not continuous as in the bulk but discrete, due to the confinement of the electron wave function to the physical dimensions of the particle [14].

Synthesis of e.g. Ag, Au, Co or Pt nanocrystals is possible by employing soft templates in a reverse micelle, by embedding nanoparticles in a layer of ligand or stabilizing agents and laser ablation.
By controlling the reaction temperature and reagent concentration influencing the nucleation, growth, and termination of nanocrystals is possible. The properties of such metal nanoparticles are various. An example is the ability of Cu, Pt, Pd, or Ni nanoparticles to absorb CO and perform a catalytic oxidation of CO into CO_2.

2.8 Chemical compounds

2.8.1 Copper:

This transition metal is a light red, soft but viscous solid. It crystallizes in cubic close packing and appears in five different oxidation states (+II is the most common). It features many properties e.g. a high electric and a high thermal conductivity. Due to these characteristics, copper is used in a variety of applications. Moreover, its alloys with zinc (brass) and with tin (bronze) are used for coins, coating etc. Another feature is its biostatic. Bacteria and many other forms of organisms cannot grow on it. This property is used for many application e.g. toilet hardware, computer keyboards, health club equipment, and shopping cart handles [29].

Copper is the most frequent of the coin metal with $5 \cdot 10^{-3}$ wt% in the geosphere. It is present in nature mostly as oxides, sulphides and carbonates. For its production, mostly the sulphides are mined and melted-metallurgical manufactured. Another source for copper is recycling of scrap metal [29].

2.8.2 Carbon dioxide CO_2

Figure 2-10 Structure of carbon dioxide

Carbon dioxide is a colourless and odourless gas, which is found naturally in the earth's atmosphere as a trace gas at a concentration of about 0.04 percent by volume. Its molecular weight is 44.01 g/mol. Some physical properties of carbon dioxide are: ρ=1.997 g/L (0°C), melting point -57°C (5,158 bar), sublimation point -78.5°C and PEL (permissible exposure limit) of 9000 mg/m^3.

Several natural sources include volcanos, geysers, hot springs or metabolization of carbohydrate and lipids for energy production and respiration in aerobic organism. Most of the carbon dioxide is produced by combustion of carbonaceous substances.

CO_2 is used in many applications, e.g. in food industry as an additive, as precursor to chemicals, inert gas, fire extinguisher, as supercritical fluid etc. The supercritical point of CO_2 is described on page 3. Some of the advantages for the use of CO_2 are, that it is non-toxic, non- flammable and non- explosive. CO_2 is well soluble in water and forms carbonic acid, whereas this formation is favoured under high pressure.

Most of the carbon dioxide is transformed into sugar and oxygen by plants. Other parts remain in the atmosphere or dissolve in the sea.

The so-called carbon circle describes production and decomposition of this compound. The carbon dioxide for the experiments was obtain by Linde Gas and has a purity of >99.5 %.

2.8.3 Polycarbonate

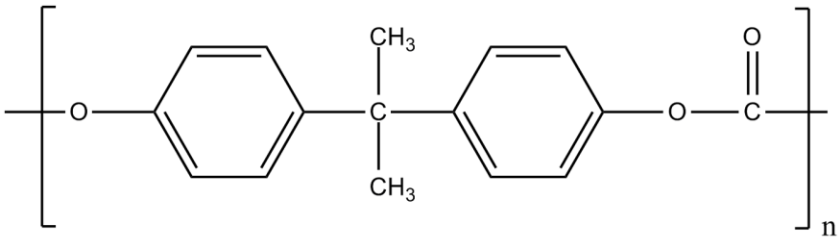

Figure 2-11 Structure of Polycarbonate

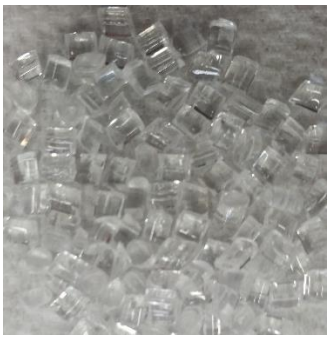

Figure 2-12 pure and transparent polycarbonate

The polycarbonate LEXAN Resin 121 kindly provided by the Saudi Arabian Basic Industries Corporation (SABIC) with a cylindrical particle size of approximately 3-4 mm was used as raw material for the experiments.

Polycarbonate is a thermoplastic, mostly amorphous polymer, which is a polyester of the carbonic acid containing a carbonate group. Regarding its characteristics, the polymer has a high stiffness, high strength, hardness and impact resistance. Moreover, it is a good insulator (S= $1.0^{17}\Omega\cdot cm$) and has low thermal conductivity (1.25 $\frac{Jg}{°C}$) [30].

In reference to its chemical resistance, polycarbonate is not soluble in water, oils and grease, but well soluble in haloalkanes (e.g. DCM), alkali water solutions, amines and ammonia [31].

The polymers T_G at atmospheric pressure is between 140 and 150°C and flows above 155°C. Referring to the company's data sheet the present polymer's glass transition temperature lies at 145°C [32]. At this temperature, a reversible transition in amorphous materials from a hard state into a molten or rubber-like state takes place.

Concerning its production, polycondensation between a diol (e.g. bisphenol A) and phosgene ($COCl_2$) is most widely used for its preparation. Typical processing techniques are injection moulding and extrusion into tubes. Typical applications are data storage likes CDs, as well as construction material e.g. domelights, medical applications, components in phones and several special applications.

2.8.4 Dithizone

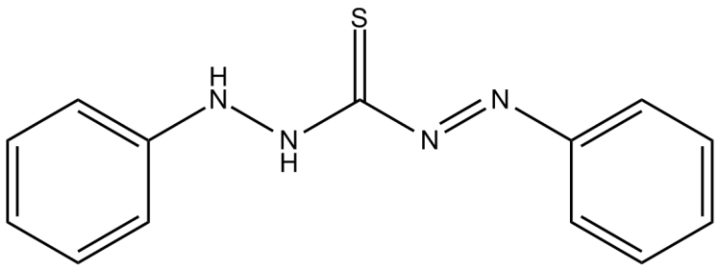

Figure 2-13 Structure of dithizone

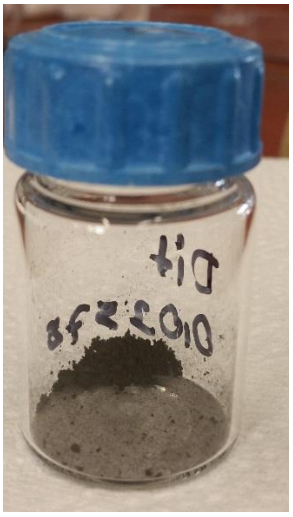

Figure 2-14 Pure dithizone

Diphenylthiocarbazone is a violet-black crystalline powder, which is an excellent chelat ligand for the formation of complexes with a variety of heavy metals. One method for its preparation is the reaction of phenylhydrazine with carbon disulphide. The final formation dithizone results from the dehydration of the intermediate diphenylthiocarbazide.

Regarding its solubility, dithizone is insoluble in water and inorganic acids, slightly soluble in ethanol and hydrocarbons and well soluble in haloalkanes.

In basic solution, dithizone is yellow in colour and present as completely dissociated alkali metal dithizonate.

In aqueous solutions, dithizone acts as a monobasic acid (Reaction 1), while the second hydrogen cation is removed at a pH above 12 (Reaction 2).

$$H_2Dz \rightleftharpoons H^+ + HDz^-$$ Reaction 1

$$HDz^- \rightleftharpoons H^+ + Dz^{-2}$$ Reaction 2

Based on a strong absorption in the visible light region, which metal dithizone complexes have, dithizone is used for determining trace metals via spectrophotometric and colorimetric measurements. Furthermore, dithizone is used for extractive titration as well.

2.8.4.1 Dithizonate complexes and their formation:

For the reactive group of dithizone two different forms are present, the enol and keto form. Heavy metals can replace either one or both hydrogen atoms. This leads to the formation of two different complexes:

- primary (monobasic or keto)
- secondary (dibasic or enol)

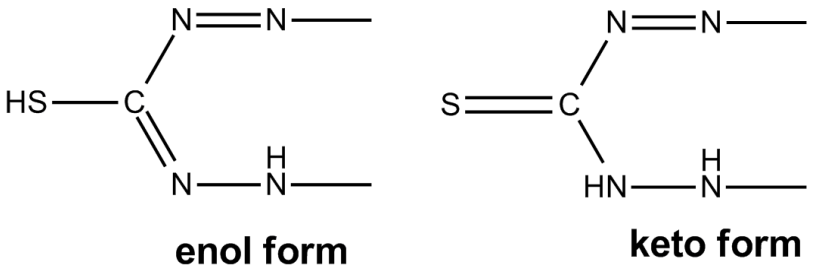

Figure 2-15 Enol and keto form of dithizone

Secondary dithizonates are less stable and less soluble in organic solvents than primary dithizonates. Furthermore, only few metals form secondary dithizonates. Regarding the formation of the complexes, primary dithizones are preferentially formed in acidic solution, whereas the secondary ones are formed preferably in alkaline media or with a deficiency of dithizone [33]. One further preparation method for the secondary dithizonates is the acidic treatment of the primary complex and its transformation into the secondary form. Figure 2-17 illustrates the bonding between two dithizone molecules and a metal.

Examples for such dithizonates are with copper, iron, nickel (violet in colour), zinc and lead (red in colour) or mercury, which is yellow in colour. Depending on the respective literature, dithizone is known to react with 20 to 35 metals [33] [34]. Figure 2-16, illustrates in continuous lines, metals that form stable dithizone complexes are.

Mn	Fe	Co	Ni	Cu	Zn	Ga	Ge	As	Se
Tc	Ru	Rh	Pd	Ag	Cd	In	Sn	Sb	Te
Re	Os	Ir	Pt	Au	Hg	Tl	Pb	Bi	Po

Figure 2-16 Metals that form dithizone complexes [35]

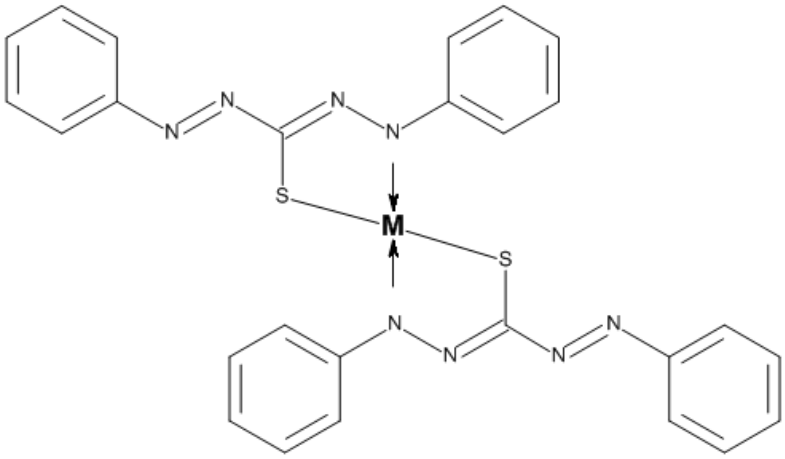

Figure 2-17 Bonding between two dithizone molecules and a metal X

Two copper dithizonate complexes were used for the experiments. Copper (II) forms two types of complexes with dithizone, whereas their composition depends on the pH of the aqueous phase during the preparation and on the relative concentration of the used components. For further information for the preparation of the two complexes, see chapter 3.5.

2.8.5 Primary copper(II) dithizonate

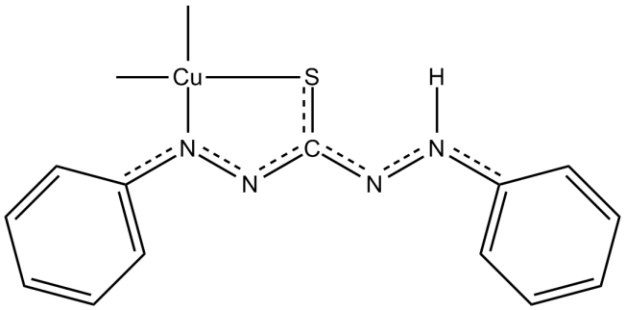

Figure 2-18 Proposed structure of primary copper(II) dithizonate [34]

The primary form of the Cu(II) dithizones is violet-black in colour. In comparison to the secondary form of this complex, the primary form is more stable and has a greater importance [33]. Primary Cu(II) dithizone is preferentially formed in acidic solutions.

Furthermore, it is possible to transform the secondary form to the primary form of this complex by treatment with acids. The crystalline powder is insoluble in water, partly in ethanol and good in chloroform and dichloromethane.

Figure 2-18 illustrates the primary form of Cu(II) dithizonate, where one H atom of dithizone is removed and the ligand has a denticity of two.

2.8.6 Secondary copper(II) dithizonate

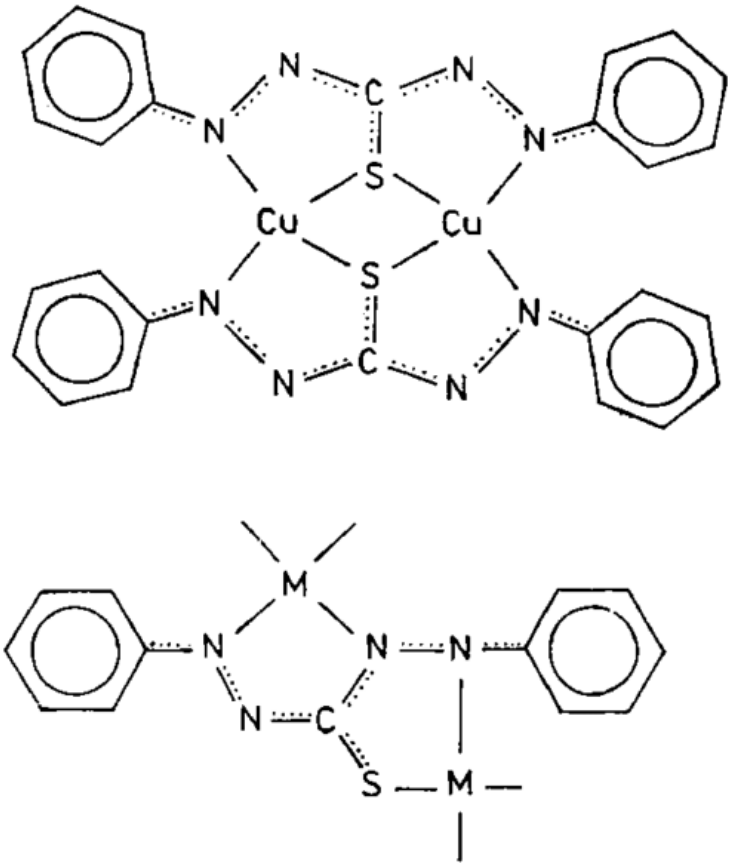

Figure 2-19 Proposed structure of secondary copper(II) dithizonate [34]

Secondary copper(II)dithizonate is brown in colour and contains copper and dithizone in the molecular properties 1:1 [36]. The complex is preferentially formed in alkali solutions. Figure 2-19 illustrates the proposed structure of secondary copper(II) dithizonate, whereas its structures has led to many debates [36]. In the secondary form 2 H atoms are removed (the thiol- and imino-protons) and the ligand has a denticity of four via the N -atoms.

The crystalline glittering powder is insoluble in water, partly in ethanol and good in chloroform and dichloromethane. The melting point of the secondary copper(II) dithizonate complex is between 198 and 200°C [36]. This temperature lies above the glass transition temperature of PC of approximately 143°C. By thermal reduction of the polymer sample and releasing of Cu, secondary copper(II) dithizonate was an ideal candidate for impregnation.

For the synthesis of these two complexes, see chapter 3.5.

2.8.7 Hexafluoroacetylacetnatecopper (Cu(II)(hfac)$_2$)

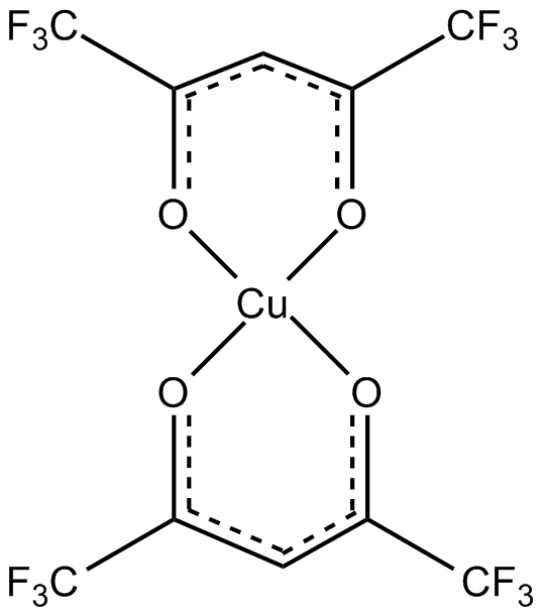

Figure 2-20 Structure of hexafluoroacetylacetnate- copper

Hexafluoroacetylacetnatecopper is an unsaturated complex, which is purple in colour and green in its hydrate form. Both forms are solid powders. The molecular weight of this complex is 477.65 g/mol for the anhydrous form and its melting point is between 130 - 134°C. Since Cu(hfac)$_2$ has a high solubility in supercritical CO_2 with $1.520 \cdot 10^{-3}$ mol complex/ mol CO_2 at 103.4 bar and 40°C, it has been used in many applications for depositing Cu films on polymers [37]. Regarding its solubility Cu(hfac)$_2$ dissolves in alcohol and ketones.

2.8.8 Copper salts:

For the experiments, three different copper salts were used and their properties studied and compared. The salts served as copper source for the experiments.

2.8.8.1 Copper(II) nitrate trihydrate $Cu(NO_3)_2 \cdot 3\,H_2O$

Copper(II) nitrate is an inorganic compound, which forms deep blue crystals. Five different hydrates exist, of which the trihydrate and hexahydrate are the most common ones. Some of its properties are: 187.56 g/mol (anhydrous form) 241.60 g/mol (trihydrate form),

decomposition at 256 °C (anhydrous), while the salt decomposes at lower temperature, the more water is bound.

Regarding the solubility of its hydrate forms in water: trihydrate: 381 g/100 mL (40 °C) and hexahydrate: 243.7 g/100 mL (80 °C) in water. One of its major applications is the conversion to copper(II) oxide, which is used as a catalyst. Moreover, its solutions are used in polishing agents for metals and in textiles. The copper(II) nitrate trihydrate for the experiments was obtained by Sigma- Aldrich >99.9%.

2.8.8.2 Copper(II) sulphate petahydrate $CuSO_4 \cdot 5\ H_2O$

Copper(II) sulphate is an inorganic, grey- white powder, which is very well soluble in water and forms bright blue pentahydrates. The hydrate loses two water molecules at 63°C, two more at 109°C, the last water molecule at a temperature of 200°C. The decomposition temperature is at around 560°C. The compound is used for producing copper containing dyes, fireworks and herbicide, fungicide and pesticide. Moreover, copper(II) sulphate has toxicological effects, e.g. anirritating effect on the gastrointestinal tract and on basis of its good solubility in water, contaminations of the environment occur rather easily.

The copper(II) sulphate was obtained by Sigma- Aldrich >99.9%.

2.8.8.3 Copper(II) chloride $Cu(Cl)_2$

Is a brown solid, which forms a blue- green dihydrate. The compound is well soluble in water, but also dissolves in organic solvents like ethanol or methanol. Copper(II) chloride is used as Cu- catalyst in the Wacker process, as catalyst in production of chlorinde and several organic synthetic applications. One possible preparation method of this salt is the chlorination of copper.

The copper(II) chloride was obtained by Sigma- Aldrich >99.9%.

3 Experimental

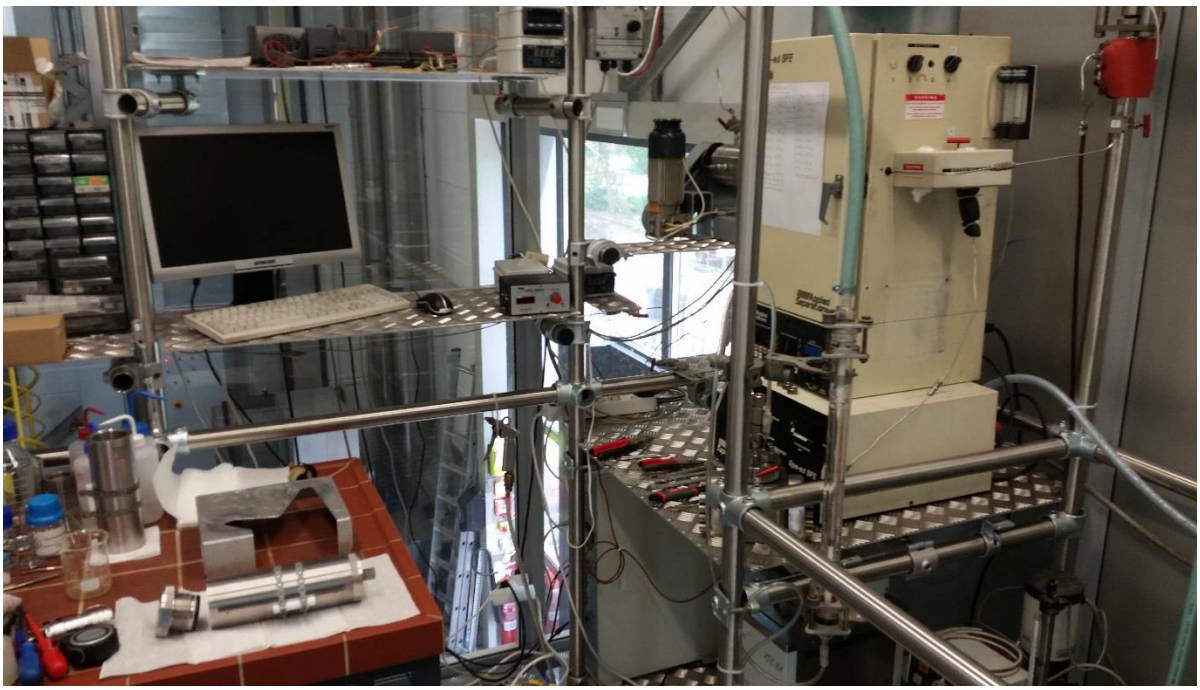

Figure 3-1 Experimental set-up

Figure 3-1 illustrates the experimental set-up including most parts of the equipment. The pressure facility is located at the Graz University of Technology, Institute of Chemical Engineering and Environmental Technology.

The following chapter presents the experimental set-up and explains the procedures and processes used for these experiments.

Moreover, the most important chemical compounds and the analytical background are going to be introduced and explained.

3.1 Equipment for the impregnation process

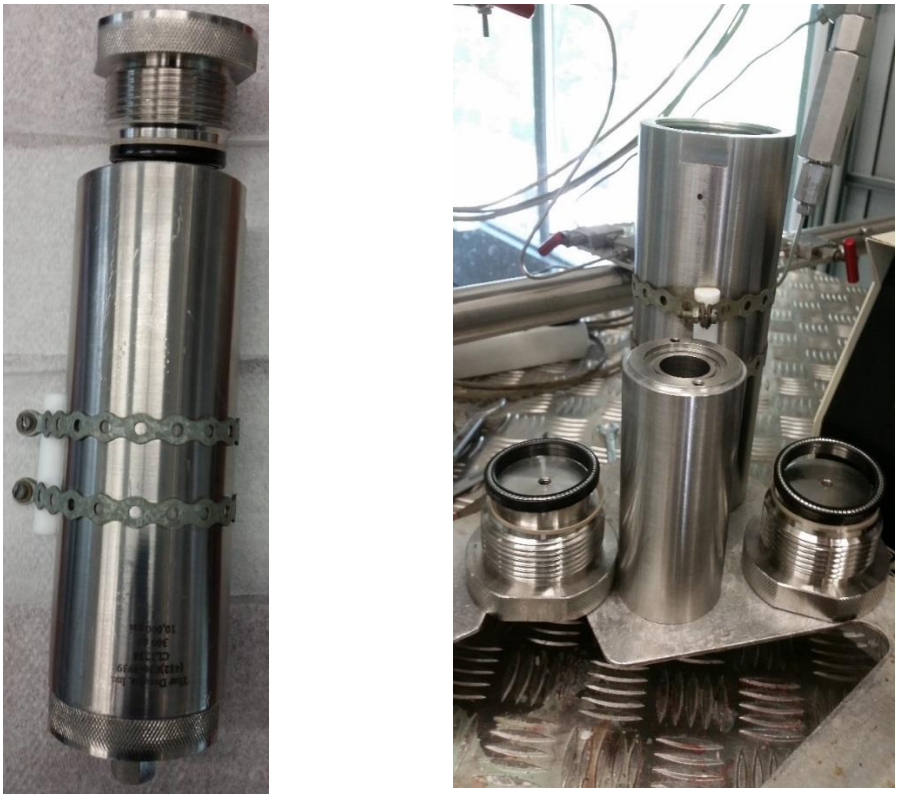

Figure 3-2 High pressure vessel with cylindrical inlet

Name	Thar Design, Inc.
Volume [ml]	~300
Height (excluding 2 caps) [mm]	213
Height (including 2 caps) [mm]	235
Diameter [mm]	76
Pressure range	up to 10,000 Psi (~690 bar)

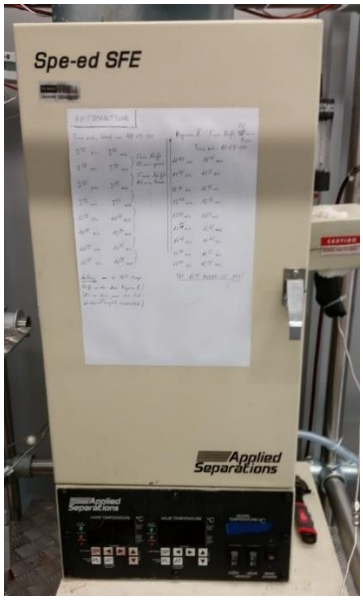

Figure 3-3 Heating chamber and valve for depressurization

Name	Spe-ed SFE by Applied Separation USA	**Name**	Kämmer Typ KA by Flowserve Ltd.
Temperature range [°C]	Up to ~250	**Supply air [bar]**	3
		Temperature range [°C]	-40 to 80

Figure 3-4 Gear pump and the high pressure pump used for the experiments

Name	Spe-ed SFE by Applied Separation USA
Pressure range	up to 10,000 Psi (~690 bar)

The gear pump (Figure 3-4) was developed by the ETH Zurich, Switzerland and home -made according their design and description.

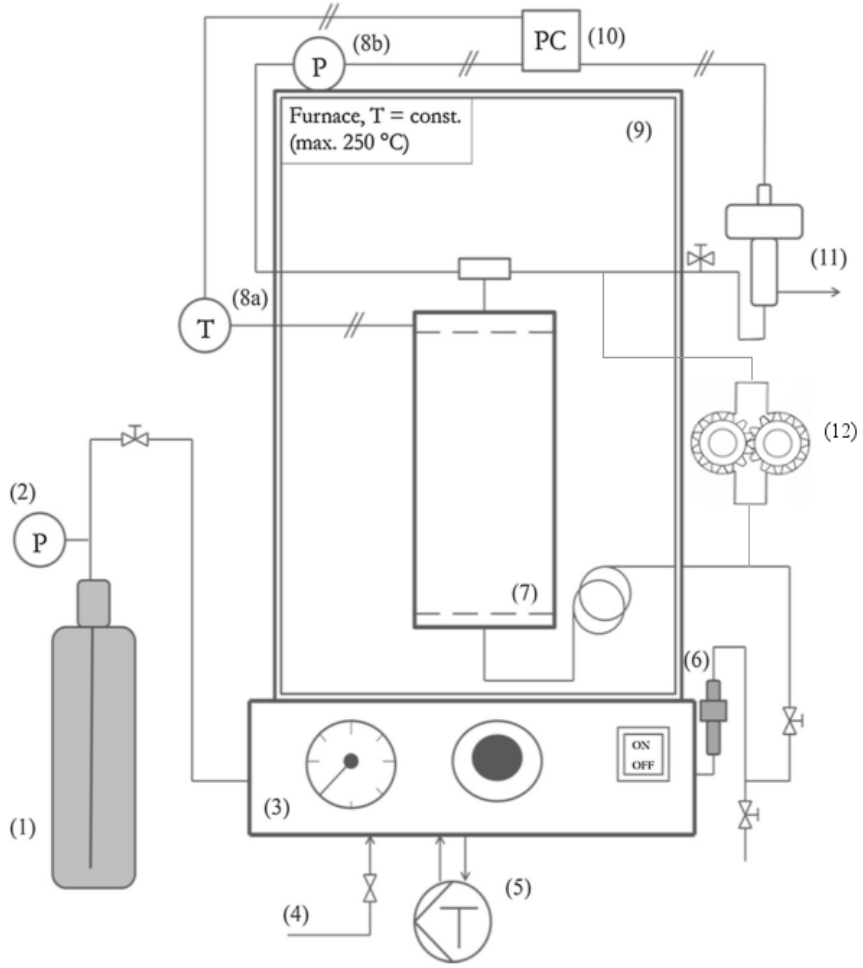

Figure 3-5 Experimental setup for the impregnation process [38]

The liquid CO_2 is stored in cylinders (1), which are equipped with a dip tube and a manometer (2) in a safety box (not pictured). To enter the system, the CO_2 flows from the cylinder with a pressure of 50- 55 bar to the liquid CO_2 pump (3 and Figure 3-4). The liquid CO_2 pump operates with pressurised air up to 5 bar (4) and is cooled to 5- 7°C by a recirculation cooling bath (5) in order to maintain CO_2 in liquid form.

Compressed CO_2 leaves the system through a check valve (6) and flows either to the view cell (not shown here, see Figure 3-6) or into the high-pressure vessel (7, Figure 3-2). By this, the vessel can be pressurized to the desired pressure To obtain isothermal conditions, the vessel is placed in an insulated furnace (9, see Figure 3-3), which can be heated up to 250°C. Pressure and temperature are monitored by indicators (8a) and (8b). A gear pump (12, Figure 3-4) connected to the high pressure vessel, allows cycling of $scCO_2$ at given pressure and temperature values and increases mixing effect. The metering valve (Figure 3-3) is connected to the computer (10) via an interface (not pictured), which allows controlling the depressurization process. This step is essential at the end of the impregnation process to achieve an unique and controlled pressure decrease. The obtained data are transmitted and saved by the computer (10).

3.2 High-pressure view cell

Figure 3-6 High- pressure view cell in water bath and in closed condition

For studying the solubility of the complexes a high- pressure view cell was installed. For the preparation, the sample was first inserted into a vial and then into the cell. After closing of the cell and connecting to the CO_2 pipes, it was filled with 4 – 5 bar of pressure. For mixing within the high-pressure view cell, a magnetic stirrer was placed below the cell. To obtain isothermal conditions, the cell was placed in a water bath whose temperature was controlled by a thermostat. After reaching the operating temperature (usually 40 – 50°C), the cell was pressurized up to 100 bar.

Once the desired pressure had been reached, the solubility of the sample was observed via a small view glass. To depressurize the cell, an outlet needle valve was opened. Thus, no controlled decompression was applied this time.

3.3 Analytical set-up

For the analysis of the products and to determine the copper content different analytical setups were used. The combination of these methods indicated the impregnation success:

- ICP-OES
- ICP- MS
- SEM- EDX
- UV- VIS

3.3.1 Inductively coupled plasma optical emission spectrometry – ICP-OES

ICP-OES is a type of emission spectroscopy, which used for the determination of trace metals up to a concentration of ~ 4mg/kg (4 ppm). To produce excited atoms and ions that emit electromagnetic radiation as so called inductively coupled plasma (ICP) is used, while a flame with a temperature in a range from 6,000 – 10,000K is produced. The emitted electromagnetic radiation has a characteristic wavelength for a specific element. For further information, regarding this analytical technique the author recommends Modern Analytic Chemistry by Harvey, David (2000).

For the determination of the copper content, the polycarbonate matrix had to be prepared. For this a microwave (Anton Paar Multiwave 3000 SOLV) assisted digestion in HNO_3 (subb)/HCl (Suprapur, Merck) was used. After further preparation and dilution, the copper content was determined with the ICP-OES (Spectro Ciros Vision FVE 12).

With this technique, the total copper content of the impregnated material was measured.

The analysis of the products was carried out at the Institute of Analytical Chemistry and Food Chemistry (ACFC) at the Graz University of Technology.

The measurements were carried out by Dipl.-Ing. Dr.techn. Wiltsche.

3.3.2 Inductively coupled plasma mass spectrometry - ICP-MS

ICP-MS is a type of mass spectroscopy, which is used for the determination of metals and non-metals up to detection limit below a ppb (ng/g).

The method (ICP) for ionization of the atoms is the same as has been used for ICP-OES. In contrast to the OES technique, the ionized sample is separated and quantified using a mass spectrometer, usually a quadrupole. Moreover, in comparison to OES this method has many advantages e.g. better precision and sensitivity. The preparation was the same as for the ICP-OES technique.

The analysis of the products was carried out through the Institute of Analytical Chemistry and Food Chemistry (ACFC) at the Graz University of Technology.

The measurements were carried out by Dipl.-Ing. Dr.techn. Wiltsche.

3.3.3 Scanning electron microscope SEM

With the SEM technique it is possible to produces images of e.g. polycarbonate samples by scanning them with a focused beam of electrons. The electrons enter the samples surface with an energy of 0.5- 30 kV and interact with the atoms of the sample, producing low energy secondary electrons. With this signal, (secondary electrons) information about the sample's surface topography and composition with a resolution better than 1 nm can be obtained.

The goal using this method was to determine possible copper deposits within the polymer matrix and to observe the penetration depth of the copper ions. Moreover, it was essential to determine the particle size and distribution.

For the analysis, the samples had to be prepared by cutting the material with a diamond blade into a suitable shape. For better resolution, the polymer surface was covered with carbon powder.

The scanning of the polycarbonate samples was carried out in cooperation with FELMI Graz.

3.3.4 Energy-dispersive X-ray spectroscopy EDX

EDX is an analytical X-ray technique, which is used for determining the elemental composition of a sample. For the analysis, a high-energy beam of electrons, protons or X-radiation is focused into a sample, producing a characteristic X- ray emission spectrum.

Usually this technique is coupled with SEM constituting a method to identify the elemental composition of a defined spot on the samples surface.

The aim using EDX for the experiments was to obtain information about the elemental composition of the deposits within the polymer matrix.

Coupled with SEM, EDX does not need any further sample preparation.

The analysis of the polycarbonate samples was carried out at in cooperation with FELMI Graz.

3.3.5 Ultraviolet- visible spectroscopy (UV-VIS)

UV - VIS spectroscopy is a type of absorption spectroscopy, which measures the absorption of molecules in the electromagnetic spectrum between 200- 400 nm (UV) and 400- 800 nm (VIS). With the UV - VIS spectroscopy it is possible to measure the concentration of a chemical species. The shorter wavelength and higher energy radiation causes many organic compounds to undergo electronic transitions. By absorbing the energy from the UV or visible light one of the molecule's electrons jumps from a lower energy to a higher energy molecular orbit.

The mathematical background is described by the Beer- Lambert law, which states that the absorbance of a solution is directly proportional to the concentration of the absorbing species in the solution and the path length. Usually the path length is fixed, therefore it is possible to calculate the concentration of the absorbing species in a solution with the following formula:

$$A_\lambda = lg\frac{I_0}{I} = \varepsilon \cdot c \cdot L \qquad \text{(Equation 5)}$$

Where A_λ is the measured absorbance, I_0 is the intensity of the incident light at a given wavelength, I is the transmitted intensity, L is the path length trough the sample (usually 1 cm), c is the concentration of the absorbing species, and ε is the so-called extinction coefficient, which is unique for each species and wavelength. This method was used for the analysis of the total dithizone content of the polycarbonate sample. For the experiments UV- spectrometer UV- 1800 Shimadzu (Figure 3-7) was used.

Figure 3-7 UV- spectrometer UV- 1800 Shimadsu

Calibration curve for determination of dithizone concentration

For the determination of the dithizone content, the polycarbonate samples (DPC samples) were dissolved in DCM. The aim of this step was to decompose the polymer matrix and determine the total dithizone of the impregnated material. By preparation of solutions with well-defined dithizone content, a calibration curve was generated. After analysis of the polycarbonate samples and the solutions for the calibration curve, the dithizone content was calculated with linear regression and the Beer- Lambert law. For the dilution series, it is important to calibrate at such concentrations, where the assumed dithizone concentration of the polycarbonate sample is estimated. With recalculation/linear regression of the measured extinction and inserting in the calibration curve it was possible to calculate the dithizone content of the polycarbonate samples. The path length (the length of the cuvette) was 1 cm.

3.4 Impregnation process

3.4.1 Preparation of the equipment

The experiments began by switching on the insulated furnace and the cooling unit for the high-pressure pump. For the experiments, the temperature of the cooling unit was between 4-6°C and for the furnace between 50- 60°C, to preheat the vessel.

3.4.2 Preparation for the impregnation process

For the impregnation process, the vessel was filled with the polycarbonate sample and additives (e.g. solvent and complex). Two different inlets (Figure 3-9 and Figure 3-10) were used. After insertion of the inlets and the samples, the vessel was sealed and connected with the CO_2 lines. To gain an isothermal setting the insulated furnace was set to the final temperature for the experiments. In the meantime, the CO_2 pump was filled with a pressure of 50- 55 bar.

3.4.3 Filling of the vessel with CO_2 and impregnation

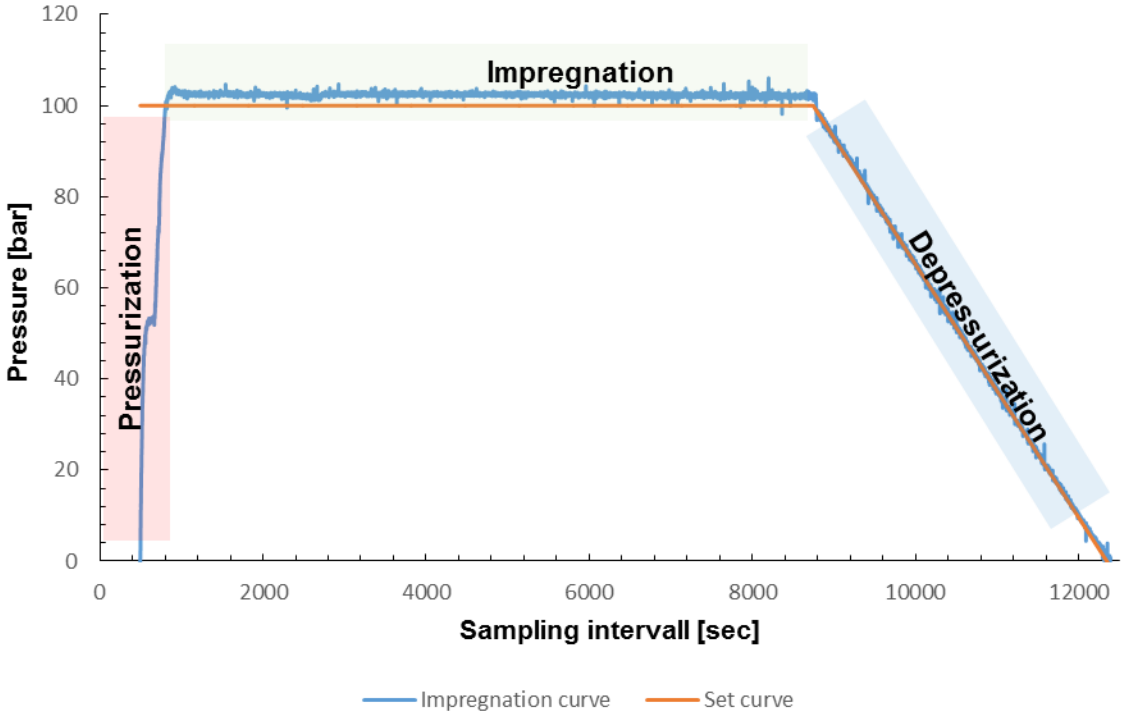

Figure 3-8 Impregnation curve of IM_14_2

At the required temperature, the valve, which connects the pump with the vessel was opened and the vessel is filled with CO_2 (red area in Figure 3-8). For the experiments, different pressures were adjusted, with the settings being regulated by the pump. After the desired

pressure was reached, the valves of the CO_2 connection to the vessel, the pump and the pressurised air to the pump were closed. From this point on the isothermal and isobaric conditions were controlled through a lab view program (LabView 7.0) (green impregnation area in Figure 3-8). To obtain a mixing effect inside the impregnation vessel the gear pump was switched on for most of the experiments. After the given impregnation time, depressurization of the system started, controlled by a Kämmer valve (blue area in Figure 3-8). By a linear depressurization curve, which was programed before this step, continuous pressure decrease was established. After full depressurization to atmospheric conditions and shut down of the system, the vessel was opened, emptied and carefully cleaned with ethanol.

Afterwards, the samples were cleaned with ethanol, air-dried and delivered for further analysis.

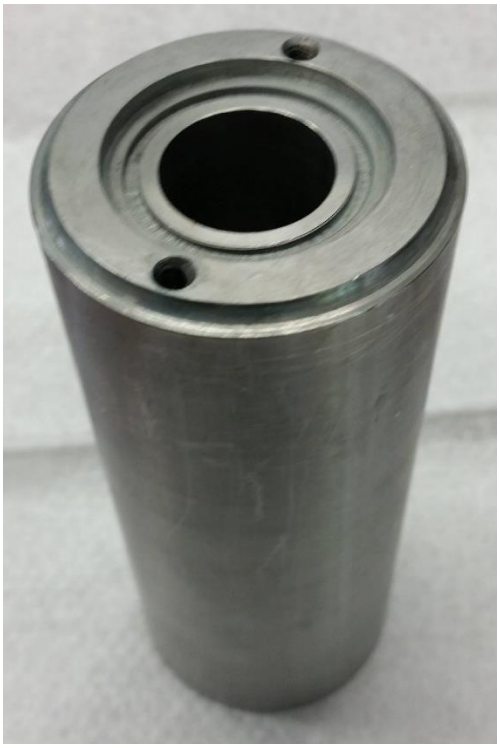

Figure 3-9 Cylindrical Inlet 1

Figure 3-10 Inlet 2 with grid

	Technical details Inlet 1	Technical details Inlet 2
Outer diameter [mm]	52	52
Height [mm]	130	103
Volume [mL]	~50	~140
Material	Stainless steel	Aluminium

3.5 Complex synthesis

Two different copper(II)dithizonate complexes were synthesized for the experiments (see chapter 2.8.4.1). Both synthetic routes were prepared by the method given by Irving and Kiwan [36]. As described earlier Copper (II) forms two types of complexes with dithizone, whereas their composition depends on the pH of the aqueous phase during the preparation and on the relative concentration of the applied components [36].

3.5.1 Secondary copper(II) dithizonate (CuDz)

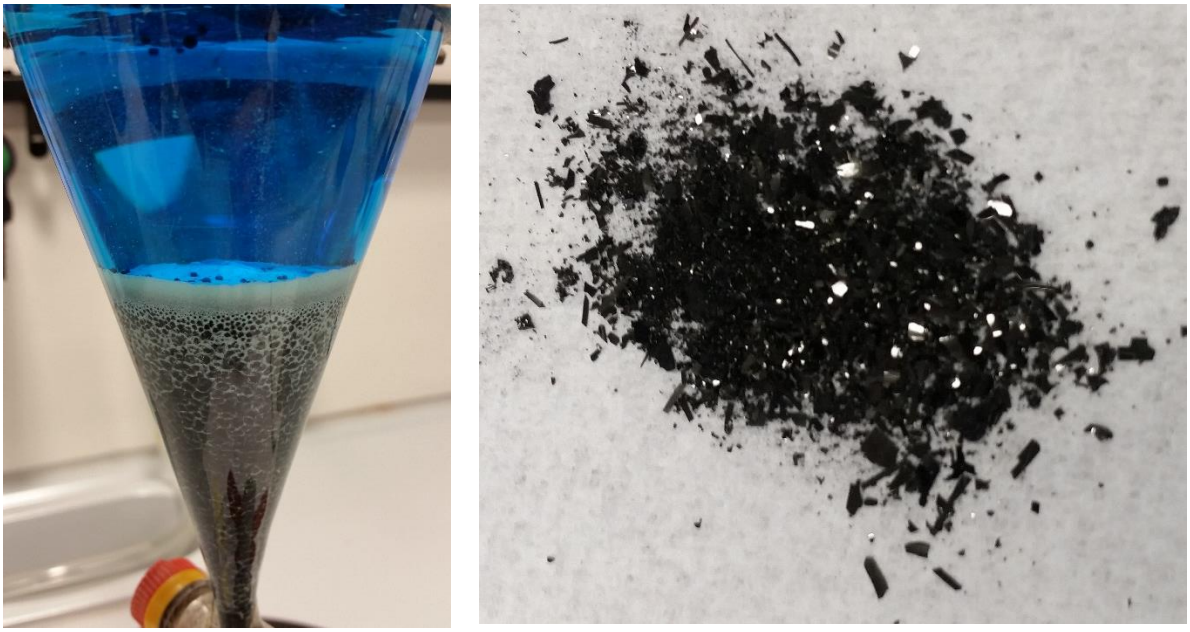

Figure 3-11 Raw product sec. copper(II) dithizonate and purified product

For the synthesis of this complex 25.01 g (≈0.1 mol) of copper sulphate pentahydrate ($Cu(SO)_4 \cdot 5H_2O$) were dissolved in 100 mL distilled water and 0.5 g (≈0.002 mol) of pure dithizone ($C_{13}H_{12}N_4S$) dissolved in 50 mL of chloroform (Merck, purity >99.9%). Both solutions were mixed and mechanically shaken. To obtain a pH of ca. 6 about 15 mL of an aqueous ammonia solution were added (Riedel-de Haën 33%).

Two phases (light blue upper phase and brown- black lower phase, with white spots Figure 3-11) were formed and transformed into a beaker. After 2 h stirring, the organic layer was withdrawn and washed 5 times with distilled water to remove the copper sulphate and copper hydroxide.

The black - violet solution was dried with anhydrous sodium sulphate and the solvent removed by suction in vacuum. The residue was washed in a few mL of hexane and dried by vacuum. The final product was dried for 1.5 h in a drying oven at around 90°C.

3.5.2 Primary copper(II) dithizonate ($Cu(HDz)_2$)

Figure 3-12 Raw product and purified product of the synthesis of primary copper(II) dithizonate

For the preparation of primary copper(II) dithizonate 0.5301 g (≈0.002 mol) of copper sulphate pentahydrate were dissolved in 50 mL of distilled water and 0,5 g (≈0.02 mol) dithizone in 50 mL of chloroform. These solutions were merged and few mL of hydrochloride (Roth, Rotipran 37%) were added to reach a pH of around 2.

The solution was stirred for 1 h and shaken for 10 min. For a clear separation of the two phases, the solution was left in the fume hood for two days to achieve complete sedimentation of the lower phase. The black - violet solution was separated, washed for several times with distilled water, dried with anhydrous sodium sulphate and the solvent removed by rotary evaporator in vacuum. A black - glittering powder was obtained. The synthesis of this complex was carried out twice, whereas the procedure for the second synthesis was changed. This change includes a higher sample weight for dithizone (1.0216 g/ ≈0.004 mol), in order to obtain more material for further impregnation experiments.

3.6 Systems used for impregnation

Four different methods were considered and investigated. The goal was to determine which method is the most effective one to impregnate a polymer matrix. Moreover, the parameters for the experiments were changed to define the most effective impregnation method. This includes changes of:

Table 3-1 Experimental parameters

	Range	Unit	Unit symbol
Temperature	40 – 50	Celsius	°C
Pressure	100 – 250	bar	bar
Impregnation-time	1 – 24	hour	h
Co- solvent	EtOH and Water	-	-
Salt	$Cu(NO_3)_2$, $Cu(SO_4)$, $CuCl_2$	-	-
Gear pump and period of use	0-50	minutes	min
Ultrasound	0 – 6	minutes	min
Milieu	Neutral and basic	-	-
Inlets	Cylindrical and with sieve	-	-
Depressurization	0.5 – 1	hour	h

Temperature: The temperature range for the experiments was between 40 and 50°C, whereas temperature has a great influence on the impregnation process. On the one hand, an increased temperature favours the solubility of additives, but on the other hand in connection with high pressure an increased temperature disfavours the physical properties of the polycarbonate (see chapter 2.8.3), including viscosity, permeability, interfacial tension, and glass transition temperature.

Pressure: The effects of increased pressure during the impregnation process are similar to an increased temperature. Pressure also has an effect on the solubility of the impregnation solute. The pressure range for the experiments was between 100 – 300 bar.

Time for the impregnation: The time for the impregnation process is essential for its success. On the one hand, CO_2 takes about 1 h to enter the polymer matrix, but on the other hand, an equilibrium and saturation is reached after a certain time [39]. Therefore, it is important to determine a suitable impregnation time for the process, which covers all requirements. Moreover, high-pressure over a long period of time, favours crystallization of the polycarbonate samples and crystallized polycarbonate is harder to impregnate [40]. The time range for the experiments was between 1 to 24 h.

Co-solvent: The main reason for using co-solvent was to increase the solubility of the additives in the system. Co-solvents which were used for the experiments were water and ethanol. The influence of solvent mixtures (e.g. water/ethanol with CO_2) were studied. Literature showed, that with co- solvents an increased diffusion coefficient of an additive over that with pure CO_2 can be achieved [2]. Adding of a co-solvent provides more controllable process parameters and allows the impregnation of thermally labile and metastable materials under lower temperature and pressure. However, addition of a co- solvent also favours crystallization of the polymer matrix, which is clearly limiting the applicable impregnation time. This crystallization phenomenon has to be avoided, since crystalline regions are hard to impregnate due to the anomalous behaviour of the polymer.

Moreover, water in combination of CO_2 gets acidic and forms carbonic acid:

$$CO_2 + H_2O \rightleftharpoons H_2CO_3 \rightleftharpoons H^+ + HCO_3^- \quad \text{Reaction 3}$$

This illustrates, that the pH of the solution is strongly influenced by adding co-solvents. The calculated and measured pH for a water/ supercritical CO_2 system varies between 2.80 and 2.95 (between a temperature of 25– 70°C and a pressure of 71– 202 bar) [41].

Several papers were published to determine the equilibrium between water-ethanol- CO_2 [42] [43]. Generally speaking, ethanol dissolves well in supercritical CO_2 and, poorly in water and therefore two phase are formed.

Applied copper salt: For the experiments different sources for copper were used. Examples were copper nitrate, copper sulphate and copper chloride. (see chapter 2.8) To choose a suitable salt, its solubility in CO_2 and the reaction between the copper salt and dithizone was important. Since most copper salts are poorly soluble in scCO_2 co-solvents (water and ethanol) were used. Moreover, the choice of the anion (e.g. nitrate) for the impregnation process was important (e.g. change of the pH can be obtained).

Gear pump: To achieve an increased mixing effect and for promotion of the equilibrium, installation of a gear pump was crucial. By stirring the solution, mass transfer in the fluid phase (which is controlled by diffusion) is enhanced. By this impregnation time could be remarkably reduced.
A further reason for using a gear pump was to reach better homogeneity on the impregnated samples. For reproducibility and for obtaining constant results, an excellent mixing is essential.

Ultrasound: An ultrasound device (Hielscher UP400S, Germany, P = 400 W, f = 24 kHz) was used to increase the dispersivity of additives in solvents. Sonication was performed at room

temperature at 100 % amplitude and 1.0 cycle. The solution was ice-cooled during the treatment. By the use of ultrasound, the formation of bigger clusters upon dissolution of the complexes in ethanol can be avoided. This is essential, because such big size aggregates cannot be impregnated due to steric effects.

Milieu: Acids and bases were added into the system to determine which pH was the most adequate for the process. One reason is the behaviour of copper salts in different milieus. The formation of copper dithizonates differ in acidic and basic environment, in particular, copper salts act differently at high and at low pH. To change the pH of the system acids (HCl/HNO_3) and bases (mostly KOH) were used. It has to be noted, that ions of the dissolved salts and cosolvents like water also had a major impact on the resulting pH of the impregnation solution.

Inlets: Two different inlets were used for the experiments. Thereby, the volume of the impregnation vessel and the arrangement of the polymer samples could be changed. For more information, see chapter 3.1

3.7 Four different systems for the impregnation process

3.7.1 Polycarbonate with Hexafluoroacetylacetnatecopper (Cu(hfac)$_2$)

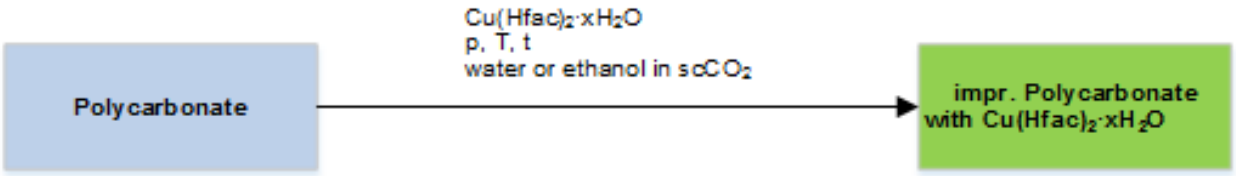

Figure 3-13 Schematic model of the polycarbonate hexafluoroacetylacetnatecopper process

Hexafluoroacetylacetnatecopper has many beneficial properties, which include good solubility in CO_2 ($1.520 \cdot 10^{-3}$ mol complex/ mol CO_2 at 103.4 bar and 40°C), long shelf life; high vapour pressure, easiness in handling and a variety of references. Generally speaking, β- diketonates e.g. Cu(Hfac)$_2$ dissolve well in $scCO_2$ [44]. The goal for this system was to use the good solubility and form aggregates within the polymer matrix directly. Similar to the following systems, different parameters were used, to investigate their effect on the impregnation. The sample weight for the polycarbonate was usually around 3 g. The sample weight for the complex was around 0.02- 0.05 g.

Table 3-2 Summary of polycarbonate with hexafluoroacetylacetnatecopper experiments

Experiment	Pressure [bar]	Temperature [°C]	Time [h]	Solvent	Inlet*	Sample weight copper [g]	Ratio PC to complex
IM_15	300	40	4	CO_2	1	0.003	1:155
IM_16	200	40	3	CO_2	1	0.007	1:60
IM_17	200	40	2	EtOH	1	0.007	1:60
IM_18	100	40	3	CO_2	2	0.007	1:60
IM_29	100	40	2	H_2O	1	0.006	1:47
IM_30	100	40	1	CO_2	1	0.005	1:50

* 1 for Inlet 1 and 2 for Inlet 2 with grid

For the experiments, IM_15 and IM_16 no gear pump was used.

3.7.2 Polycarbonate with copper(II) dithizonates (CuDz and $Cu(HDz)_2$)

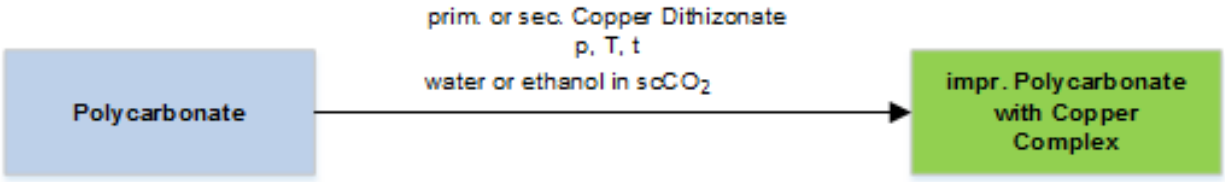

Figure 3-14 Schematic model of polycarbonate and copper dithizonate complex process

For this system, two different complexes were synthesized (see chapter 3.5). In a previous work it was found that dithizone has a good solubility in $scCO_2$. The assumption was that a copper dithizonate complex combines a good solubility in $scCO_2$, with a decent metal source. The goal was to achieve a successful insertion of the complexes into the polymer matrix. The assumption was, that both complexes are soluble in $scCO_2$ and after entering the matrix, copper complex aggregates within the polymer are formed. For the experiments primary copper(II) dithizonate and secondary copper(II) dithizonate were used. The secondary form has a poor solubility regarding $scCO_2$ (see chapter 4.2). As Figure 3-14 illustrates polycarbonate and the copper complex were placed in the vessel using two different inlets for the reactor. The experiments were carried out with changing parameters to determine the most efficient way for the impregnation.

Table 3-3 summarized the experiments carried out with the dithizonate complexes:

For the analysis of the products, ICP-OES and ICP-MS were used. For the experiments IM_31 and IM_36 a gear pump was used.

Table 3-3 Summary of the impregnation of PC with dithizonate complexes

Experiment	Complex	Pressure [bar]	Temperature [°C]	Time [h]	Solvent	Inlet*	Sample weight copper [g]	Ratio complex to PC
IM_5	sec.	200	40	6	CO_2	1	0.003	1:67
IM_6	sec.	150	40	3	CO_2/EtOH	2	0.002	1:139
IM_7	sec.	150	40	3	CO_2/EtOH	1	0.002	1:138
IM_8	sec.	150	40	3	CO_2/EtOH	2	0.002	1:136
IM_9	prim.	150	40	3	CO_2	1	0.002	1:136
IM_10	prim.	150	40	3	CO_2/EtOH	1	0.001	1:189
IM_12	prim.	150	40	3	CO_2/EtOH	1	0.001	1:170
IM_13	prim.	300	50	3	CO_2	1	0.002	1:133
IM_31	prim.	150	40	2	EtOH/H_2O/CO_2	1	0.002	1:110
IM_36	prim.	100	40	24	CO_2	1	0.017	1:14

* 1 for Inlet 1 and 2 for Inlet 2 with grid

3.7.3 *In situ* polycarbonate with dithizone and copper salt

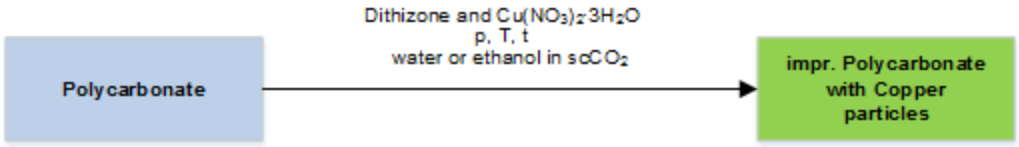

Figure 3-15 Schematic model of polycarbonate *in-situ* process

The aim for this system was an *in situ* formation of copper dithizonates during the process and a direct impregnation within the matrix. For this, accretion of dithizone within the polymer and an interaction of the copper ions of the salt with the dithizone occurred. For these experiments different co-solvents were added to the $scCO_2$. Similar to the previous system ICP-OES and ICP-MS were used to determine the total copper content. No gear pump was used in any of the experiments

Table 3-4 Summary of the in situ experiments

Experiment	Pressure [bar]	Temperature [°C]	Time [h]	Solvent	Inlet*	Sample weight copper [g]	Ratio salt to PC
IM_1	200	50	4	H_2O	2	0.026	1:20
IM_2	200	50	2	EtOH	2	0.005	1:101
IM_3	200	40	2	H_2O	1	0.342	1:1.5
IM_4	200	40	2	EtOH/H_2O	1	0.264	1:2

* 1 for Inlet 1 and 2 for Inlet 2 with grid

3.7.4 2- step process

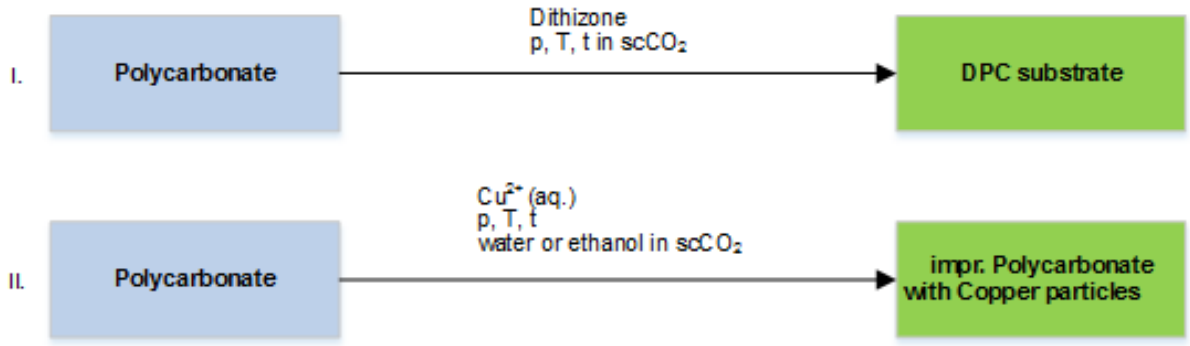

Figure 3-16 Schematic model of the 2- step process

For the 2- step process, polycarbonate was first impregnated with dithizone to produce so called DPC (dithizonized polycarbonate). The second step was the impregnation of DPC with a copper salt, whereas different parameters were investigated. Two approaches were important to study. On the one hand, the aim was to find the most efficient procedure to impregnate polycarbonate with dithizone. On the other hand, it was investigated under which conditions and parameters the impregnation of DPC with copper is favoured. Table 3-5 illustrates the summary of the different parameters used for the first step and

Table 3-6 shows a summary for the second step. For the experiments IM_24 and IM_28 a gear pump was used. According to observations carried out in the high-pressure view cell, it was found, that dithizone had a slight solubility in $scCO_2$. Therefore, one impregnation (IM_14) was performed without adding ethanol as a cosolvent to the system. However, by this, remarkably lower dithizone content in the PC matrix was achieved.

Table 3-5 Summary of the DPC prodction (first step)

Experiment	Pressure [bar]	Temperature [°C]	Time [h]	Solvent	Inlet*	Ratio PC. to Dit
DPC_1**	150	40	4	EtOH	1	-
IM_14/DPC_2	300	50	3	CO_2	2	1:67
IM_24/DPC_3	150	40	2	EtOH	1	1:132
IM_28/DPC_4	100	40	2	EtOH	1	1:121
IM_35/DPC:5	100	40	2	EtOH	1	1:116

* 1 for Inlet 1 and 2 for Inlet 2 with grid ** DPC_1 was prepared by Simon Alkin [38]

For the experiments IM_14_1 and IM_14_2 no gear pump was used.

Table 3-6 Summary of the second step

Experiment	DPC source	Solvent	Inlet*	Milieu	Sample weight copper [g]	Ratio PC to salt
IM_14_1	IM_14	EtOH	1	Neutral	0.078	1:5
IM_14_2	IM_14	H_2O	1	Basic	0.079	1:5
IM_20	DPC_1	H_2O	2	Basic	0.123	1:5
IM_21	DPC_1	EtOH	1	Neutral	0.119	1:5
IM_25	IM_24	H_2O	2	Basic	0.123	1:8
IM_26	IM_24	H_2O	2	Basic	0.121	1:4
IM_27	IM_24	H_2O	2	Basic	0.070	1:7
IM_32	IM_28	H_2O	2	Basic	0.086	1:6
IM_33	IM_28	H_2O	1	Basic	0.084	1:6
IM_34	IM_28	H_2O	2	Basic	0.087	1:6
IM_37	IM_35	H_2O	1	Neutral	0.097	1:6
IM_38	IM_35	H_2O	1	Acidic	0.080	1:6
IM_41	IM_35	H_2O	1	Basic	0.95	1:7

* 1 for Inlet 1 and 2 for Inlet 2 with grid

For all experiments 100 bar, 40°C and 2 h of impregnation time were used.

4 Results

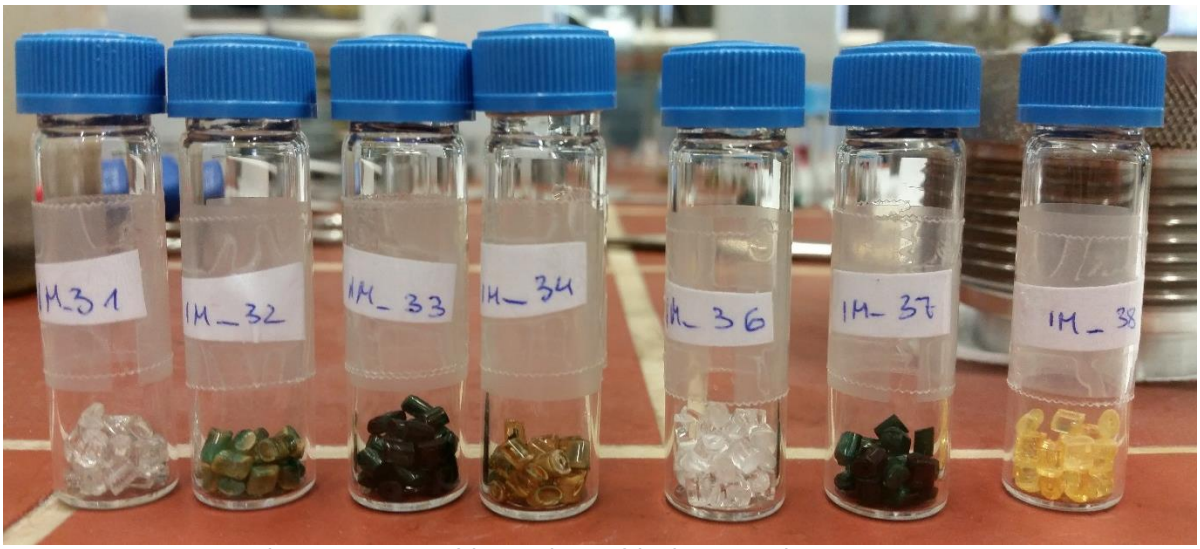

Figure 4-1 Some of the products of the impregnation processes

Different approaches were studied in order to achieve a successful impregnation of a polycarbonate matrix with copper nanoparticles. For this, four different systems were investigated. To measure the success of an impregnation process, two main parameters were introduced. Firstly, the total copper concentration within the polymer matrix determined by ICP-OES and ICP_MS.

And secondly, the distribution and visualization of copper aggregates within the polymer matrix, measured by SEM that was coupled to EDX.

4.1 Calculation of the efficiency of the impregnation process

For measuring the success of an experiment, its efficiency was calculated. For this, the total copper content (in g), which was inserted into the system via a copper salt or complex was determined, divided by the copper content inside the polymer matrix (after the impregnation process) and multiplied with 100 to obtain the percentage.

$$\frac{obtained\ Copper\ content\ after\ exp.}{total\ copper\ content} \cdot 100 = Efficiency \qquad \text{(Equation 6)}$$

4.2 Results of the high pressure view cell

To estimate the solubility of dithizone and the secondary copper dithizonate in $scCO_2$, both compounds were insert into the cell and dissolved under supercritical conditions.

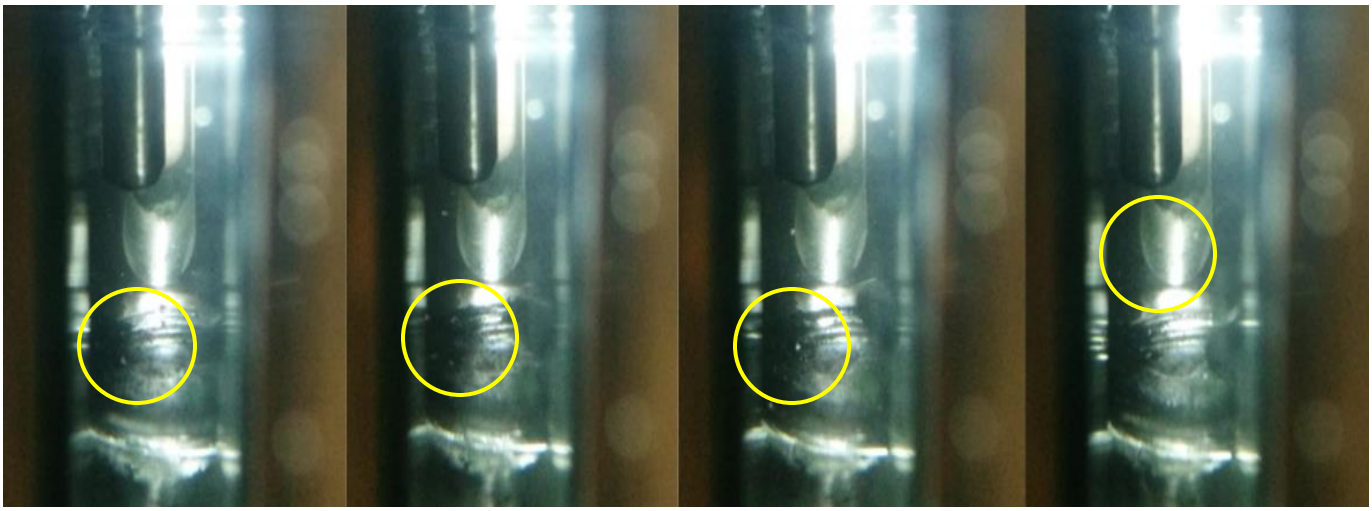

Figure 4-2 Secondary copper dithizonate in $scCO_2$

As illustrated in Figure 4-2 the secondary form of this complex did not dissolve in $scCO_2$. The small, bright points represent complex particles (yellow ring in figure above).

Residues of the complex within the vial confirmed this observation after the experiments were finished. For more information regarding solubility of this compound, more accurate measuring methods are necessary. Measuring the solubility and the dissolution kinetics of a given compound in $scCO_2$ is a complicated task and is out of the scope of this study.

Figure 4-3 Primary copper dithizonate in scCO2

Figure 4-4 Dissolved dithizone in scCO2

Similar results were obtained with the primary form of this complex (yellow ring). No dissolution was achieved with this complex. Dithizone (Figure 4-4) showed a very good solubility in $scCO_2$. After few minutes the fluid became lightly green, but mostly transparent, which indicates a nearly complete dissolution. The observation indicates suitable properties of dithizone for impregnation in $scCO_2$.

4.3 Results of the four impregnation processes

4.3.1 Polycarbonate with hexafluoroacetylacetonate ($Cu(hfac)_2$)

Six experiments with hexafluoroacetylacetonate were performed, whereas five samples were measured for their total copper content via ICP-OES. Figure 4-5 illustrates the products, which were obtained in IM_15 and IM_30. As the two figures demonstrate no change in colour within the polymer matrix occurred. Parts of the complex precipitated on the surface of the polymer. Whereas the residue of the complex changed in colour from yellow to white and a change of the complexes texture was observed to adhere. After cleaning of the product in ethanol most of the complex was removed from the polymer. Only small aggregates were still present on the surface. It is not totally clear, which sort of transformation occurred during the process.

Figure 4-5 Polycarbonate product IM_15

Table 4-1 Results for the hexafluoroacetylacetnate copper experiments

Experiment	Cu content [mg/kg]	Efficiency of impregnation [%]	Pressure [bar]	Temperature [°C]
IM_15	<LOQ	0.00	300	40
IM_16	5 ± 1	0.23	200	40
IM_17	<LOQ	0.00	200	40
IM_18	no data	no data	100	40
IM_29	<LOQ	0.00	100	40
IM_30	5 ± 0.7	0.19	100	40

As Table illustrates, IM_16 and IM_30 were the only successful experiments in this series with an efficiency of 0.23% and 0.19%. Both had a copper content of around 5 mg/kg, whereas the other experiments (IM_15, IM_17 and M_29) were under the limit of quantitation with 4 mg/kg for the ICP-OES. As Table 3-2 illustrates, IM_16 and IM_30 shared the same experimental parameters, except for pressure. Solvents like water or ethanol had no positive impact for the impregnation process with this complex. Moreover, although literature states that higher pressure, leads to better solubility results, pressure did not have any influence on the results.

The high solubility of hexafluoroacetylacetonate is one possible reason for a lack of finding copper aggregates within the polymer matrix. The complex enters and leaves the polymer matrix during the impregnation process, whereas none of the complex precipitates and forms aggregates within the matrix. Most of the complex precipitates during the depressurization on the surface.

4.3.2 Polycarbonate with copper(II) dithizonates

Figure 4-6 Polycarbonate product IM_5

Figure 4-7 Polymer product of IM_31

Table 44-2 Results of the polycarbonate with copper(II) dithizonates experiments

Experiment	Complex	Cu content [mg/kg]	Efficiency of impregnation [%]	Pressure [bar]	Temperature [°C]
IM_5	sec.	no data	0	200	40
IM_6	sec.	no data	0	150	40
IM_7	sec.	no data	0	150	40
IM_8	sec.	<LOQ	0	150	40
IM_9	prim.	no data	0	150	40
IM_10	prim.	no data	0	150	40
IM_12	prim.	5 ± 1	0.84	150	40
IM_13	prim.	no data	0	300	50
IM_31	prim.	9 ± 2	0.99	150	40
IM_36	prim.	<LOQ	0	200	40

Four experiments with the secondary copper dithizonate and 7 with primary were performed for this series. For determining the copper content of IM_5, IM_7, IM_9 and IM_10, the samples were measured with ICP-OES or ICP-MS. Different pressures, co- solvents and arrangements were utilized. Figure 4-6 and Figure 4-7 show products of this impregnation series. The resulting samples were transparent in colour with small black complex congregations within the polymer tunnel in the middle. After cleaning of the polymer with its indentations, most of the complex was removed. Since after washing no colour change within the polymer was observed, the assumption was made that no successful impregnation with the secondary

complex has been achieved. A significant amount of the complex remaining within the expansion valve confirmed this assumption. For the following experiments, ethanol was used as a co- solvent. To prevent precipitation of the complex in the co-solvent ultrasound was used before impregnation. Only one sample of the secondary complex series was measured with ICP-OES. The result for IM_9 is listed in Table 4 and no impregnation higher 4 ppm (LOQ of ICP-OES) was achieved by using this complex. Better results were obtained with the primary form of the dithizone complex. IM_12 and IM_31 achieved a copper concentration of 5 ± 1 and 9 ± 2 mg/kg. For both experiments a pressure of 150 bar and a temperature of 40°C was used, therefore additional parameters were influencing this system. As illustrated in Table 3-3 for IM_11 ethanol and for IM_31 a mixture of ethanol/water was used as co- solvent and the cylindrical set- up gave generally better results. For both experiments, a gear pump was used, but the mixing time was longer in IM_31. Therefore, a better homogeneity and mixing was achieved in IM_31. It seems, that the impregnation time and depressurization had a minor influence while applying water as a co-solvent and the pH of the system had a major impact on this sorption. As Reaction 3 illustrates, water in combination with CO_2 forms an acidic milieu. In this milieu, the complex is present in a different form and appears to have a better interaction with the polymer matrix.

4.3.3 *In si*tu polycarbonate with dithizone and copper salt

Figure 4-5 Polycarbonate obtained IM_1

Figure 4-6 Polycarbonate obtained in IM_3

Table 4-1 Results of the *in-situ* polycarbonate with dithizone and copper salt experiments

Experiment	Cu content [mg/kg]	Efficiency of impregnation [%]	Pressure [bar]	Temperature [°C]
IM_1	<LOQ	0	200	50
IM_2	no data	0	200	50
IM_3	<LOQ	0	200	40
IM_4	<LOQ	0	200	40

The aim for this series was the in situ formation of a copper dithizonate within the polymer matrix. Figure 4-5 and Figure 4-6 illustrate the polycarbonate after the impregnation process of IM_1 and IM_3. The product was transparent or lightly green coloured. The greenish colour came from dithizone, which is present inside the polymer matrix. Nevertheless, the first interpretations of the results implied an unsuccessful impregnation with copper. Table 4-1 summarizes the results of the ICP-OES measurement for the Experiments IM_1- IM_4. For IM_2 no data is available. None of the experiments had a copper content higher than 4 mg/kg (LOQ of ICP-OES). The dithizone within the polymer matrix did not interact with the copper ions of the salt. One reason is the better solubility of dithizone in $scCO_2$. Salt in the water or ethanol phase has no affinity towards in $scCO_2$. Therefore, both phases hardly interact with each other and formation of a complex is hindered. Additionally, a lack of mixing (no gear pump was used) disfavoured intermixing of the two phases. Since no evidence for copper dithizone complexes was found that high pressure and a temperature of 40°C disfavours the in situ formation of copper dithizone complexes and no impregnation of the polymer matrix can be achieved by this method.

4.3.4 2-step impregnation process

After performing and testing three different impregnation systems, it was observed, that *in situ* complex formation turned out to be complicated due to the complex equilibrium behaviour of the system. Therefore, experiments were carried out to obtain complexation within the polymer matrix in two distinct steps.

In this section, both steps will be discussed. For the first part, the impregnation of the polycarbonate with dithizone is studied and the sample measured via UV-VIS spectroscopy. For the second part, the copper content was determined via ICP-OES.

1. **First step- dithizone impregnation of polycarbonate:**

Figure 4-7 Product of IM_14_1

As Figure 4-7 illustrates, the product of this impregnation series was deep green. This indicates a dithizone impregnation within the polymer matrix. To prove this successful impregnation, dithizone concentration was measured via UV/VIS spectroscopy.

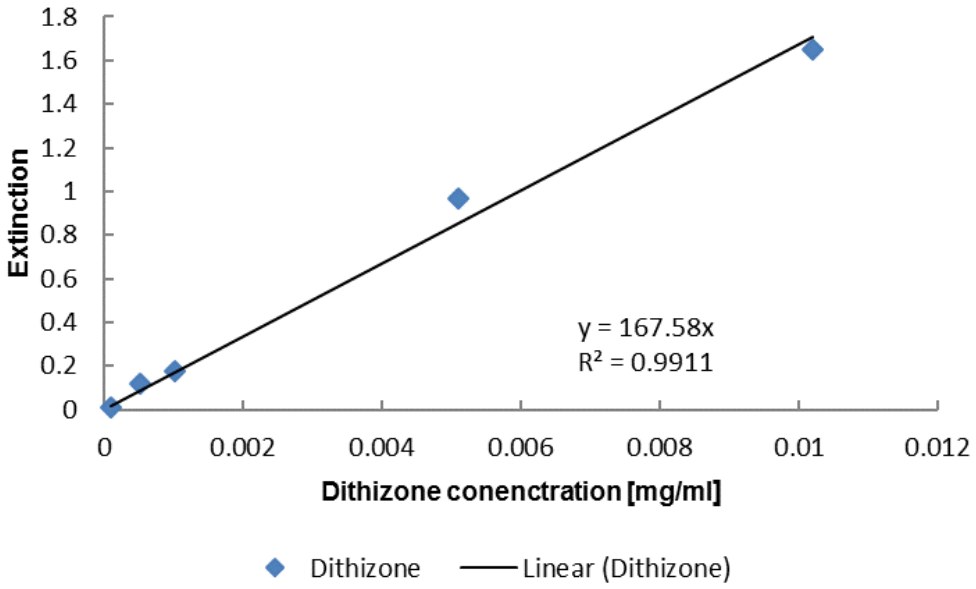

Figure 4-8 UV- VIS calibration for dithizone impregnation of the polycarbonate

Figure 4-11 illustrates the calibration curve for the dithizone determination. Five calibration points were measured and a linear regression was carried out. With the ascertained parameters, the total dithizone content was calculated. As mentioned before, dithizone reacts with a variety of metal ions. The resulting complexes are deeply coloured. Therefore, a change in colour of the calibration solutions occurs rather easy and it is essential to work accurately. Even slight colour changes, which are invisible for the eye, can cause some failure during calibration.

Table 4-2 Results of the dithizone polycarbonate experiments

Experiment	For experiments	Dithizone concentration [mg (Dit)/g(PC)]	Pressure [bar]	Temperature [°C]
DPC_1	IM_20 and IM_21	0.179	150	40
DPC_2 (IM_14)	IM_14_1 and IM_14_2	No data	300	50
DPC_3 (IM_24)	IM_26 and IM_27	0.110	150	40
DPC_4 (IM_28)	IM_32, IM_33 and IM_34	0.085	100	40
DPC_5 (IM_35)	IM_37 and IM_38 and IM_41	0.097	100	40

Two of the measured dithizone values were outside the calibration range. By assuming an insignificant statistical error, the calculated dithizone concentrations were expected to be correct. As Table 4-2 illustrates all of the impregnation experiments showed a successful dithizone impregnation of the polycarbonate. For IM_14 no sample was left to measure the dithizone concentration. Regarding the dithizone content with a co-solvent, impregnation at

higher pressure (150 bar compared to 100 bar) favours the impregnation. Moreover, combining high pressure with a co-solvent generates crystalline products as it has already been described in literature [39]. Comparing DPC_4 and DPC_ 5 (same parameters, DPC_5 had longer mixing time) shows the importance of good mixing.

As mentioned before the set-up has a significant role as well. For better homogeneity, a cylindrical set-up is preferred. By this, the vessel had less volume with a narrower diameter, which causes better flow distribution of the $scCO_2$ during sorption when stirring the solution.

2. **Second step- copper impregnation of DPC:**

Figure 4-9 Products of the 2- step impregnation (IM_ and IM_)

As Figure 4-9 illustrates the colour range of the products was from green to golden yellow. It has to be assumed, that a significant amount of dithizone was extracted from the polycarbonate. In combination with a co-solvent and higher pressure crystalline products were obtained.

Table 4-3 Results of the ICP-OES measurement for the 2- step impregnation process

Experiment	DPC source	Cu content [mg/kg]	Pressure [bar]	Temperature [°C]
IM_14_1	IM_14	45±2	100	40
IM_14_2	IM_14	109±3	100	40
IM_20	DPC_1	90±3	100	40
IM_21	DPC_1	10,9±0,3	100	40
IM_25	IM_24	9,2±0,3	100	40
IM_26	IM_24	15±7	100	40
IM_27	IM_24	< LOQ	100	40
IM_32	IM_28	< LOQ	100	40
IM_33	IM_28	67±7	100	40
IM_34	IM_28	6±4	100	40
IM_37	IM_35	< LOQ	100	40
IM_38	IM_35	< LOQ	100	40
IM_41*	IM_35	379.35	100	40

*IM_41 was measured by IKEMA d.o.o in Lovrenc na Dravskem Polju, Slovenia

The results in Table 4-3 indicate a high standard deviation for the copper concentrations. This results from an insufficient homogeneity induced by the set-up. However, the cylindrical set-up gives higher copper concentrations, even the copper range is differing a lot. The best result was IM_41 with ≈380 ppm. Comparing the total copper amount and combing it with the dithizone loading of the first step, no direct correlation can be found. In theory, more dithizone loading gives more bounded cooper. IM_25, IM_26 and IM_27 are exemplify, that the dithizone loading has only a small influence. DPC_3 (IM_24) had a dithizone concentration of 0.101 mg/g PC and the results for IM_25-IM_27 were lower than the average.

For a successful impregnation, using KOH or a likewise base is essential. IM_37, which had similar parameters as the other experiments (except for the lack of KOH) had a copper concentration lower than the limit of quantification of the ICP-OES. The base might deprotonate dithizone and favours coordination with copper. Moreover, KOH favours the formation of $Cu(OH)_2$, which might be more soluble in supercritical CO_2 or interacts better with dithizone.

$$Cu(NO_3)_2 + 2\,KOH \rightarrow Cu(OH)_2 + 2\,KNO_3 \qquad \text{Reaction 4}$$

Generally speaking, $Cu(OH)_2$ is nearly insoluble in water and probably poorly soluble in $scCO_2$ (no literature data were found). The equilibria between supercritical CO_2, H_2O and the interaction of the cooper salt with the polymer matrix is still not fully understood. One possible reaction which might occur during the impregnation, is the reaction between $Cu(OH)_2$ and H_2CO_3, which is formed during the process in combination with H_2O.

$$Cu(OH)_2 + H_2CO_3 \rightarrow CuCO_3 + 2\,H_2O \qquad \text{Reaction 5}$$

Since H_2CO_3 is a weak acid, a reaction with $Cu(OH)_2$ is not certain to occur but may influence the impregnation process by changing the pH of the system.

Regarding the role of dithizone during the impregnation process, it seems that a maximum dithizone concentration for copper impregnation exists. Two approaches can be defined to understand the mechanism for binding copper:

1. Copper binds with dithizone and clusters or aggregates of copper within the polymer are formed. The amount of coordinating copper ions at the dithizone is saturated and a maximum amount for copper to bind exists. The base might deprotonate dithizone and favours binding of copper.

2. An interaction between the carbonyl group of the polycarbonate and the copper occurs and a weak bond (van der Waals or Coulomb interaction) is formed. Figure 4-10 illustrates this interaction. Copper acts as an electrophilic group and the oxygen atom of the carbonyl group as nucleophile.

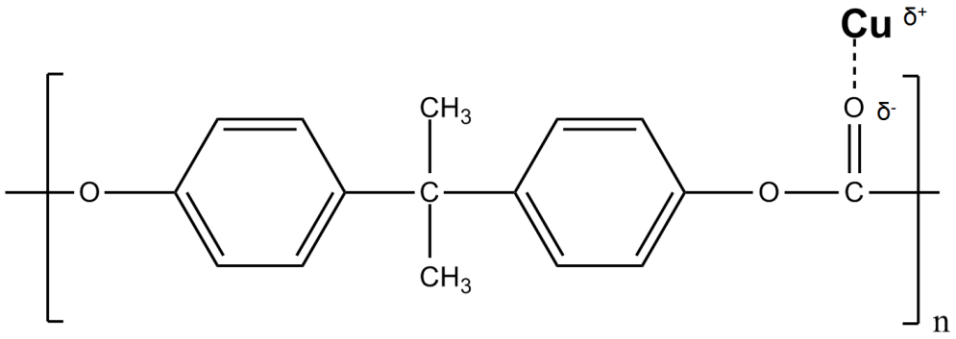

Figure 4-10 Interaction between polycarbonate and copper

None of the two approaches completely explain the resulting copper concentrations and there are pros and cons for both theories. Additionally, to help understanding the most likely mechanism 2 experiments were carried out. In both experiments, no dithizone was used as additive and impregnation of polycarbonate with only copper salt were carried out.

Table 4-4 Results of IM_22 and IM_23

	Pressure [bar]	Temperature [°C]	Time [h]	Solvent	Set-up	Gear pump [min]	Copper content [mg/kg]
IM_22	100	40	2	EtOH	2	39	78±18
IM_23	100	40	2	H_2O/KOH	2	30	4±1

As the results in Table 4-4 illustrate, a successful impregnation to a certain copper level might be achieved without dithizone. However, it has to be mentioned, that only two experiments were carried out and standard deviation was high in IM_22. Moreover, EtOH dissolves better in supercritical CO_2 and different mechanism might occur in this system.

4.3.5 Scanning electron microscope SEM coupled with EDX

To visualize a successful impregnation within the polymer matrix, SEM of IM_14_2 (109±3mg/kg) was performed. Moreover, this technique was used to observe the depth of penetration, the distribution of copper within the polymer and the size of occurring aggregates.

To determine the metal, which was present within the polymer, EDX scanning was carried out. The parameters, obtained through these techniques, were indicators for a successful impregnation process and guidelines for future impregnation experiments.

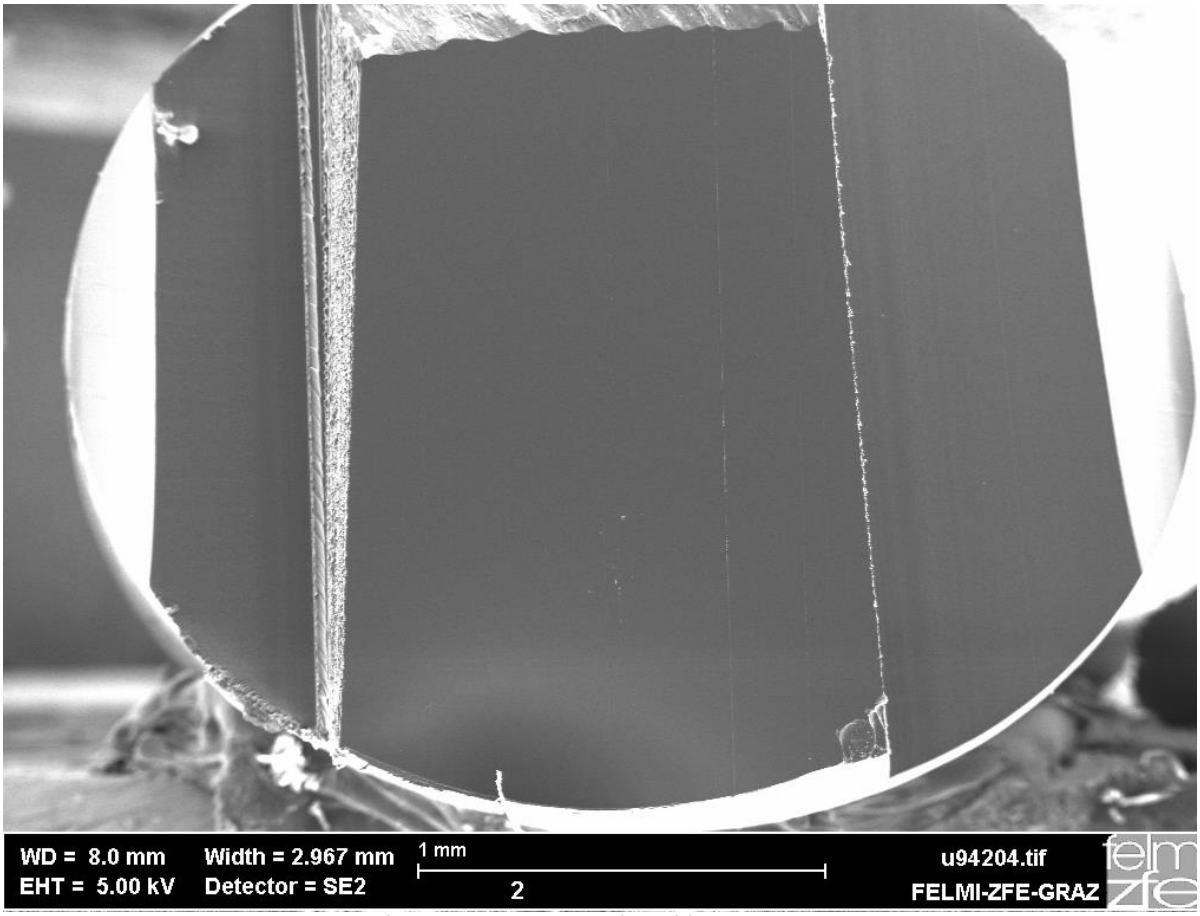

Figure 4-11 Cross section of the IM_14_2

Figure 4-11 illustrates a secondary electron's image of a cross section (IM_14_2) and shows the elliptical shape of the polymer granulate. By using the bar on the bottom of the image, the length of the sample can be estimated. The bright lines are bruises induced by the diamond knife during the sample preparation. On closer examination, small bright points deep inside the polymer matrix were observed. These points were interpreted as metal aggregates. To determine the aggregates composition, EDX was performed. Figure 4-12 and Figure 4-13 show two examples for these points. Both points have an estimated size of 5-600 nm. By backscattering the image, clear shapes of the aggregates can be observed.

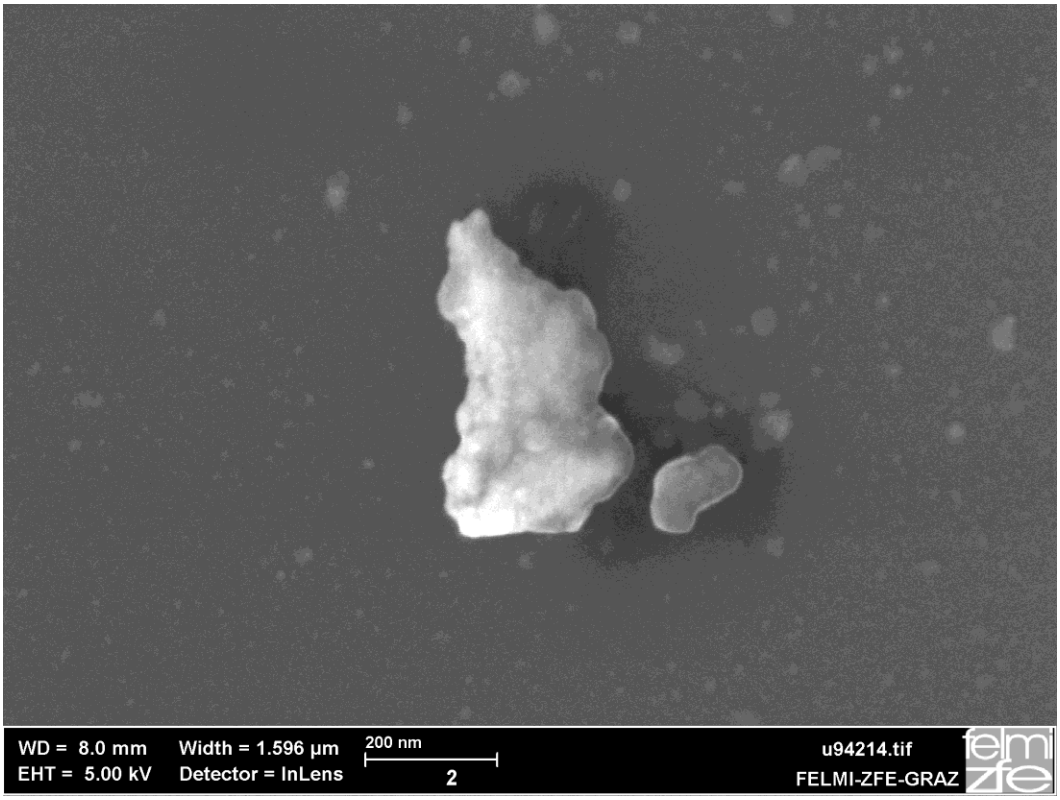

Figure 4-12 Bright point within the polymer matrix I

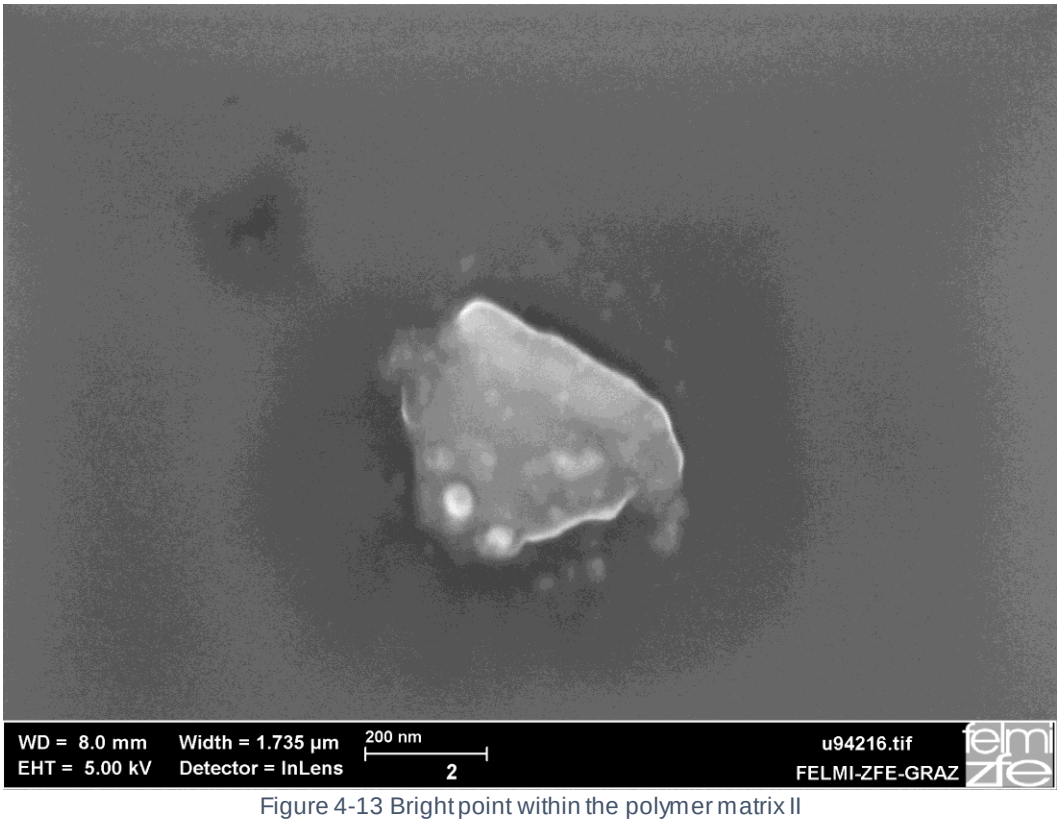

Figure 4-13 Bright point within the polymer matrix II

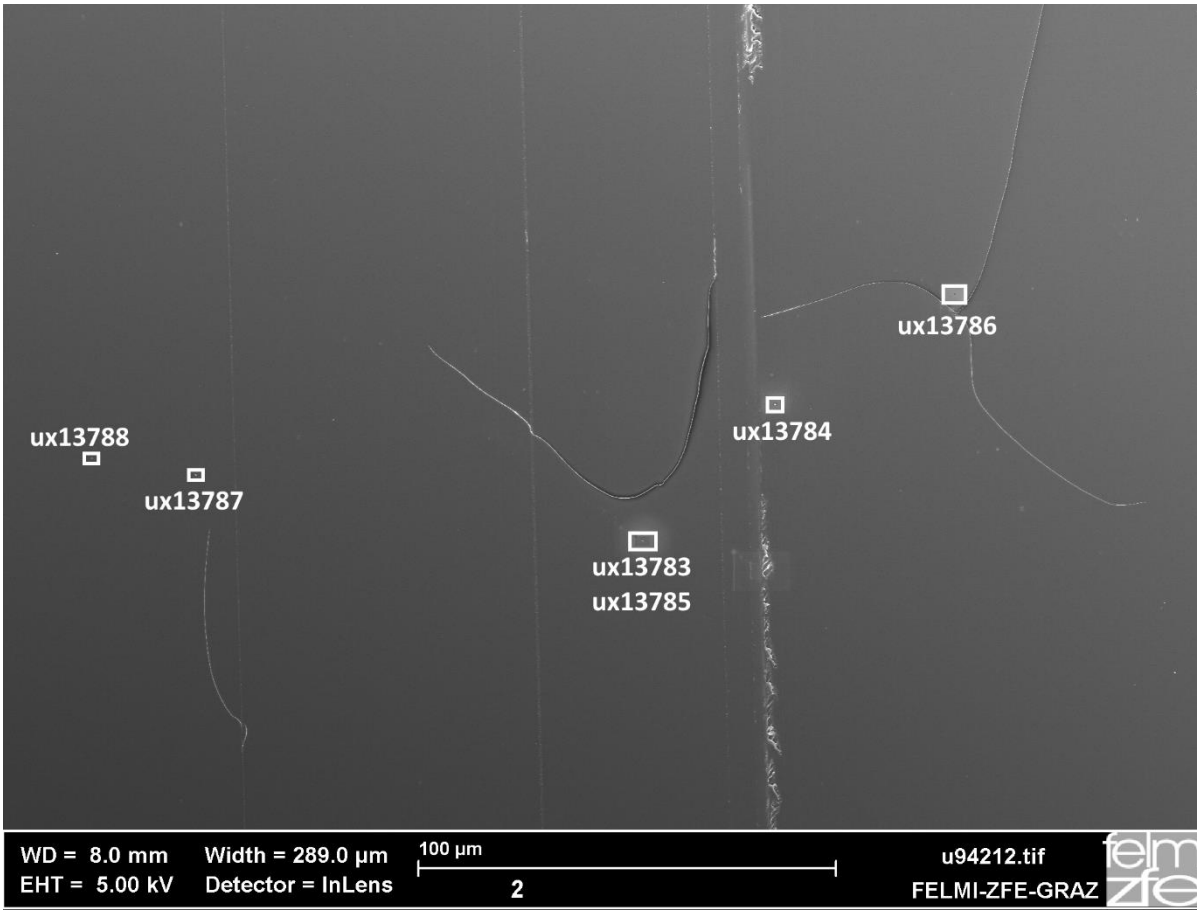

Figure 4-14 Local section of SEM IM_14_2

For this local section, five EDX measurements (Figure 4-14) were performed. To get the EDX spectra, an electric potential of 5 kV and 20 kV acceleration voltage was used. The following figures illustrate the results/spectra of these measurements. To obtain a clear cut from other signals, first the background was scanned.

Figure 4-15 illustrates the background scanned by EDX. Carbon and oxygen peaks result from the polycarbonate structure mostly containing these two elements (for the structure, chapter 2.8.3).

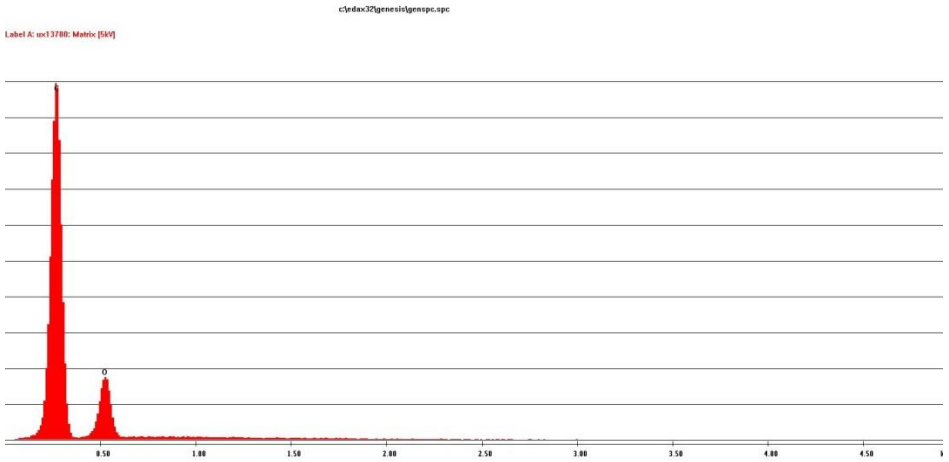

Figure 4-15 EDX spectrum of the background (IM_14_2)

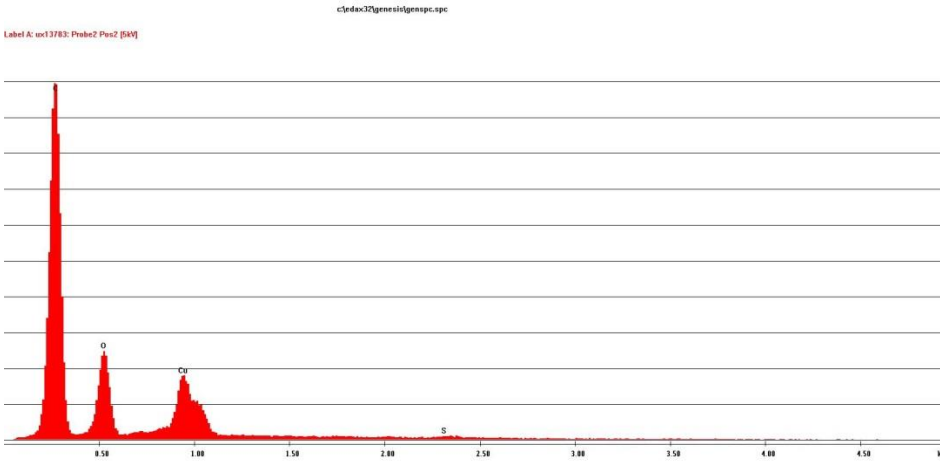

Figure 4-16 EDX spectrum of ux13783 (IM_14_2)

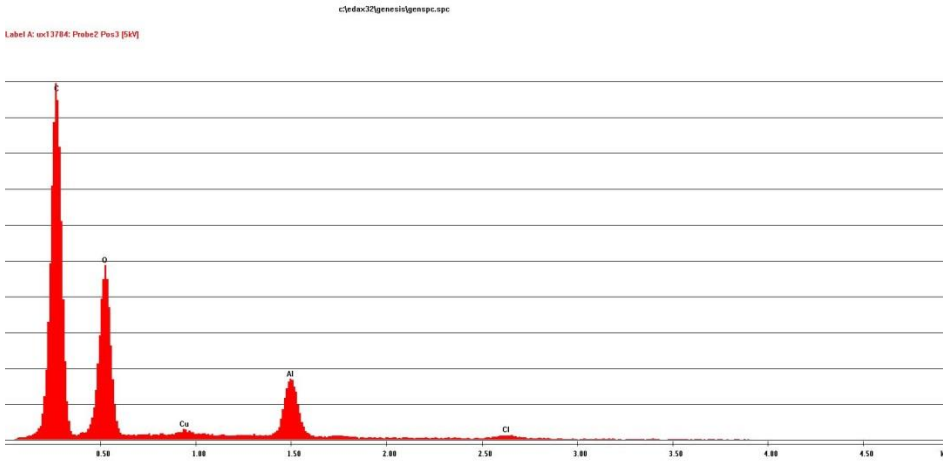

Figure 4-17 EDX spectrum of ux13784 (IM_14_2)

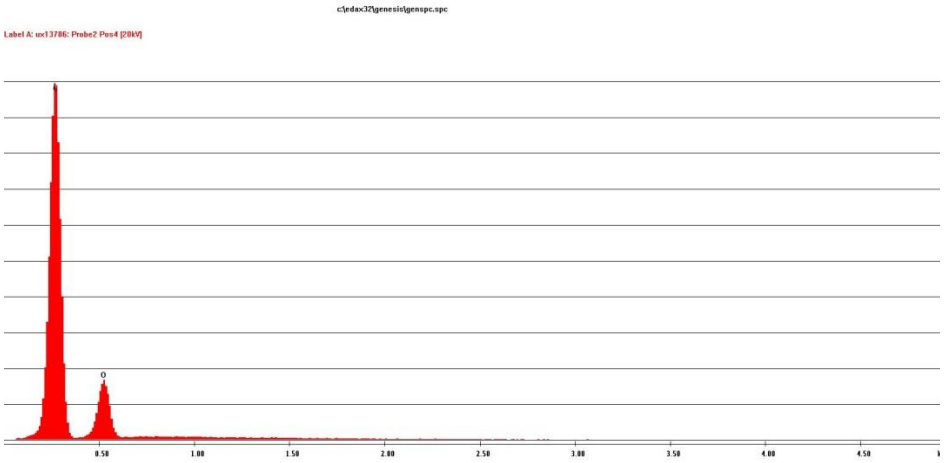

Figure 4-18 EDX spectrum of ux13786 (IM_14_2)

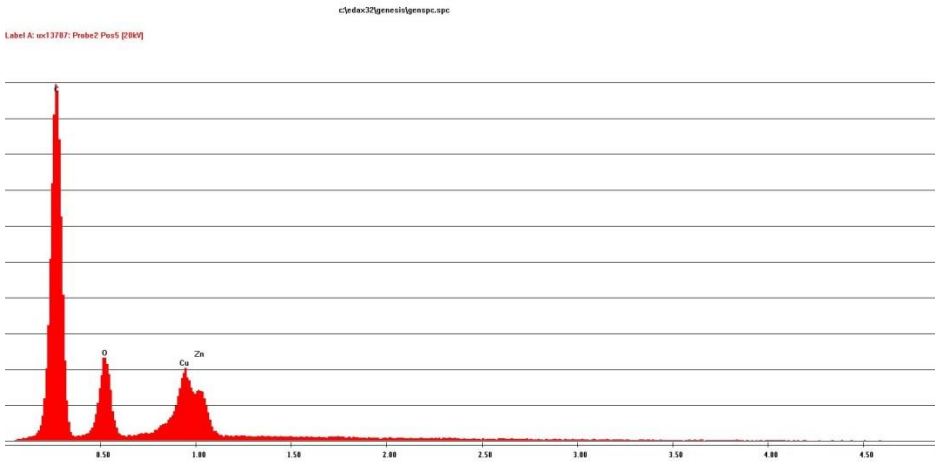

Figure 4-19 EDX spectrum of ux13787 (IM_14_2)

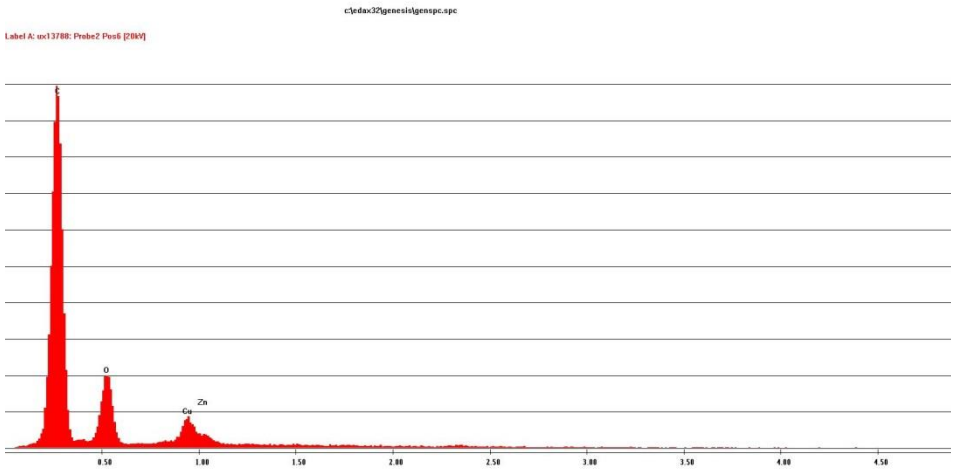

Figure 4-20 EDX spectrum of ux13788 (IM_14_2)

All EDX spectra showed clear peaks for copper (except of ux13786). In some spectra (e.g. ux13788) a second peak next to copper can be observed. This peak represents the element zinc, which might result from sample preparation. However, this peak can also come from the K_β signal of the copper. An alumina peak in ux13784 is clearly a contamination coming from the diamond knife, which was used to create a cross section of the sample.

The previous spectra prove that in IM_14_2 (except of ux13786) copper was present deep inside the polymer matrix.

Combing the results of the SEM images and the EDX spectra, it has been proved that formation of copper aggregates within the polymer matrix occurred and a homogenous impregnation was achieved.

5 Conclusion and perspectives

The objective of this work was to create an alternative and efficient impregnation method for polycarbonate. Furthermore, the ambitions were high to achieve an impregnation of copper nanostructures deep inside the polymer matrix by the usage of the intrinsic advantages of $scCO_2$. For the impregnation process, dithizone as a new carrier molecule was introduced and its potential was investigated.

Four different approaches were established and compared to each other. 3 of those 4 methods produced impregnated polycarbonate products. An *in situ* formation of copper dithizonate within the matrix was not fully achieved.

The copper concentration in the polymer lay between 4 mg/kg and approximately 380 mg/kg. The highest concentrations were obtained by the 2- step impregnation. Experiments performed at a temperature of 40°C, a pressure of 100 bar and an impregnation time of 2 h produced the highest copper content. Increasing temperature and impregnation time leads to crystallization of the polymer and to a complicated impregnation.

In order to obtain high concentrations, the presence of a base (e.g. KOH) is necessary. However, all of the experiments showed high standard deviations. This indicates problems with homogeneity. Comparing the two inlets, the cylindrical one gave higher copper concentration with lower standard deviation. Regarding additional solvents (water and ethanol), the usage of water resulted in better copper load for the 2-step process.

In conclusion, water in combination with KOH is to favour. However, to obtain more information regarding the mechanisms, further studies are required.

One of the advantages of the 2-step process is that a better control of this system can be achieved. By loading the polycarbonate sample first with a defined amount of dithizone, the resulting copper concentration can be estimated. Regarding the copper bonding, two explanations are possible: binding of copper with dithizone and interaction between copper and a carbonyl group. In reality, it is most likely that both phenomena contribute to the formation of copper aggregates and further investigations have to be performed. Moreover, the oxidation state of the copper as well as the question if reduction (either by thermally or chemically) of the metal is necessary have to be considered.

Nevertheless, SEM in combination with EDX showed discrete copper deposits and indicated a successful impregnation by the 2-step impregnation process.

For future projects, it would be important to determine the maximum available dithizone loading concentration in polycarbonate and to investigate the formation of copper aggregates within the polymer matrix.

Moreover, it is necessary to study the polymers properties, which might have changed containing a remarkable amount of metal.

In light of all observations and results, the impregnation of polycarbonate with copper nanostructures in supercritical CO_2 has great potential. Since dithizone binds a variety of metals, the number of possible application is numerous.

Thus, further investigations have to be done, but this method could be a new promising technique to produce metal containing polymers.

Literature

1. Yeo, S.-D. & Kiran, E. Formation of polymer particles with supercritical fluids: A review. *J. Supercrit. Fluids* **34,** 287–308 (2005).
2. Erkey, C. Preparation of metallic supported nanoparticles and films using supercritical fluid deposition. *J. Supercrit. Fluids* **47,** 517–522 (2009).
3. Kikic, I. & Vecchione, F. Supercritical impregnation of polymers. *Curr. Opin. Solid State Mater. Sci.* **7,** 399–405 (2003).
4. Smith, R. M. Nomenclature for supercritical fluid chromatography and extraction. *Pure Appl. Chem.* **65,** 2397–2403 (1993).
5. Jessop, P. G. & Leitner, W. *Chemical Synthesis Using Supercritical Fluids*. (*Wiley-VCH, Weinheim* 1999).
6. Jessop, P. & Leitner, W. *Chemical synthesis using supercritical fluids*. (Wiley-VCH, 1999).
7. Kemmere, M. & Meyer, T. *Supercritical carbon dioxide: in polymer reaction engineering*. (Wiley-VCH, 2006).
8. Kazarian, S. G. Polymer Processing with Supercritical Fluids. *Polym. Sci.* **42,** 78–101220 (2000).
9. Nalawade, S. P., Picchioni, F. & Janssen, L. P. B. M. Supercritical carbon dioxide as a green solvent for processing polymer melts: Processing aspects and applications. *Prog. Polym. Sci.* **31,** 19–43 (2006).
10. Bach, E., Cleve, E. & Schollmeyer, E. Past, present and future of supercritical fluid dyeing technology - an overview. *Rev. Prog. Color. Relat. Top.* **32,** 88–102 (2002).
11. Sabirzyanov, A., Il'in, A., Akhunov, A. & Gumerov, F. Solubility of water in supercritical carbon dioxide. *High Temp.* **40,** 231–234 (2002).
12. Haruki, M., Kobayashi, F., Kishimoto, K., Kihara, S. & Takishima, S. Measurement of the solubility of metal complexes in supercritical carbon dioxide using a UV–vis spectrometer. *Fluid Phase Equilib.* **280,** 49–55 (2009).
13. Diplomarbeit: Sieberer, R. Gewinnung von cholagogahaltigen Extrakten aus den Natturstoffen Baldrian, Löwenzahn, Schafgarbe, Mariendistel und Scholkraut durch Hochdruckextraktion mit Kohlendioxid (1998).
14. Kemmere, M. F. Supercritical Carbon Dioxide for Sustainable Polymer Processes. *Supercrit. Carbon Dioxide Polym. React. Eng.* 1–14 (2006). doi:10.1002/3527606726.ch1
15. Nicolais, L. & Carotenuto, G. *Metal-Polymer Nanocomposites*. *Metal-Polymer Nanocomposites* (2005). doi:10.1002/0471695432
16. Siemann, U. Solvent cast technology - A versatile tool for thin film production. *Prog. Colloid Polym. Sci.* **130,** 1–14 (2005).
17. Braun, D., Cherdron, H., Rehahn, M., Ritter, H. & Voit, B. *Polymer synthesis: theory and practice*. (2005).
18. Prut, E. V & Zelenetskii, A. N. Chemical modification and blending of polymers in an extruder reactor. *Russ. Chem. Rev.* **70,** 65–79 (2007).

19. Zhang, Y. & Erkey, C. Preparation of supported metallic nanoparticles using supercritical fluids: A review. *J. Supercrit. Fluids* **38,** 252–267 (2006).

20. Sun, Y. *et al.* Solubility and diffusion coefficient of supercritical-CO2 in polycarbonate and CO2 induced crystallization of polycarbonate. *J. Supercrit. Fluids* **95,** 35–43 (2014).

21. Berens, A. R., *et.al*., Application of compressed carbon dioxide in the incorporation of additives into polymers. *J. Appl. Polym. Sci.* **46,** 231–242 (1992).

22. Wissinger, R & G. & Paulaitis, M. E. Swelling and sorption in polymer–CO_2 mixtures at elevated pressures. *J. Polym. Sci. Part B Polym. Phys.* **25,** 2497–2510 (1987).

23. Kiran, E. Debenedetti,P. G., Peters C. J., *Supercritical Fluids Fundamentals and Applications*. (Springer Science+Business Media, BV., 1994).

24. von Schnitzler, J. & Eggers, R. Mass transfer in polymers in a supercritical CO2-atmosphere. *J. Supercrit. Fluids* **16,** 81–92 (1999).

25. Berens, A. R. & Huvard, G. S. Interaction of Polymers with Near-Critical Carbon Dioxide. 207–223 (1989). doi:10.1021/bk-1989-0406.ch014

26. Tomasko, D. L. *et al.* A review of CO(2) applications in the processing of polymers. *Ind. Eng. Chem. Res.* **42,** 6431–6456 (2003).

27. Shieh, Y. T. & Lin, Y. G. Equilibrium solubility of CO_2 in rubbery EVA over a wide pressure range: Effects of carbonyl group content and crystallinity. *Polymer (Guildf).* **43,** 1849–1856 (2002).

28. Kazarian, S. G., Vincent, M. F., Bright, F. V., Liotta, C. L. & Eckert, C. a. Specific intermolecular interaction of carbon dioxide with polymers. *J. Am. Chem. Soc.* **118,** 1729–1736 (1996).

29. Holleman, A. & Wiberg, E. *Lehrbuch der Anorganischen Chemie*. *Journal of Chemical Information and Modeling* **53,** (1995).

30. Sabic. LEXAN ™ Resin 121. <https://www.sabic-ip.com/gepapp/eng/weather/weatherhtml?sltUnit=SI&sltRegionList=1002002000&sltPrd=1002003008&sltGrd=1002010815&sltModule=DATASHEETS&sltType=Online&sltVersion=Internet&sltLDAP=0.> (09.08.2016)

31. Bürkle GmbH. Chemische Beständigkeit von Kunststoffen. **49,** 1–35 (2010).

32. Zhang, Z. & Handa, Y. P. An in situ study of plasticization of polymers by high-pressure gases. *J. Polym. Sci.* **36,** 977–982 (1998).

33. Star, J. *The Solvent Extraction of Metal Chelates*. *The Solvent Extraction of Metal Chelates* (1964).

34. Robisch G. & Herrma W., Zur Existenr und Struktur der sekundaren Dithizonate. **515,** 230–240 (1984).

35. Irving. H & Cox, J. J. 289. Studies with dithizone. Part VIII. Reactions with organometallic compounds. *J. Chem. Soc.* 1470–1479 (1961).

36. Irving H & Kiwan A. M., Studies with dithizone: Part XXV. Secondary copper(II) dithizonate. *Anal. Chim. Acta* **56,** 435–446 (1971).

37. Cabanas, A., Blackburn, J. M. & Watkins, J. J. Deposition of Cu films from supercritical fluids using Cu(I) b-diketonate precursors. *Microelectron. Eng.* **64,** 53–61 (2002).

38. Varga, D. *et al.* Supercritical fluid dyeing of polycarbonate in carbon dioxide. *J. Supercrit. Fluids* **116,** 111–116 (2016).

39. Tang, Z., Youshuang, C., Mouhua, W. Specific properties improvement of polycarbonate induced by irradiation at elevated particular temperature. *Radiat. Phys. Chem.* **96,** 171–175 (2014).

40. Gross, S. M., Roberts, G. W., Kiserow, D. J. & Desimone, J. M. Crystallization and solid-state polymerization of poly(bisphenol A carbonate) facilitated by supercritical CO2. *Macromolecules* **33,** 40–45 (2000).

41. Toews, K. L., Shroll, R. M., Wai, C. M. & Smart, N. G. pH-Defining equilibrium between water and supercritical CO_2 - Influence on SFE of organics and metal-chelates. *Anal. Chem.* **67,** 4040–4043 (1995).

42. Adrian, T., Wendland, M., Hasse, H. & Maurer, G. High-pressure multiphase behaviour of ternary systems carbon dioxide–water–polar solvent: review and modeling with the Peng–Robinson equation of state. *J. Supercrit. Fluids* **12,** 185–221 (1998).

43. Durling, N. E., Catchpole, O. J., Tallon, S. J. & Grey, J. B. Measurement and modelling of the ternary phase equilibria for high pressure carbon dioxide-ethanol-water mixtures. *Fluid Phase Equilib.* **252,** 103–113 (2007).

44. Kondoh, E. & Kato, H. Characteristics of copper deposition in a supercritical CO_2 fluid. *Microelectron. Eng.* **64,** 495–499 (2002).

List of figures

List of tables

List of abbreviations

CO_2	Carbon dioxide
PC	Polycarbonate
SCF	Supercritical Fluid
$scCO_2$	Supercritical carbon dioxide
ICP-OES	Inductively coupled plasma optical emission spectroscopy
ICP-MS	Inductively coupled plasma mass spectrometry
UV/VIS- spectroscopy	Ultraviolet–visible spectroscopy
SEM	Scanning electron microscope
p_C	Critical pressure
T_C	Critical temperature
T_G	Glass transition temperature
wt%	Weight percent
DCM	Dichloromethane
H_2O	Water
EtOH	Ethanol
IM_X	Impregnation Experiment X
DPC	Dithizone impregnated polycarbonate
Dit	Dithizone
Prim.	Primary
Sec.	Secondary
p	Pressure
T	Temperature
t	Time
Depr. -time	Time for depressurization

Appendix

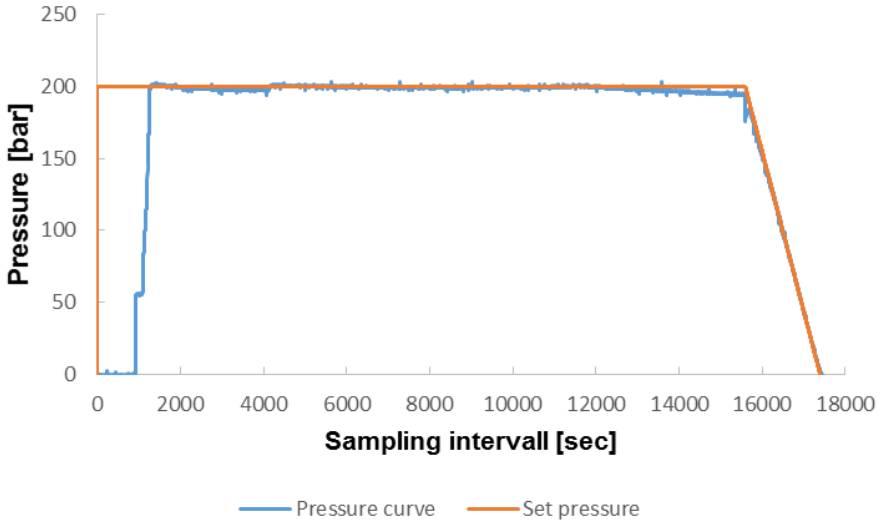

Method	*In situ*
p [bar]	200
T [°C]	50
T [h]	4
Gear pump	No
Ultra-sound	No
Co-solvent	H_2O
Inlet	2
Milieu	Neutral
Depr.-time	1

Figure 0-1 Pressure curve IM_1

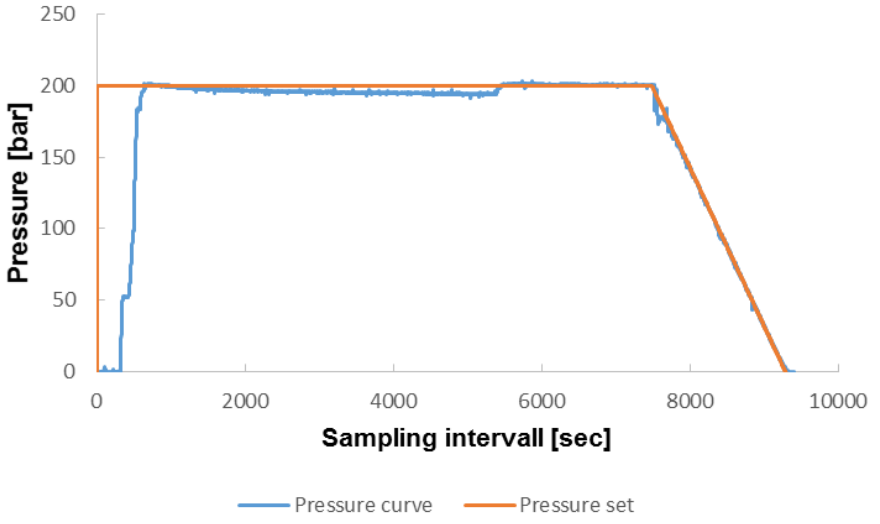

Method	*In situ*
p [bar]	200
T [°C]	50
T [h]	2
Gear pump	No
Ultra-sound	No
Co-solvent	EtOH
Inlet	2
Milieu	Neutral
Depr.-time	1

Figure 0-2 Pressure curve IM_2

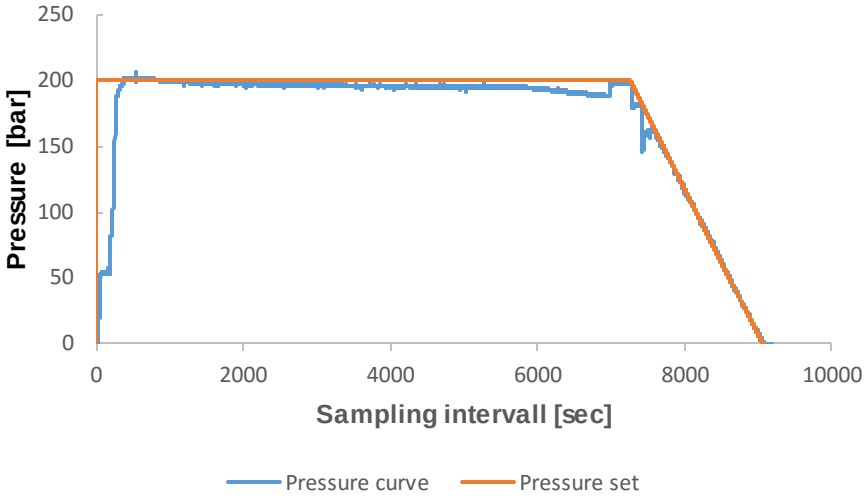

Method	*In situ*
p [bar]	200
T [°C]	40
T [h]	2
Gear pump	No
Ultra-sound	No
Co-solvent	H_2O
Inlet	1
Milieu	Neutral
Depr.-time	1

Figure 0-3 Pressure curve IM_3

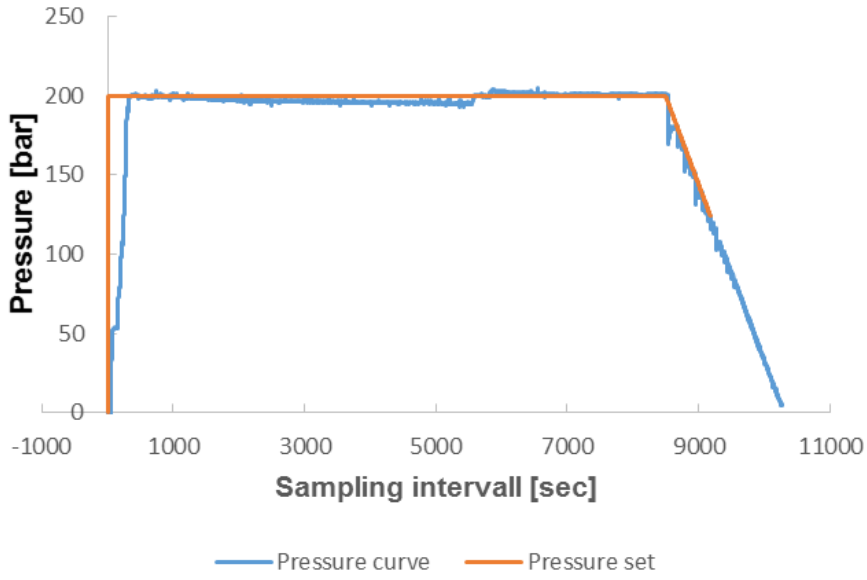

Method	*In situ*
p [bar]	200
T [°C]	40
T [h]	2
Gear pump	No
Ultra-sound	No
Co-solvent	H_2O/ EtOH
Inlet	1
Milieu	Neutral
Depr.-time	1

Figure 0-4 Pressure curve IM_4

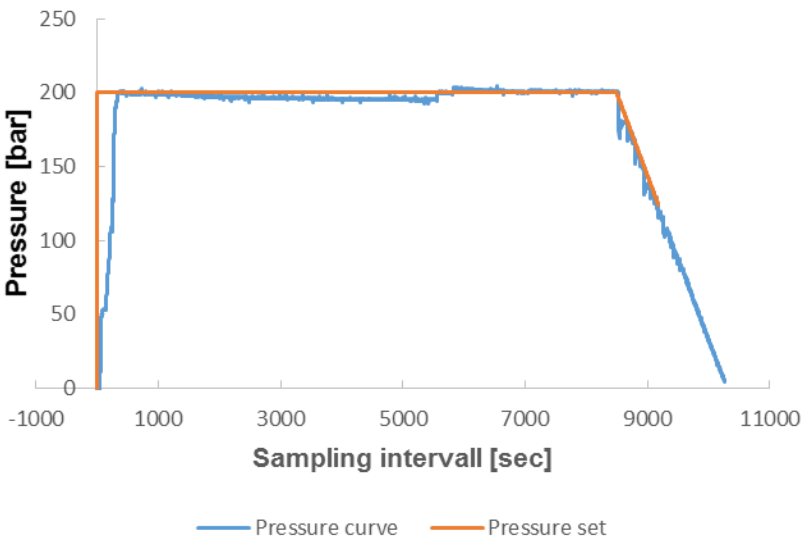

Method	sec.
p [bar]	200
T [°C]	40
T [h]	6
Gear pump	No
Ultra-sound	No
Co-solvent	-
Inlet	1
Milieu	Neutral
Depr.-time	1

Figure 0-5 Pressure curve IM_5

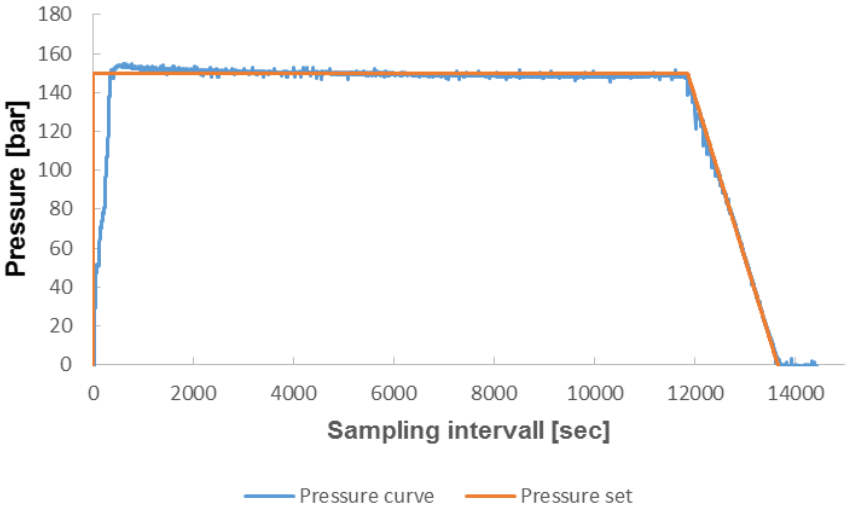

Method	sec.
p [bar]	150
T [°C]	40
T [h]	3
Gear pump	No
Ultra-sound	Yes
Co-solvent	EtOH
Inlet	1
Milieu	Neutral
Depr.-time	1

Figure 0-6 Pressure curve IM_7

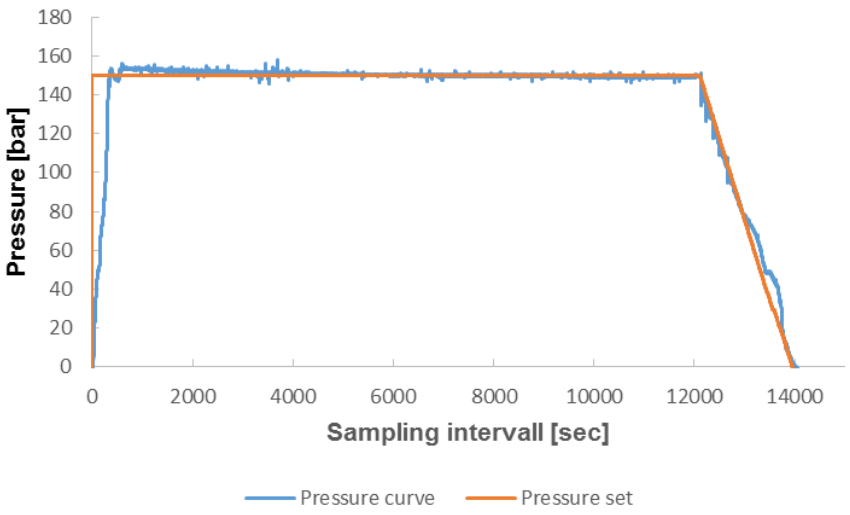

Figure 0-7 Pressure curve IM_8

Method	sec.
p [bar]	150
T [°C]	40
T [h]	3
Gear pump	No
Ultra-sound	Yes
Co-solvent	EtOH
Inlet	2
Milieu	Neutral
Depr.-time	1

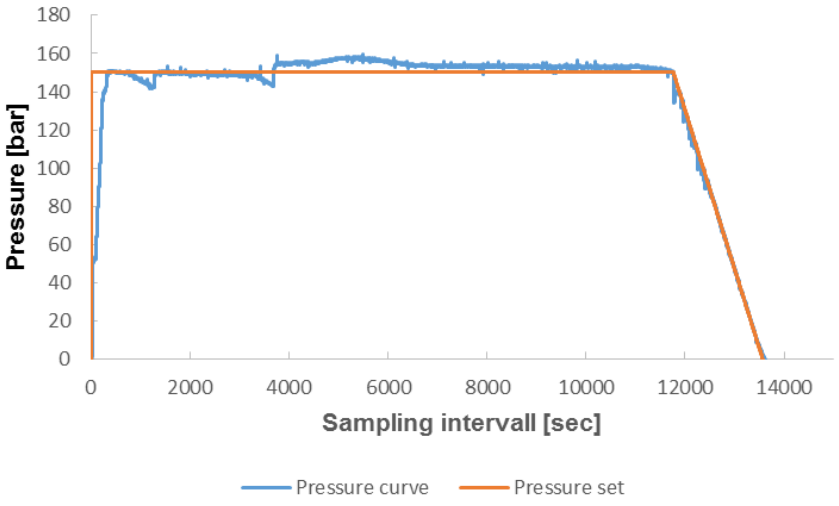

Figure 0-8 Pressure curve IM_9

Method	prim.
p [bar]	150
T [°C]	40
T [h]	3
Gear pump	No
Ultra-sound	Yes
Co-solvent	-
Inlet	1
Milieu	Neutral
Depr.-time	1

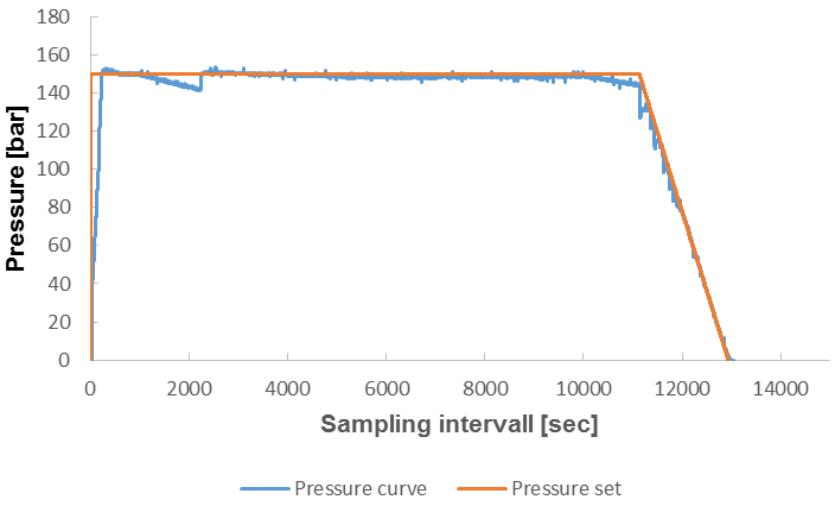

Figure 0-9 Pressure curve IM_10

Method	prim.
p [bar]	150
T [°C]	40
T [h]	3
Gear pump	No
Ultra-sound	Yes
Co-solvent	EtOH
Inlet	1
Milieu	Neutral
Depr.-time	1

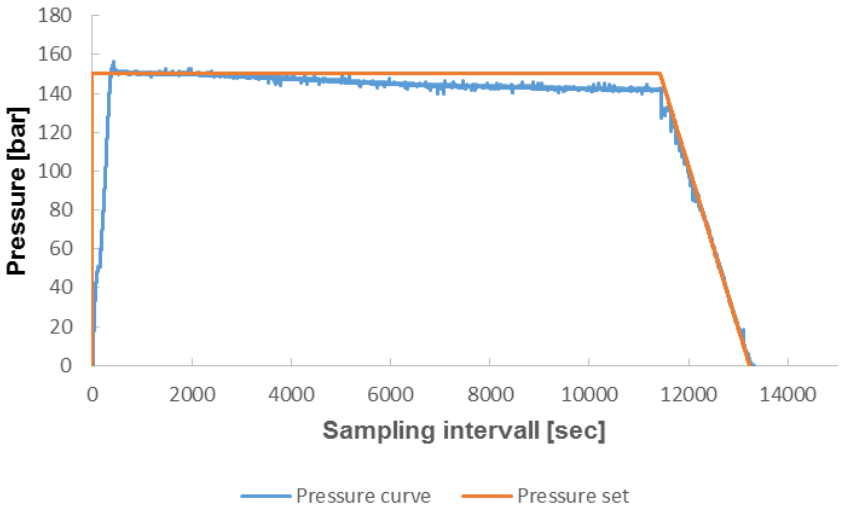

Figure 0-10 Pressure curve IM_12

Method	prim.
p [bar]	150
T [°C]	40
T [h]	3
Gear pump	No
Ultra-sound	Yes
Co-solvent	EtOH
Inlet	1
Milieu	Neutral
Depr.-time	1

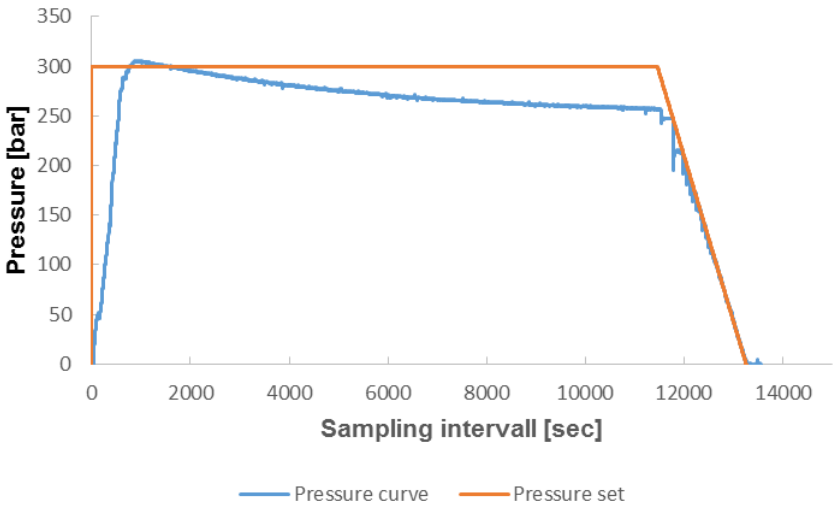

Figure 0-11 Pressure curve IM_13

Method	prim.
p [bar]	150
T [°C]	40
T [h]	3
Gear pump	No
Ultra-sound	Yes
Co-solvent	EtOH
Inlet	1
Milieu	Neutral
Depr.-time	1

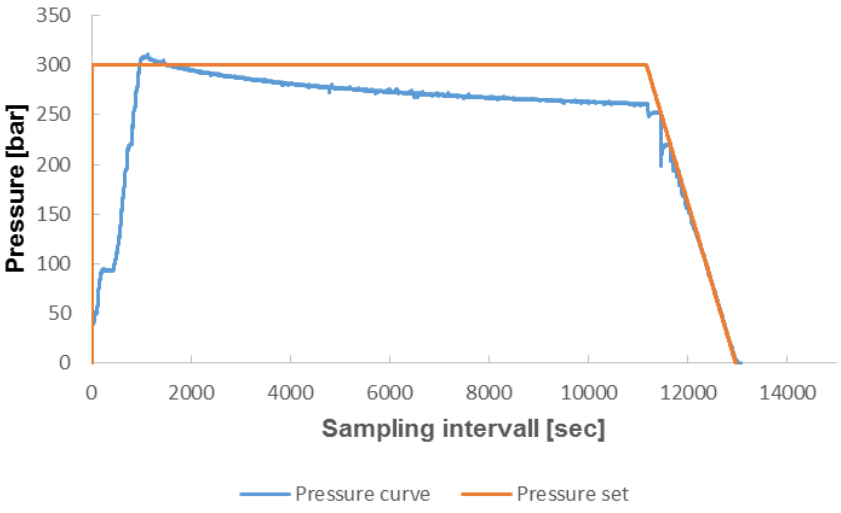

Figure 0-12 Pressure curve IM_14

Method	DPC
p [bar]	300
T [°C]	40
T [h]	3
Gear pump	Yes
Ultra-sound	No
Co-solvent	-
Inlet	1
Milieu	Neutral
Depr.-time	1

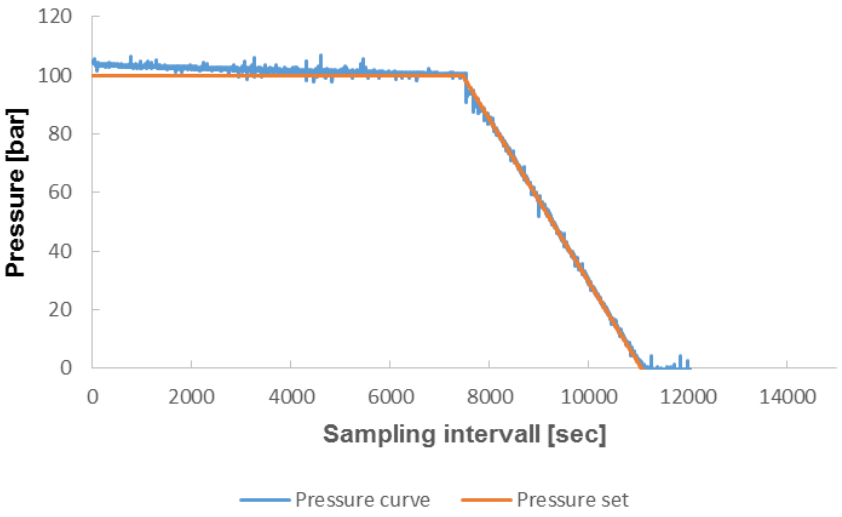

Figure 0-13 Pressure curve IM_14_1

Method	2-Step
p [bar]	100
T [°C]	40
T [h]	2
Gear pump	Yes
Ultra-sound	No
Co-solvent	EtOH
Inlet	1
Milieu	Neutral
Depr.-time	1

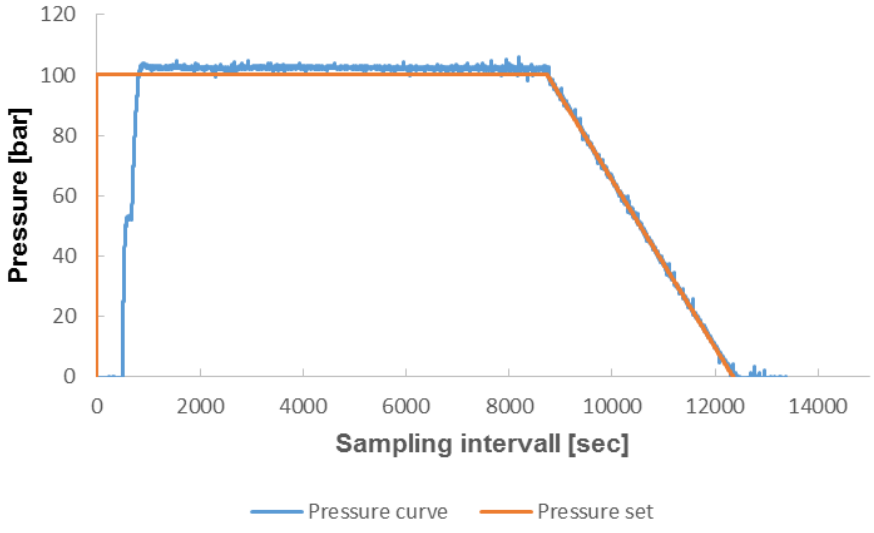

Figure 0-14 Pressure curve IM_14_2

Method	2-Step
p [bar]	100
T [°C]	40
T [h]	2
Gear pump	Yes
Ultra-sound	No
Co-solvent	H_2O
Inlet	1
Milieu	Basic
Depr.-time	1

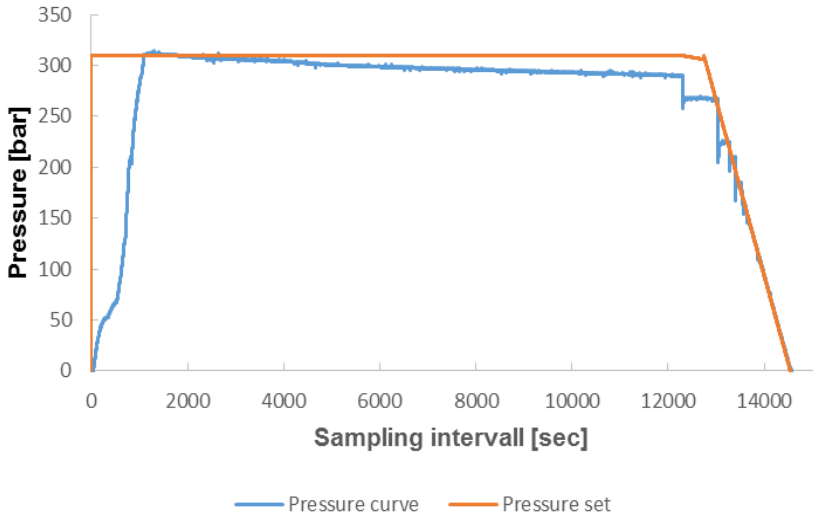

Figure 0-15 Pressure curve IM_15

Method	$Cu(hfac)_2$
p [bar]	300
T [°C]	40
T [h]	4
Gear pump	Yes
Ultra-sound	No
Co-solvent	-
Inlet	1
Milieu	Neutral
Depr.-time	1

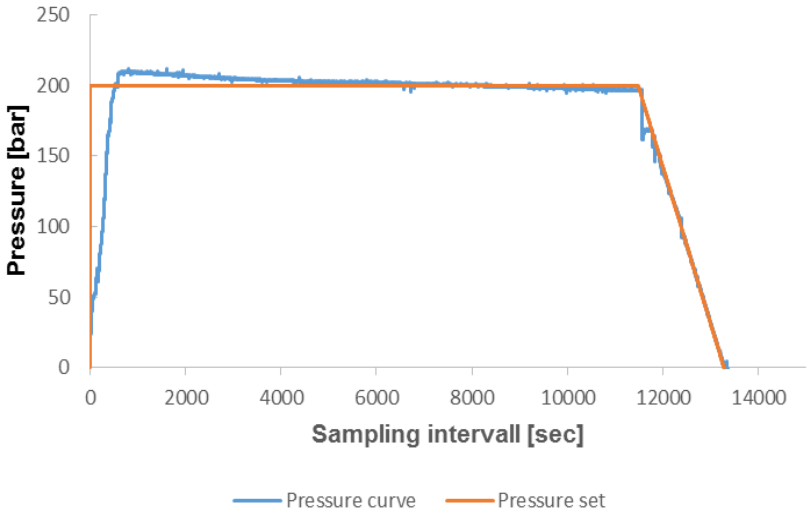

Figure 0-16 Pressure curve IM_16

Method	$Cu(hfac)_2$
p [bar]	200
T [°C]	40
T [h]	3
Gear pump	Yes
Ultra-sound	No
Co-solvent	-
Inlet	1
Milieu	Neutral
Depr.-time	1

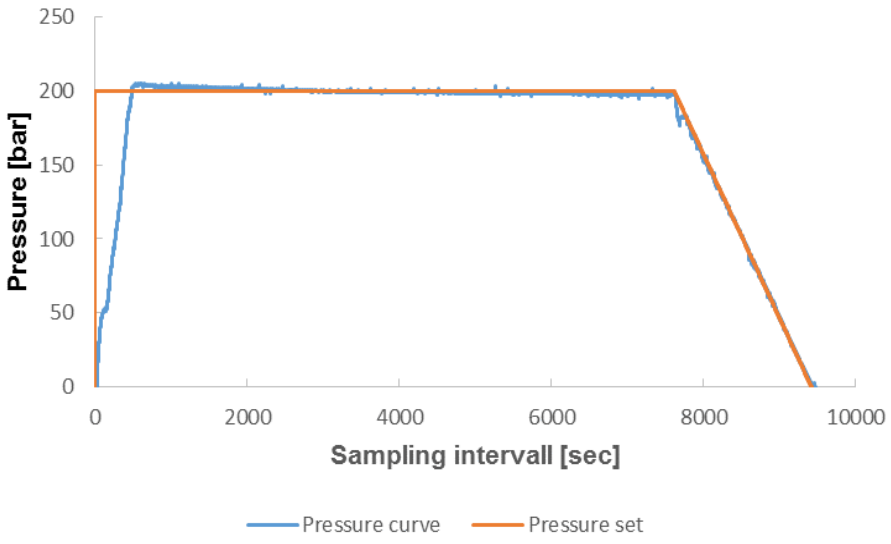

Method	$Cu(hfac)_2$
p [bar]	200
T [°C]	40
T [h]	3
Gear pump	Yes
Ultra-sound	No
Co-solvent	EtOH
Inlet	1
Milieu	Neutral
Depr.-time	1

Figure 0-17 Pressure curve IM_17

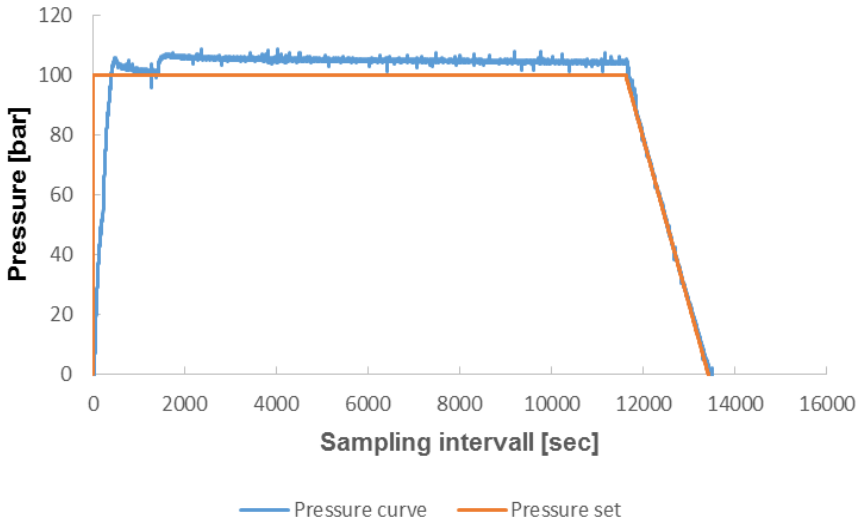

Method	$Cu(hfac)_2$
p [bar]	200
T [°C]	40
T [h]	3
Gear pump	Yes
Ultra-sound	No
Co-solvent	-
Inlet	2
Milieu	Neutral
Depr.-time	1

Figure 0-18 Pressure curve IM_18

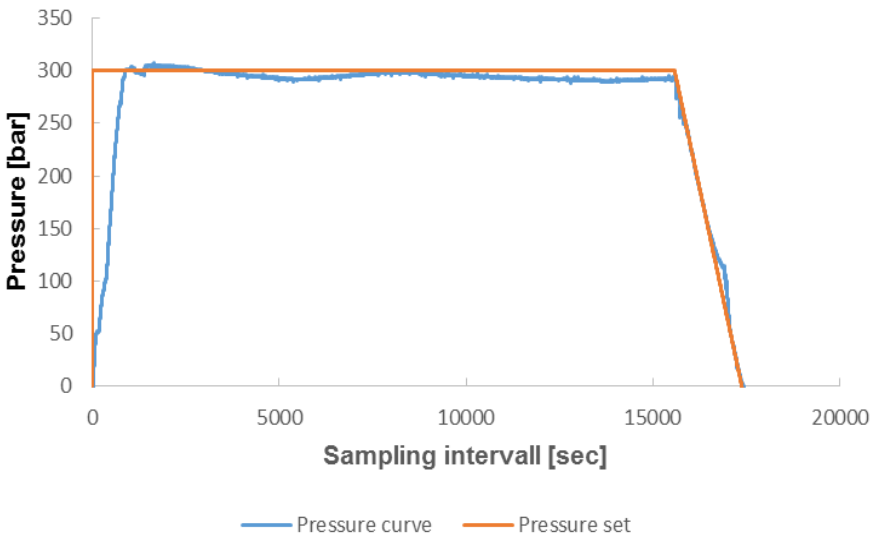

Figure 0-19 Pressure curve IM_19

Method	DPC
p [bar]	300
T [°C]	45
T [h]	4
Gear pump	Yes
Ultra-sound	No
Co-solvent	-
Inlet	2
Milieu	Neutral
Depr.-time	1

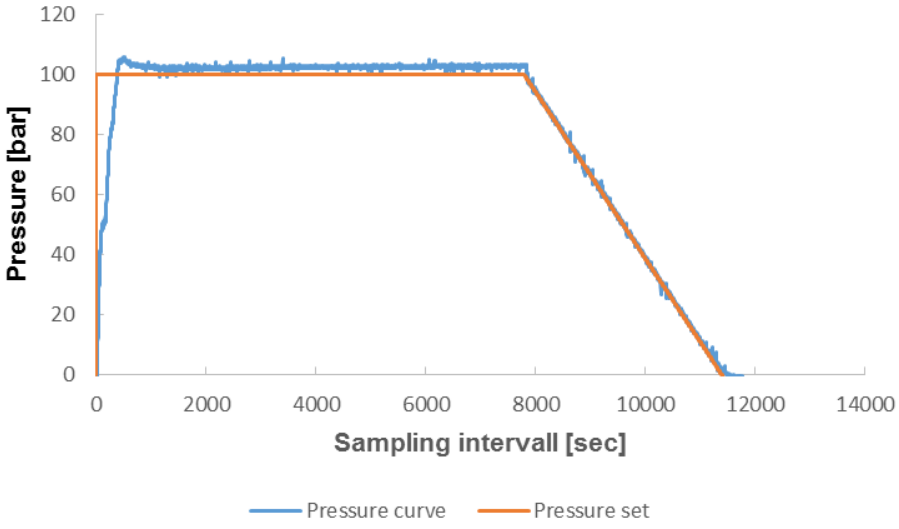

Figure 0-20 Pressure curve IM_20

Method	2-Step
p [bar]	100
T [°C]	40
T [h]	2
Gear pump	Yes
Ultra-sound	No
Co-solvent	H_2O
Inlet	2
Milieu	Basic
Depr.-time	1

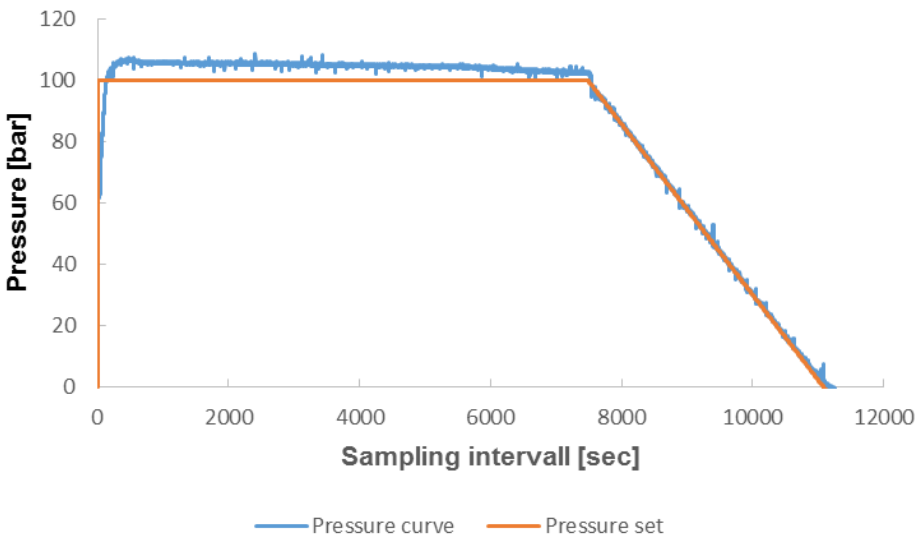

Method	2-Step
p [bar]	100
T [°C]	40
T [h]	2
Gear pump	Yes
Ultra-sound	No
Co-solvent	EtOH
Inlet	1
Milieu	Basic
Depr.-time	1

Figure 0-21 Pressure curve IM_21

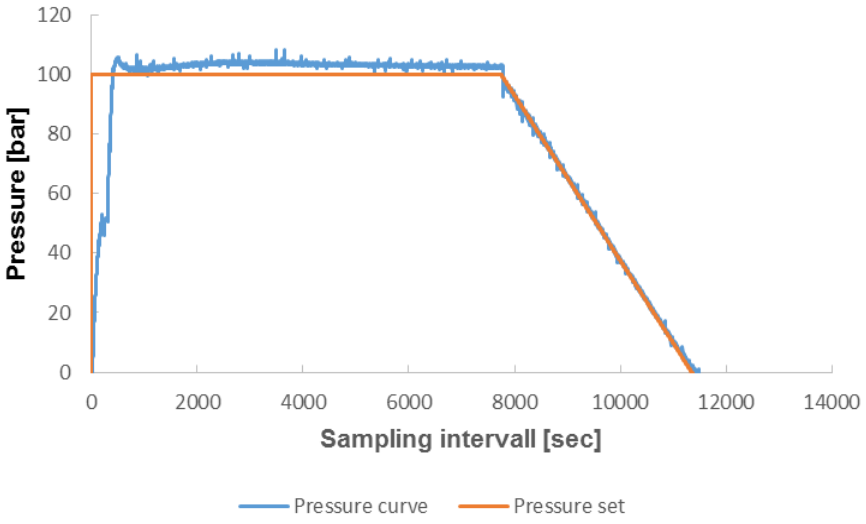

Method	Salt only
p [bar]	100
T [°C]	40
T [h]	2
Gear pump	Yes
Ultra-sound	No
Co-solvent	H_2O
Inlet	2
Milieu	Neutral
Depr.-time	1

Figure 0-22 Pressure curve IM_22

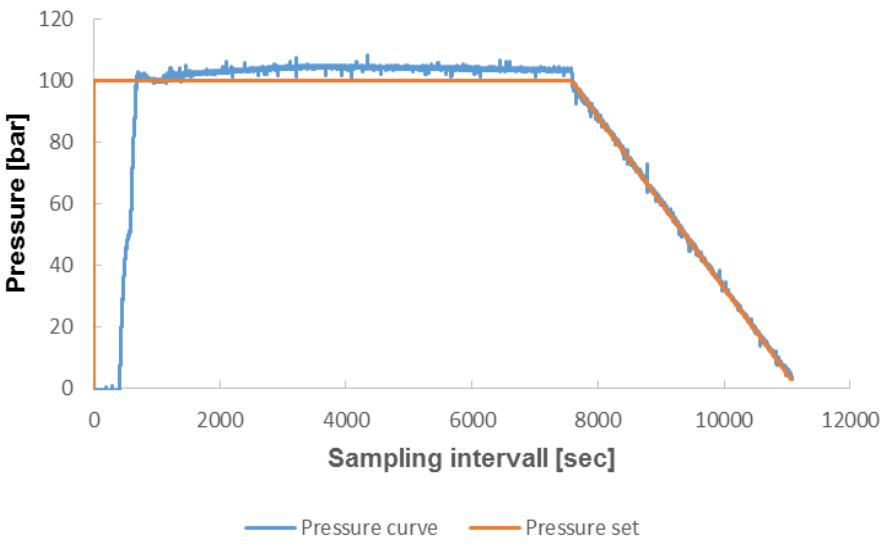

Figure 0-23 Pressure curve IM_23

Method	Salt only
p [bar]	100
T [°C]	40
T [h]	2
Gear pump	Yes
Ultra-sound	No
Co-solvent	EtOH
Inlet	2
Milieu	Neutral
Depr.-time	1

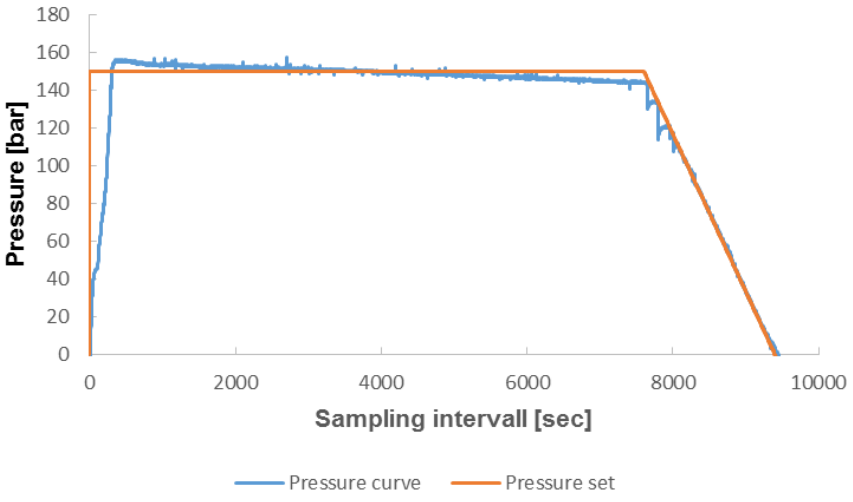

Figure 0-24 Pressure curve IM_24

Method	DPC
p [bar]	150
T [°C]	40
T [h]	2
Gear pump	Yes
Ultra-sound	No
Co-solvent	EtOH
Inlet	2
Milieu	Neutral
Depr.-time	1

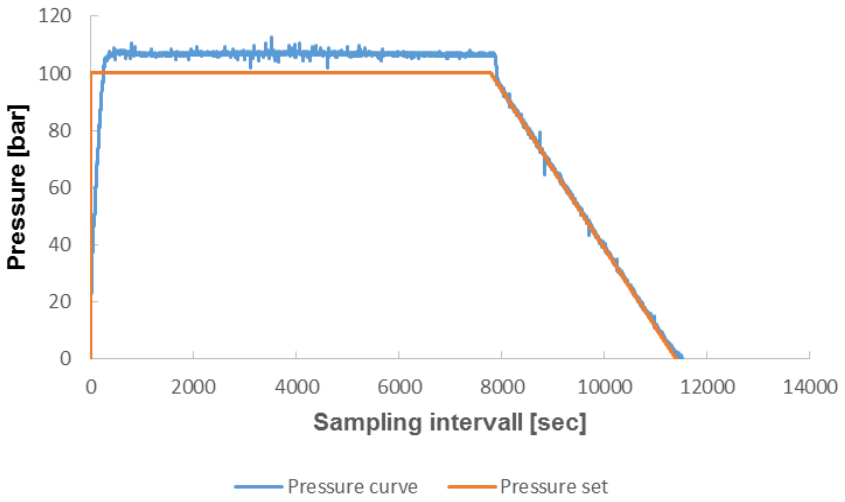

Figure 0-25 Pressure curve IM_25

Method	2-Step
p [bar]	100
T [°C]	40
T [h]	2
Gear pump	Yes
Ultra-sound	No
Co-solvent	H_2O
Inlet	2
Milieu	Basic
Depr.-time	2

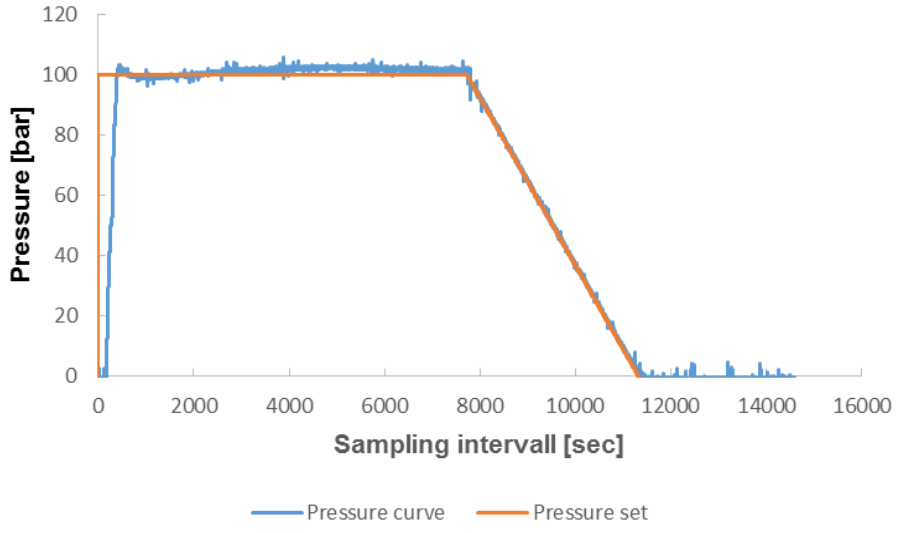

Figure 0-26 Pressure curve IM_26

Method	2-Step
p [bar]	100
T [°C]	40
T [h]	2
Gear pump	Yes
Ultra-sound	No
Co-solvent	H_2O
Inlet	2
Milieu	Basic
Depr.-time	1

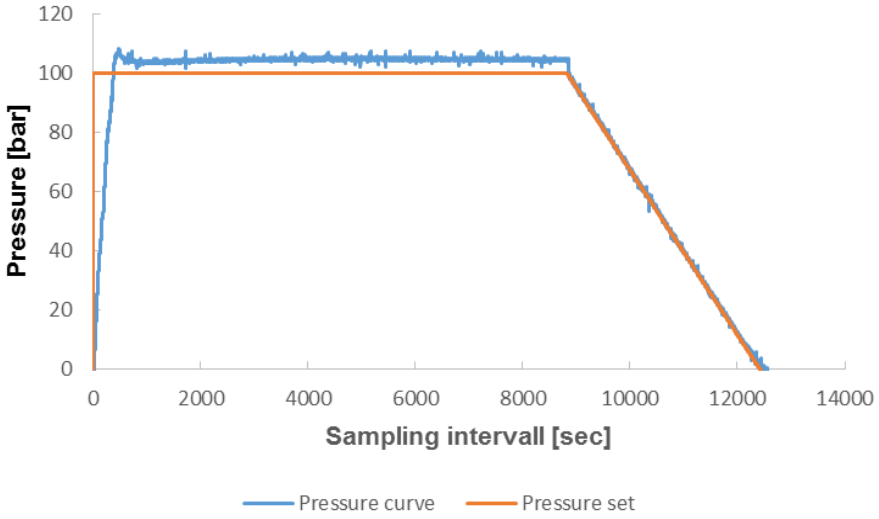

Figure 0-27 Pressure curve IM_27

Method	2-Step
p [bar]	100
T [°C]	40
T [h]	2
Gear pump	Yes
Ultra-sound	No
Co-solvent	H_2O
Inlet	2
Milieu	Basic
Depr.-time	1

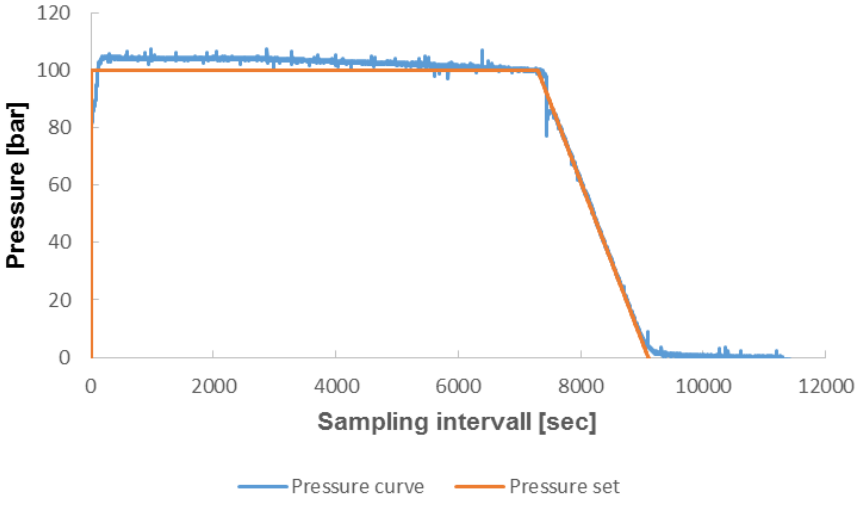

Figure 0-28 Pressure curve IM_28

Method	DPC
p [bar]	100
T [°C]	40
T [h]	2
Gear pump	Yes
Ultra-sound	No
Co-solvent	-
Inlet	1
Milieu	Neutral
Depr.-time	1

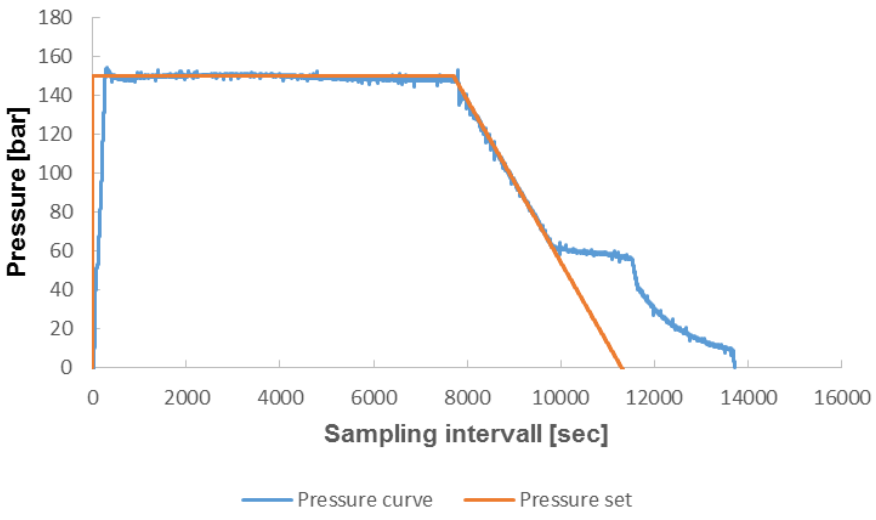

Figure 0-29 Pressure curve IM_31

Method	prim.
p [bar]	150
T [°C]	40
T [h]	2
Gear pump	Yes
Ultra-sound	No
Co-solvent	EtOH/ H_2O
Inlet	1
Milieu	Neutral
Depr.-time	1

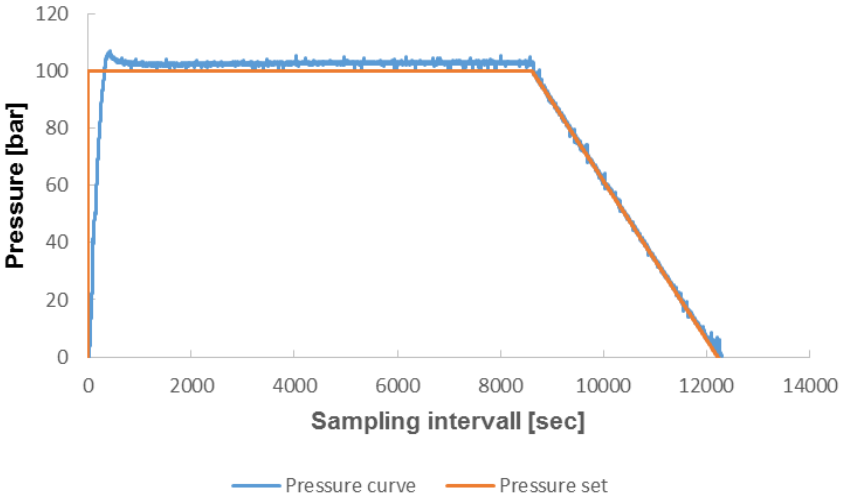

Figure 0-30 Pressure curve IM_32

Method	2-Step
p [bar]	100
T [°C]	40
T [h]	2
Gear pump	Yes
Ultra-sound	No
Co-solvent	H_2O
Inlet	2
Milieu	Basic
Depr.-time	1

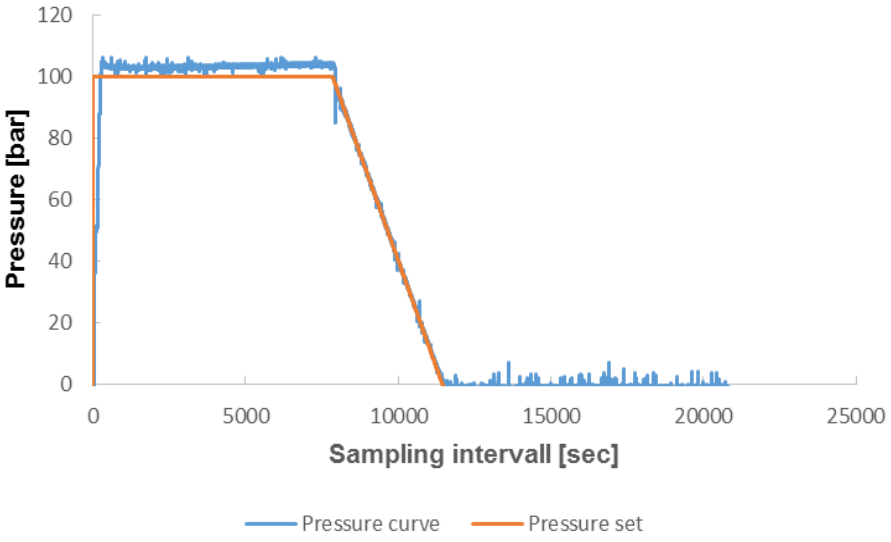

Figure 0-31 Pressure curve IM_33

Method	2-Step
p [bar]	100
T [°C]	40
T [h]	2
Gear pump	Yes
Ultra-sound	No
Co-solvent	H_2O
Inlet	1
Milieu	Basic
Depr.-time	1

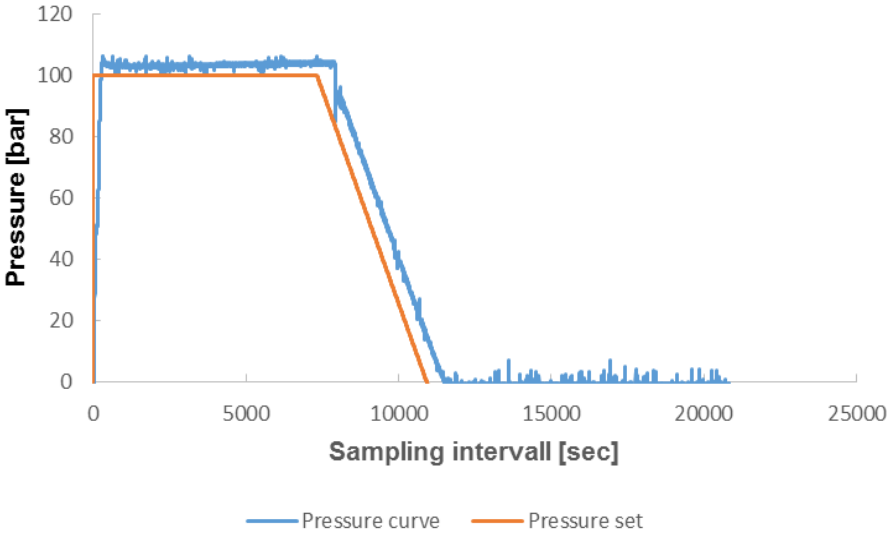

Figure 0-32 Pressure curve IM_34

Method	2-Step
p [bar]	100
T [°C]	40
T [h]	2
Gear pump	Yes
Ultra-sound	No
Co-solvent	H_2O
Inlet	2
Milieu	Basic
Depr.-time	1

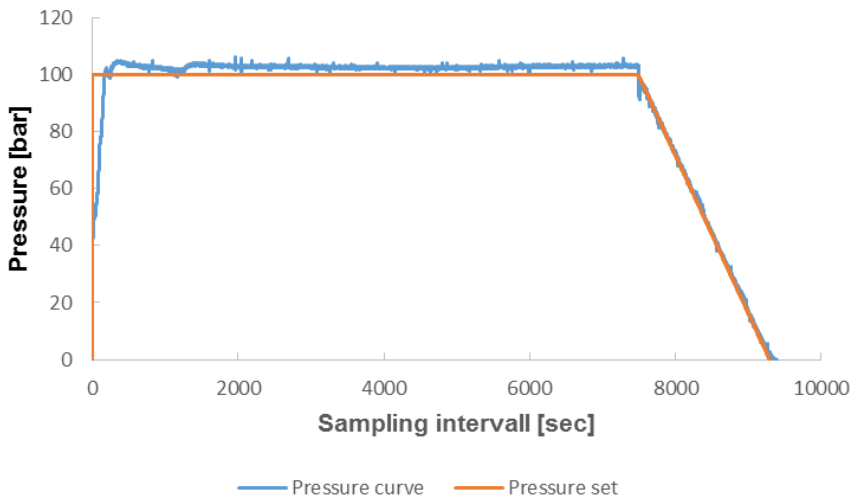

Figure 0-33 Pressure curve IM_35

Method	DPC
p [bar]	100
T [°C]	40
T [h]	2
Gear pump	Yes
Ultra-sound	No
Co-solvent	-
Inlet	1
Milieu	Neutral
Depr.-time	1

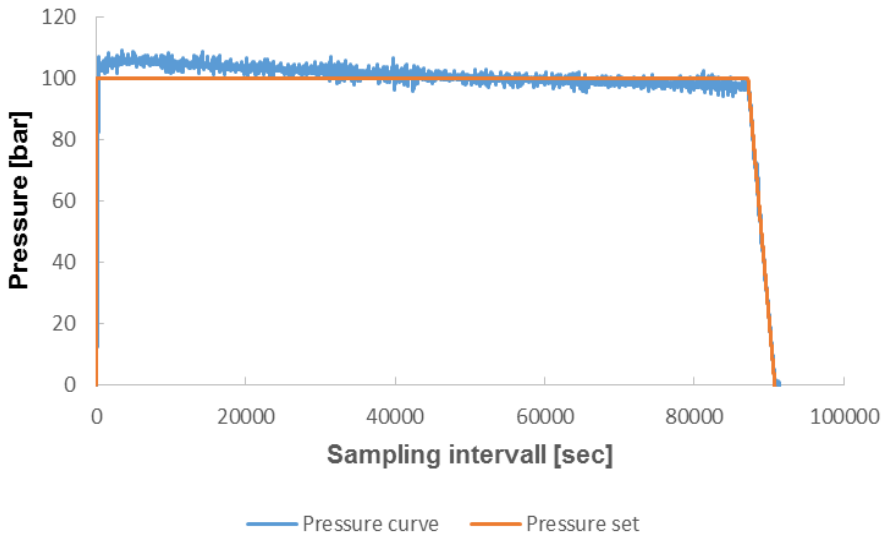

Figure 0-34 Pressure curve IM_36

Method	prim.
p [bar]	100
T [°C]	40
T [h]	24
Gear pump	Yes
Ultra-sound	No
Co-solvent	-
Inlet	1
Milieu	Neutral
Depr.-time	1

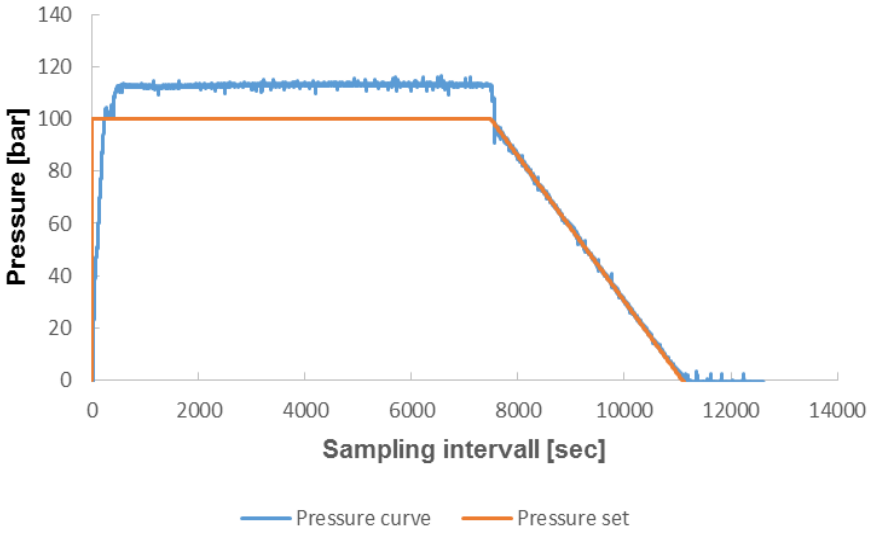

Method	2-Step
p [bar]	100
T [°C]	40
T [h]	2
Gear pump	Yes
Ultra-sound	No
Co-solvent	H_2O
Inlet	1
Milieu	Neutral
Depr.-time	1

Figure 0-35 Pressure curve IM_37

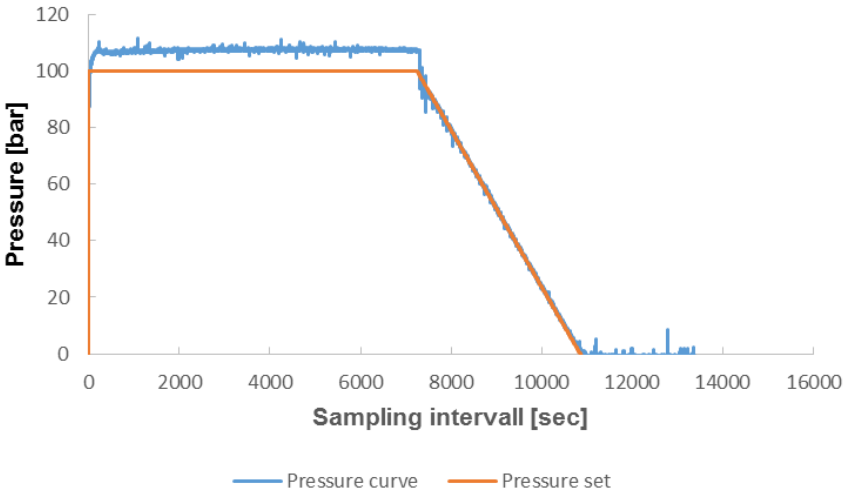

Method	2-Step
p [bar]	100
T [°C]	40
T [h]	2
Gear pump	Yes
Ultra-sound	No
Co-solvent	H_2O
Inlet	1
Milieu	Acidic
Depr.-time	1

Figure 0-36 Pressure curve IM_38